

**TRUE TRIAXIAL COMPRESSIVE STRENGTHS OF
MAHA SARA KHAM ROCK SALT**

Tanapol Sriapai

**A Thesis Submitted in Partial Fulfillment of the Requirements for the
Degree of Master of Engineering in Geotechnology**

Suranaree University of Technology

Academic Year 2010

การทดสอบค่ากำลังแรงกดในสามแกนจริงของเกลือหินชุดมหาสารคาม

นายชนพล ศรีอภัย

วิทยานิพนธ์นี้เป็นส่วนหนึ่งของการศึกษาตามหลักสูตรปริญญาวิศวกรรมศาสตรมหาบัณฑิต

สาขาวิชาเทคโนโลยีธรณี

มหาวิทยาลัยเทคโนโลยีสุรนารี

ปีการศึกษา 2553

**TRUE TRIAXIAL COMPRESSIVE STRENGTHS OF MAHA
SARAKHAM ROCK SALT**

Suranaree University of Technology has approved this thesis submitted in partial fulfillment of the requirements for a Master's Degree.

Thesis Examining Committee

(Asst. Prof. Thara Lekuthai)

Chairperson

(Assoc. Prof. Dr. Kittitep Fuenkajorn)

Member (Thesis Advisor)

(Dr. Prachya Tepnarong)

Member

(Dr. Wut Dankittikul)

Acting Vice Rector for Academic Affairs

(Assoc. Prof. Dr. Vorapot Khompis)

Dean of Institute of Engineering

ธนพล ศรีอภัย : การทดสอบค่ากำลังแรงกดในสามแกนจริงของเกลือหินซุคมหาสารคาม
(TRUE TRIAXIAL COMPRESSIVE STRENGTHS OF MAHA SARAKHAM ROCK
SALT) อาจารย์ที่ปรึกษา : รองศาสตราจารย์ ดร.กิตติเทพ เฟื่องขจร, 100 หน้า.

วัตถุประสงค์ของงานวิจัยเพื่อหาค่ากำลังการกดในสามแกนจริงของเกลือหินและเพื่อ
คาดคะเนเกณฑ์การแตกในสามมิติที่สามารถนำมาใช้วิเคราะห์หาเสถียรภาพของโพรงอากาศกักเก็บ
ในชั้นเกลือหิน เกลือหินตัวอย่างมาจากเกลือหินชั้นกลางของหน่วยหินมหาสารคาม
ในภาคตะวันออกเฉียงเหนือของประเทศไทย โดยตัวอย่างเกลือหินจะถูกตัดและฝนให้ได้รูปร่าง
บล็อกสี่เหลี่ยมมีขนาด $5 \times 5 \times 10$ ลูกบาศก์เซนติเมตร และใช้โครงกดทดสอบในสามแกนในการ
ทดสอบ ซึ่งจะประกอบกับคานคู่ให้ความเค้นด้านข้างคงที่ ในขณะที่การกดในแนวแกนจะใช้
ไฮดรอลิกปั๊ม โดยจะให้ค่าความเค้นหลักกลางคงที่โดยผันแปรตั้งแต่ 0 ถึง 80 เมกะปาสคาลและ
ค่าความเค้นหลักต่ำสุดคงที่โดยผันแปรตั้งแต่ 0 ถึง 28 เมกะปาสคาล ในขณะที่ความเค้นหลักสูงสุด
จะถูกกดให้มีค่าเพิ่มขึ้นจนกระทั่งหินแตก นอกจากนี้ทำการบันทึกการเปลี่ยนแปลงรูปร่างของ
ตัวอย่างเกลือหินในระหว่างการทดสอบในแต่ละแกน และจะใช้ในการคำนวณค่าสัมประสิทธิ์
ความยืดหยุ่นและอัตราส่วนปัวซองค์ โดยผลจากการคำนวณค่าสัมประสิทธิ์ความยืดหยุ่นและ
อัตราส่วนปัวซองค์เฉลี่ยมีค่า 22.2 ± 2.7 จิกะปาสคาล และ 0.37 ± 0.05 สำหรับเกณฑ์การแตกของ
Coulomb มีค่ามุมเสียดทานเท่ากับ 50 องศา และค่าสัมประสิทธิ์แรงเสียดทานเท่ากับ
5 เมกะปาสคาล ผลกระทบของความเค้นหลักกลางของเกลือหินสามารถอธิบายได้ดีด้วยเกณฑ์
การแตกของ modified Wiebols and Cook เกณฑ์การแตกของ Mogi จะสามารถทำนายการแตก
ของเกลือหินได้ดีเฉพาะความเค้นหลักต่ำสุด เกณฑ์การแตกของ modified Lade สามารถทำนาย
การแตกของเกลือหินได้สูงกว่าผลการทดสอบในทุกระดับของความเค้นหลักต่ำสูงสุด เกณฑ์การ
แตกของ Coulomb และเกณฑ์การแตก Hoek and Brown ไม่สามารถอธิบายความแข็งของ
เกลือหินได้ เนื่องจากทั้งสองกฎเกณฑ์ไม่มีการพิจารณาผลกระทบของความเค้นหลักกลาง
ทั้ง circumscribed และ inscribed ของเกณฑ์การแตก Drucker -Prager สามารถทำนายผลการทดสอบ
ได้ดีกว่าความเค้นหลักสูงสุดในทุกสภาวะของความเค้น

การจำลองด้วยแบบจำลองทางคอมพิวเตอร์เป็นการชี้ให้เห็นถึงผลกระทบของความเค้น
หลักกลางที่อยู่รอบ ๆ โพรงอากาศกักเก็บในเกลือหิน การจำลองใช้โปรแกรม FLAC โดยจะทำการ
ลดความดันภายในโพรง (P_{min}) ให้เหลือ 10 เปอร์เซ็นต์ และ 20 เปอร์เซ็นต์ ของความเค้นที่ด้าน
บนสุดของโพรงอากาศกักเก็บซึ่งจะมีค่าความเค้นที่มีความเบี่ยงเบนสูง ผลปรากฏว่าเมื่อทำการลด
ความดันภายในโพรงให้เหลือ 10 เปอร์เซ็นต์ จะเกิดการแตกขึ้นที่รอบ ๆ ผนังโพรงซึ่งสามารถ

ทำนายได้ด้วยเกณฑ์การแตกของ modified Wiebols and Cook เกณฑ์การแตกดังกล่าวมีความเหมาะสมมากกว่าเมื่อเปรียบเทียบกับเกณฑ์การแตกของ Coulomb เพราะเกณฑ์การแตกของ modified Wiebols and Cook มีการพัฒนามาจากผลลัพธ์ของการทดสอบกำลังกดในสามแกนจริง ซึ่งมีความน่าเชื่อถือมากกว่าเกณฑ์การแตกของ Coulomb

TANAPOL SRIAPAI : TRUE TRIAXIAL COMPRESSIVE STRENGTHS
OF MAHA SARA KHAM ROCK SALT. THESIS ADVISOR : ASSOC.
PROF. KITTITEP FUENKAJORN, Ph.D., P.E., 100 PP.

TRUE TRIAXIAL/POLYAXIAL/ROCK SALT/FAILURE/INTERMEDIATE
PRINCIPAL STRESS

The objectives of this research are to determine the true triaxial compressive strengths of rock salt and to assess the predictive capability of various multi-axial strength criteria for the rock. The salt specimens are from the Middle unit of the Maha Sarakham formation in the northeast of Thailand. The salt cores has been cut and ground to obtain rectangular blocks with a nominal dimension of $5 \times 5 \times 10 \text{ cm}^3$. A polyaxial load frame equipped with two pairs of cantilever beams used to apply constant lateral stresses (σ_2 and σ_3) to the salt specimen while the axial stress (σ_1) has been applied by a hydraulic load cell. Here the constant σ_2 is varied from 0 to 80 MPa, and σ_3 from 0 to 28 MPa while the axial stress is increased until failure. The deformations induced along the three loading directions are monitored and used to calculate the elastic modulus and Poisson's ratio of the salt. The results indicate that the elastic modulus and Poisson's ratio of the Maha Sarakham salt are averaged as $22.2 \pm 2.7 \text{ GPa}$ and 0.37 ± 0.05 . For the Coulomb criterion, the internal friction angle determined from the triaxial loading condition ($\sigma_2 = \sigma_3$) is 50° , and the cohesion is 5 MPa. The effect of σ_2 on the salt strengths can be best described by the modified Wiebols and Cook criterion. The empirical (power law) Mogi criterion tends to underestimate the salt strengths particularly under high σ_3 values. The modified

Lade criterion is the overestimates at all levels of σ_3 . The Coulomb and Hoek and Brown criteria can not describe the salt strengths beyond the condition where $\sigma_2 = \sigma_3$, as they can not incorporate the effects of σ_2 . Both circumscribed and inscribed Drucker-Prager criteria severely underestimate σ_1 at failure for all stress conditions.

A finite element analysis was performed to demonstrate the impact of the intermediated principal stress on the salt behavior around a compressed-air storage cavern subject to the designed minimum storage pressures during retrieval period. Under this condition the minimum cavern pressure (P_{\min}) is reduced to as low as 10% and 20% of the in-situ stress at the casing shoe (above the cavern top), and hence the stress states in the surrounding salt are highly deviatoric. For the minimum cavern pressure of 10% σ_{cs} failure occurs at cavern boundary as predicted by modified Wiebols and Cook criterion which is more appropriated when compared with the Coulomb criterion. This is because the modified Wiebols and Cook criterion on is developed from true triaxial test results, and hence, they can predict the stability condition more conservative than the Coulomb criterion.

School of Geotechnology

Academic Year 2010

Student's Signature_____

Advisor's Signature_____

ACKNOWLEDGMENTS

I wish to acknowledge the funding supported by Suranaree University of Technology (SUT).

I would like to express my sincere thanks to Assoc. Prof. Dr. Kittitep Fuenkajorn, thesis advisor, who gave a critical review and constant encouragement throughout the course of this research. Further appreciation is extended to Asst. Prof. Thara Lekuthai : chairman, school of Geotechnology and Dr. Prachya Tepnarong, School of Geotechnology, Suranaree University of Technology who are members of my examination committee. I am grateful Pimai Salt Company for donating salt core for testing. Grateful thanks are given to all staffs of Geomechanics Research Unit, Institute of Engineering who supported I work.

Finally, I most gratefully acknowledge my parents and friends for all their supported throughout the period of this research.

Tanapol Sriapai

TABLE OF CONTENTS

	Page
ABSTRRACT (THAI)	I
ABSTRACT (ENGLISH)	III
ACKNOWLEDGEMENTS	V
TABLE OF CONTENTS	VI
LIST OF TABLES	IX
LIST OF FIGURES.....	V
LIST OF SYMBOLS AND ABBREVIATIONS.....	VIII
CHAPTER	VIII
I INTRODUCTION	1
1.1 Background and rationale.....	1
1.2 Research objectives	1
1.3 Research methodology	1
1.3.1 Literature review	2
1.3.2 Sample preparation.....	2
1.3.3 Polyaxial strength testing	3
1.3.3 Assessment of the strength criteria	3
1.3.5 Computer simulations	3
1.3.6 Conclusions and thesis writing.....	5
1.4 Scope and limitations	5

TABLE OF CONTENTS (Continued)

	Page
1.5 Thesis contents	6
II LITERATURE REVIEW	7
III SAMPLE PREPARATION	22
IV LABORATORY TESTING	27
4.1 Introduction	27
4.2 Test equipment	27
4.3 Test method	29
4.4 Test results	32
4.4.1 Strength results	33
4.4.2 Elastic results	38
V ASSESSMENT OF THE STRENGTH CRITERIA	41
5.1 Introduction	41
5.2 Coulomb criterion	41
5.3 Modified Wiebols and Cook criteria	43
5.4 Modified Lade criterion	47
5.5 Mogi empirical 1971	49
5.6 Drucker–Prager criterion	51
5.7 Hoek and Brown criterion	54
5.8 Predictability of the strength criteria	58
5.9 Discussions of the test results	60

TABLE OF CONTENTS (Continued)

	Page
VI COMPUTER SIMULATION	61
6.1 Introduction	61
6.2 Numerical simulation	61
6.3 Results	64
6.3.1 Coulomb criterion	64
6.3.2 The modified Weibols and Cook criterion	65
VI DISCUSSIONS CONCLUSIONS AND	
RECOMMENDATIONS FOR FUTURE STUDIES	69
6.1 Discussions and conclusions	69
6.2 Recommendations for future studies	70
REFERENCES	72
APPENDICES	76
APPENDIX A. LIST OF STRESS – STRAINS CURVES.....	76
APPENDIX B. TECHNICAL PUBLICATION.....	86
BIOGRAPHY	105

LIST OF TABLES

Table	Page
3.1 Specimen dimensions prepared for polyaxial testing	24
4.1 Summary of the strength results on salt specimen of true triaxial compression tests	33
4.2 Summarizes these stress and strain values and their corresponding elastic parameters	38
4.3 Elastic parameters obtained from true triaxial testing	39
5.1 Strength calculation in terms of $J_2^{1/2}$ and σ_m	44
5.2 Modified Wiebols and Cook parameters for rock salt	46
5.3 Parameters for each failure criterion	54
5.4 Mean misfits calculated for each failure criterion	56
6.1 Material properties and strengths parameter used in FLAC simulations	60

LIST OF FIGURES

Figure		Page
1.1	Research plan	4
1.2	Polyaxial load frame.....	5
2.1	Test cell with a specimen inside ready to be transferred to the loading machine.....	8
2.2	True triaxial system used for study	11
2.3	Influence of the intermediate principal stress on the strength of Westerly granite. Rapid initial rock strength increases with increasing σ_2 can be seen for low σ_3	13
3.1	A salt specimen is dry cut by a cutting machine	23
3.2	Some salt specimens prepared for true triaxial testing.	23
4.1	Polyaxial load frame developed for compressive strength testing under true triaxial stresses	27
4.2	Directions of loading with respect to specimen shape.....	27
4.3	Cantilever beam weighed at outer end applies lateral stress to the rock specimen	29
4.4	Calibrated curves for use in polyaxial compression testing.....	30
4.5	Maximum principal stress (σ_1) at failure as a function of σ_2 for various	34

LIST OF FIGURES (Continued)

Figure	Page
4.6	Some post-test specimens. Numbers in blankets indicate [$\sigma_1, \sigma_2, \sigma_3$] at failure.....35
4.7	Results of triaxial compressive strength from polyaxial compressive strength tests in terms of Mohr's circles and Coulomb criterion.36
5.1	$J_2^{1/2}$ as a function of σ_m from testing rock salt compared with the Coulomb criterion predictions (lines).45
5.2	$J_2^{1/2}$ as a function of σ_m from testing rock salt compared with modified Wiebols & Cook criterion predictions (lines)47
5.3	$J_2^{1/2}$ as a function of σ_m from testing rock salt compared with modified Lade criterion predictions (lines).....58
5.4	Comparisons between the test results with the Mogi empirical 1971.....51
5.5	Comparisons between the test results with circumscribed Drucker- Prager criterion.....53
5.6	$J_2^{1/2}$ as a function of σ_m from testing rock salt compared with the Hoek and Brown criterion predictions (lines).....55
6.1	Finite difference mesh constructed to simulate a compressed-air storage cavern in the Maha Sarakham salt59

LIST OF FIGURES (Continued)

Figure	Page
6.2 Contours of factor of safety calculated from the Coulomb and modified Wiebols and Cook criteria for $P_{\min} = 10\% \sigma_{cs}$, r = 25 m.	63
6.3 Contours of factor of safety calculated from the Coulomb and modified Wiebols and Cook criteria for $P_{\min} = 20\% \sigma_{cs}$, r = 25 m.	64

LIST OF SYMBOLS AND ABBREVIATIONS

A	=	Parameter related to C_0 and μ_i
A'	=	Parameter related to τ_{oct} and $\sigma_{m,2}$
B	=	Parameter related to C_0 and μ_i
B'	=	Parameter related to C_0 and $\sigma_{m,2}$
C	=	Parameter related to C_0 and μ_i
C ₁	=	Parameter related to C_0 and μ_i
c	=	Cohesion
E	=	Elastic modulus
F	=	Load on rock sample
FS	=	Factor of Safety
G	=	Shear modulus
I ₁	=	The first stress invariant
I ₃	=	The third stress invariant
I ₁ '	=	The modified first of stress invariant
I ₃ '	=	The modified of stress invariant
J ₁	=	The first order of stress invariant
J ₂ ^{1/2}	=	The second order of stress invariant
J ₂ ^{1/2} ,f	=	The second order of stress invariant from FLAC program
k ₁	=	Constant value depends on the density of the soil.
m	=	Number of data sets

LIST OF SYMBOLS AND ABBREVIATION (Continued)

m'	=	Parameter related to σ_1 and σ_3
n	=	Number of data points
p_a	=	Atmospheric pressure
P_{\min}	=	minimum pressure
q	=	Parameter related to μ_i
S	=	Parameter related to S_o and ϕ
S_o	=	Cohesion
S_1	=	Maximum principal deviation
S_2	=	Intermediate principal deviation
S_3	=	Minimum principal deviation
s	=	Parameter related to σ_1 and σ_3
\bar{s}	=	mean misfit
W	=	Weight on lower bars
α	=	Parameter related to c and ϕ
β	=	Parameter related to σ_1 and σ_3
χ	=	Parameter related to principal stress
Δ	=	Volumetric strain
ϕ	=	Friction angle
$\gamma_{\text{oct,e}}$	=	Octahedral shear strain at elastic modulus point
η	=	Parameter related to ϕ
κ	=	Parameter related to c and ϕ

LIST OF SYMBOLS AND ABBREVIATION (Continued)

λ	=	Lame's constant
μ_i	=	Parameter related to ϕ
ν	=	Poisson's ratio
ρ	=	Density
σ_c	=	Uniaxial compressive strengths
σ_{cs}	=	In-situ stress at casing shoe
σ_m	=	Mean stress
$\sigma_{m,e}$	=	Mean stress at elastic modulus point
$\sigma_{m,2}$	=	Mean stress of Mogi Empirical
σ_n	=	Normal stress
$\sigma_{1,f}$	=	Maximum principal stress from FLAC program
$\sigma_{1,j}^{calc}$	=	Maximum stress predicted from strength criterion
$\sigma_{1,j}^{test}$	=	Maximum stress from test data
σ_1	=	Maximum principal stress
σ_2	=	Intermediate principal stress
σ_3	=	Minimum principal stress
τ	=	Shear stress
τ_{oct}	=	Octahedral shear stress
$\tau_{oct,e}$	=	Octahedral shear stress at elastic modulus point
ψ	=	Parameter related to principal stress

CHAPTER I

INTRODUCTION

1.1 Background and rationale

The effects of confining pressures at great depths on the mechanical properties of rocks are commonly simulated in a laboratory by performing triaxial compression testing of cylindrical rock core specimens. A significant limitation of these conventional methods is that the intermediate and minimum principal stresses are equal during the test while the actual in-situ rock is normally subjected to an anisotropic stress state where the maximum, intermediate and minimum principal stresses are different ($\sigma_1 \neq \sigma_2 \neq \sigma_3$). It has been commonly found that compressive strengths obtained from conventional triaxial testing can not represent the actual in-situ strength where the rock is subjected to an anisotropic stress state. The intermediate principal stress increase can the maximum stress at failure. As a result the failure criterion that can take into account the three-dimensional stress states has been extremely rare. The existing three dimensional failure criteria for rock are not adequate because they are not in the form that can readily be applied in the actual design and analysis of geological structures.

1.2 Research objectives

The objectives of this research are to determine the compressive strengths of rock salt subjected to anisotropic stress states, and to assess the predictive capability of three-dimensional failure criteria that can be readily applied in the design and

stability analysis of compressed-air storage cavern in rock salt. The efforts involve determination of the maximum principal stress at failure of the rock samples under various intermediate and minimum principal stresses, and determination of the most suitable multi-axial strength criterion. A polyaxial loading frame is used to apply constant σ_2 and σ_3 onto the specimen while the σ_1 is increased until failure. The applied σ_2 and σ_3 at different magnitudes are varied from 0 to 60 MPa. The failure stresses will be measured, and mode of failure will be examined. The existing three-dimensional strength criteria will be used to compare against the strength criteria above: (1) the octahedral shear strength as a function of mean stress, and (2) the major principal stress at failure as a function of the intermediate principal stress. Such criterion will be useful for determining or predicting the rock strength under anisotropic stress state of the in-situ condition.

1.3 Research methodology

The research methodology shown in Figure 1.1 comprises 7 steps; including literature review, sample preparation, polyaxial strength testing, assessment of strength criteria for salt, computer simulation, and discussions and conclusions.

1.3.1 Literature review

Literature review is carried out to study the previous researches on compressive strength in true-triaxial stress state and the effect of intermediate principal stress. The sources of information are from text books, journals, technical reports and conference papers. A summary of the literature review is given in the thesis.

1.3.2 Sample preparation

Rock samples used here have been obtained from the Middle members of the Maha Sarakham formation in the northeastern Thailand. The rock salt is relatively pure halite. Sample preparation is carried out in the laboratory at Suranaree University of Technology. Samples prepared for compressive strength test are $5 \times 5 \times 10 \text{ cm}^3$.

1.3.3 Polyaxial strength testing

The laboratory testing involves true triaxial compressive strength tests in polyaxial load frame. A polyaxial load frame shown in Figure 1.2 is equipped with two pairs of cantilever beams used to apply constant lateral stresses (σ_2 and σ_3) to the specimen while the axial stress (σ_1) is applied by a hydraulic load cell. The specimen is first confined under hydrostatic stress equivalent to the pre-defined intermediate principal stress. One of the lateral stresses is then decreased to the pre-defined minimum principal stress while the axial stress is increased until failure occurs.

1.3.4 Assessment of the strength criteria

Results from laboratory measurements in terms of the principal stresses at failure are used to formulate mathematical relations. The studied strength criteria include the Coulomb, Drucker-Prager, modified Lade, modified Weibols and Cook, Hoek and Brown, and the empirical 1971 Mogi criteria. The principal stresses can be incorporated to the strength criteria. The mean misfit (\bar{s}) is determined for each criterion

1.3.5 Computer simulations

The failure criterion is used to assess the stability of an underground storage cavern by using the finite difference code (FLAC). The multi-axial strength

criterion, calibrated from the true triaxial strength test results and the conventional approach of using the uniaxial and triaxial strength test data are used to simulate the stability conditions of the storage cavern.

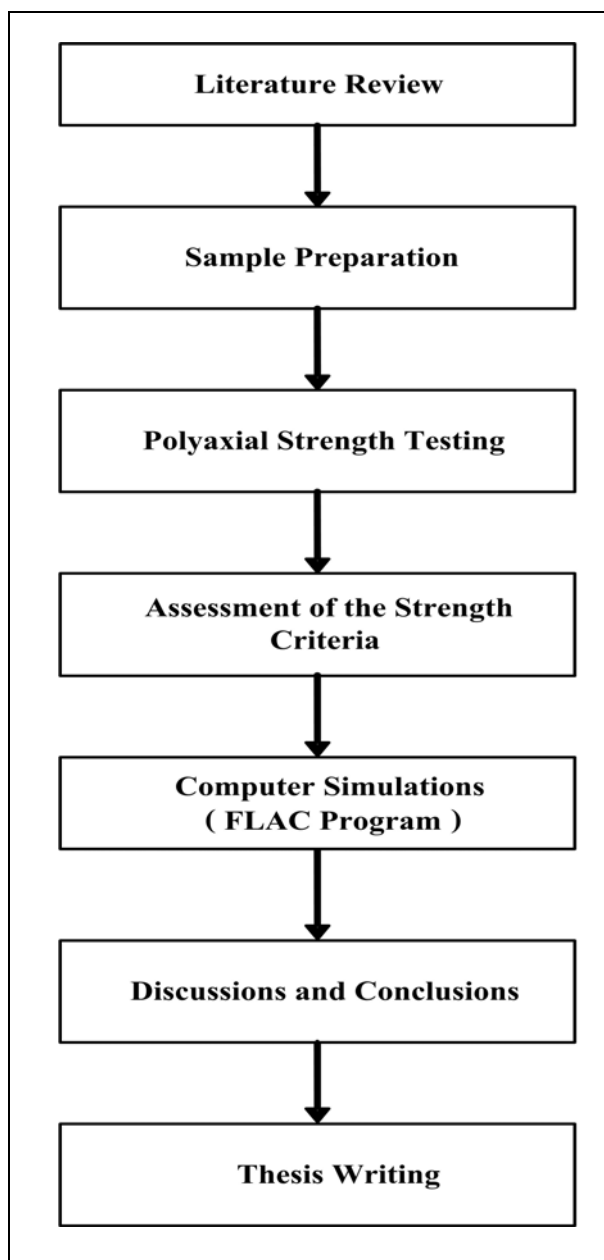


Figure 1.1 Research methodology

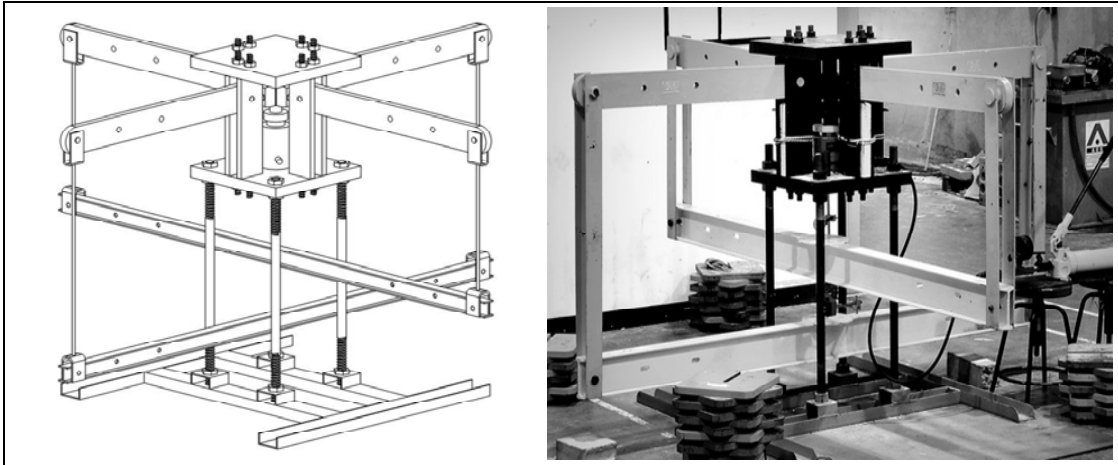


Figure 1.2 Polyaxial load frame

1.3.6 Conclusion and thesis writing

All research activities, methods, and results are documented and compiled in the thesis.

1.4 Scope and limitations

The scope and limitations of the research include as follows.

1. Laboratory experiments are conducted on rock salt specimens from Maha Sarakham formation
2. Testing is made under intermediate principal stresses ranging from 0 to 60 MPa, and the minimum principal stresses between 0 and 7 MPa
3. Up to 30 samples are tested, with the nominal sample size of $5 \times 5 \times 10 \text{ cm}^3$.
4. All tests are conducted under ambient temperature.
5. Testing is made under dry condition.
6. No field testing is conducted.
7. The research findings had been published in conference paper or journal.

1.5 Thesis contents

This research thesis is divided into seven chapters. The first chapter includes background and rationale, research objectives, research methodology, and scope and limitations. **Chapter II** presents results of the literature review to improve an understanding of rock compressive strength as affected by the intermediate principal stress. **Chapter III** describes the sample preparation. **Chapter IV** describes the polyaxial compressive strength test. **Chapter V** presents strength criteria. **Chapter VI** presents results from strength criterion calibration and compare with computer simulations. **Chapter VII** is the discussions, conclusions and recommendations for future studies.

CHAPTER II

LITERATURE REVIEW

2.1 Compressive strength of rock

Relevant topics and previous research results are reviewed to improve an understanding of rock compressive strength as affected by the intermediate principal stress. Summary of the review results is described below.

Alsayed (2002) used hollow cylinder specimens for simulating stress condition around the opening to study the behaviour of rock under a much wider variety of stress paths. The hollow cylinder specimens are used in conventional triaxial test cell, shown in Figure 2.1 It was developed by Hoek and Franklin (1970) and specially designed of internal of pressure loading configuration. Springwell sandstone specimens were subjected to under uniaxial, biaxial, triaxial and polyaxial compression, as well as indirect tension. The results obtained confirm the effect of the intermediate principal stress on rock failure and show that the apparent strength of rock is markedly influenced by the stress condition imposed. Multiaxial testing system can provide realistic prediction of the actual behaviour of rock and guide the formulation of more adequate numerical models.

Kwasniewski et al. (2003) use prismatic samples of medium-grained sandstone from Śląsk Colliery for testing under uniaxial compression, conventional triaxial compression and true triaxial compression conditions. Results of the studies show that confining pressure strongly inhibited dilatant behavior of rock samples tested under

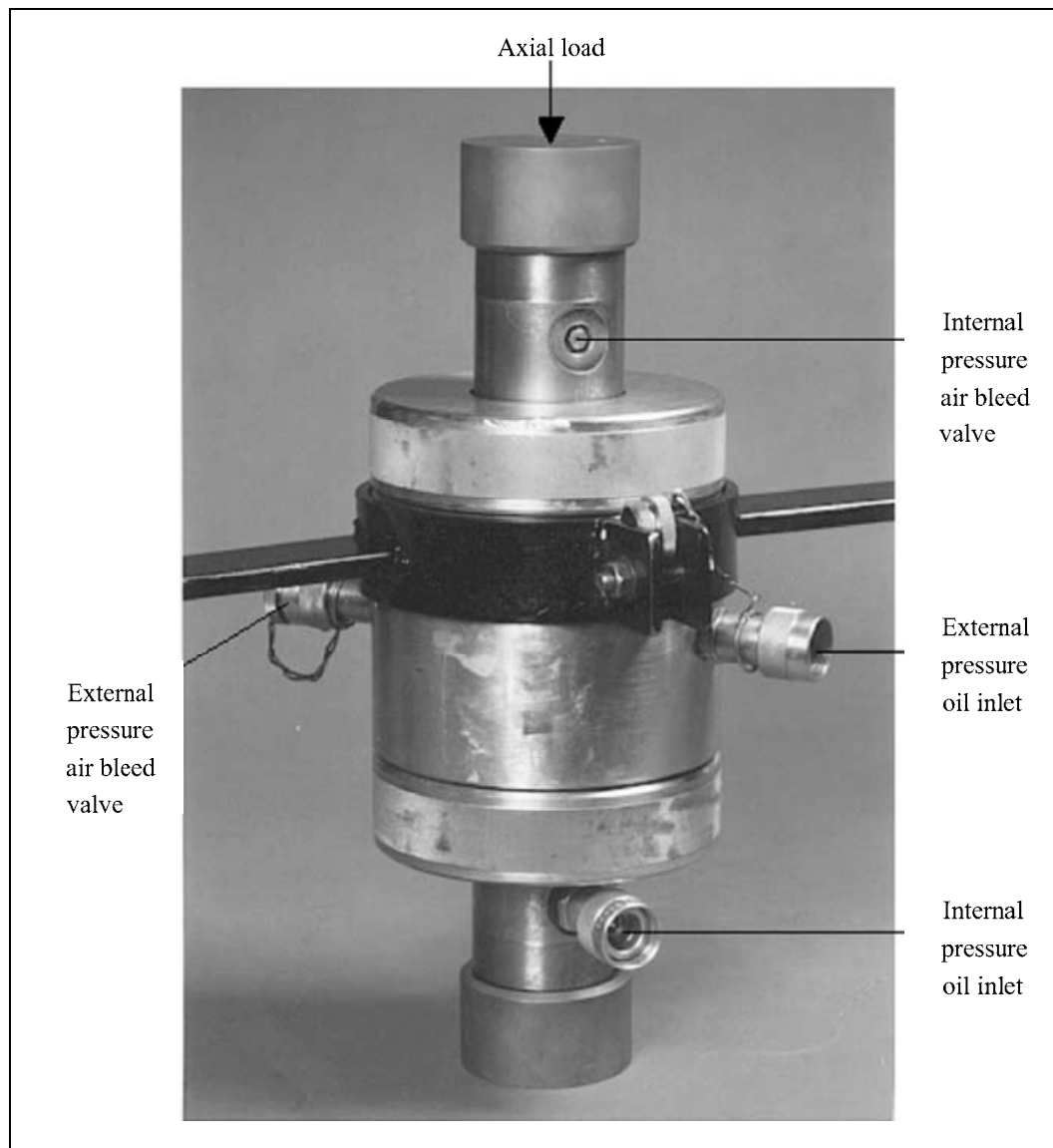


Figure 2.1 Test cell with a specimen inside ready to be transferred to the loading machine (Alsayed, 2002).

conventional triaxial compression conditions; the increasing confinement resulted in the growing compaction of the rock material. The effect of dilatancy was also highly suppressed by the intermediate principal stress. While important dilatant, negative volumetric strain corresponded to the peak differential stress at low intermediate

principal stress conditions, at high intermediate stresses the rock material was damaged to much lesser extent. As a result, faulting of rock samples in the post-peak region was much more violent and was accompanied by a strong acoustic effect.

Colmenares and Zoback (2002) examine seven different failure criteria by comparing them to published polyaxial test data ($\sigma_1 > \sigma_2 > \sigma_3$) for five different rock types at a variety of stress states. They employed a grid search algorithm to find the best set of parameters that describe failure for each criterion and the associated misfits. Overall, they found that the polyaxial criterion of Modified Wiebols and Cook and Modified Lade achieved a good fit to most of the test data. This is especially true for rocks with a highly σ_2 -dependent failure behavior (e.g. Dunham dolomite, Solenhofen limestone). However, for some rock types (e.g. Shirahama Sandstone, Yuubari shale), the intermediate stress hardly affects failure and the Mohr Coulomb and Hoek and Brown criteria fit these test data equally well, or even better, than the more complicated polyaxial criteria. The values of C_0 (uniaxial compressive strength) yielded by the Inscribed and the Circumscribed Drucker–Prager criteria bounded the C_0 (uniaxial compressive strength) value obtained using the Mohr Coulomb criterion as expected. In general, the Drucker–Prager failure criterion did not accurately indicate the value of σ_1 at failure. The value of the misfits achieved with the empirical 1967 and 1971 Mogi criteria were generally in between those obtained using the triaxial and the polyaxial criteria. The disadvantage of these failure criteria is that they cannot be related to strength parameters such as C_0 : They also found that if only data from triaxial tests are available, it is possible to incorporate the influence of σ_2 on failure by using a polyaxial failure criterion. The results for two out of three rocks that could be analyzed in this way were encouraging.

Tiwari and Rao (2004) have described physical modeling of a rock mass under a true triaxial stress state by using block mass models having three smooth joint sets. The testing used true-triaxial system (TTS) developed by Rao and Tiwari (2002), shown in Figure 2.2. The test results show the strength of rock mass (σ_1) and deformation modulus (E_j) increase significantly which is confirmed by fracture shear planes developed on σ_2 face of specimen. Most of the specimens failed in shearing with sliding in some cases. The effect of interlocking and rotation of principal stresses σ_2 and σ_3 on strength and deformation response was also investigated.

Chang and Haimson (2005) discuss the non-dilatant deformation and failure mechanism under true triaxial compression. They conducted laboratory rock strength experiments on two brittle rocks, hornfels and metapelite, which together are the major constituent of the long valley Caldera (California, USA) basement in the 2025 – 2996 m depth range. Both rocks are banded, very high porosity. Uniaxial compression test at different orientations with respect to banding planes reveal that while the hornfels compressive strength is nearly isotropic, the metapelite possesses distinct anisotropy. Conventional triaxial tests in these rocks reveal that their respective strengths in a specific orientation increase approximately linearly with confining pressure. True triaxial compressive experiments in specimens oriented at a consistent angle to banding, in which the magnitude of the least (σ_3) and the intermediate (σ_2) principal stresses are different but kept constant during testing while the maximum principal stress is increased until failure, exhibit a behaviour unlike that previously observed in other rocks under similar testing conditions. For a given magnitude of σ_3 , compressive strength σ_1 does not vary significantly in both regardless of the applied σ_2 , suggesting little or no intermediate principal stress effect. Strains measured in all

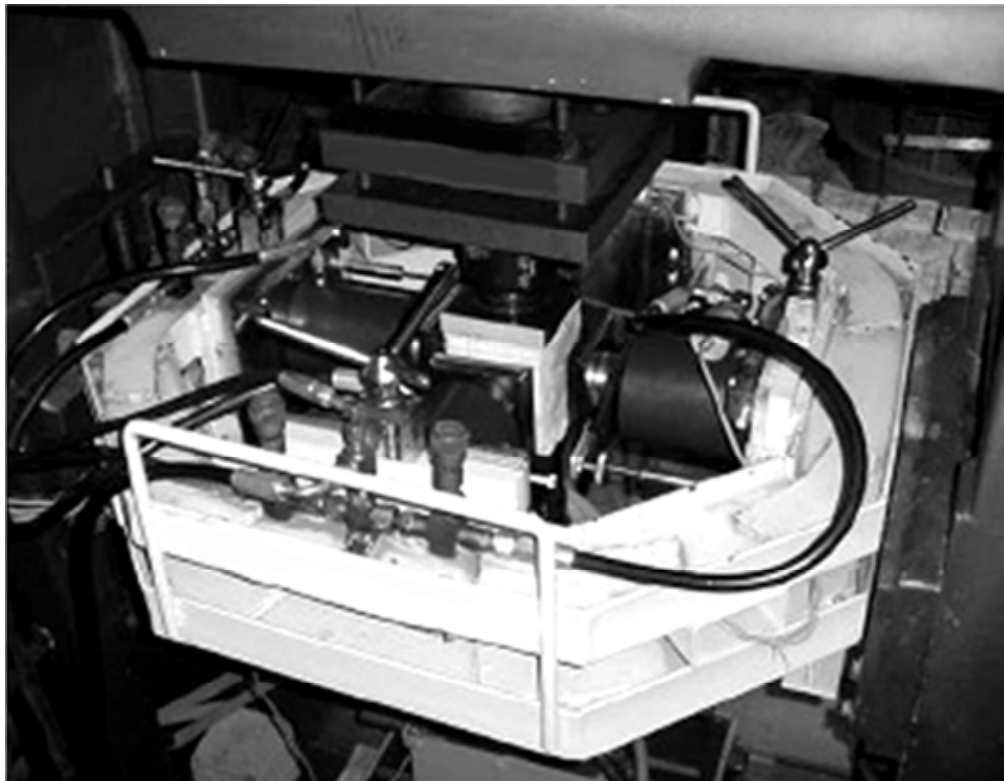


Figure 2.2 True triaxial system used for study (Rao and Tiwari, 2002).

three principal directions during loading were used to obtain plots σ_1 versus volumetric strain. These are consistently linear almost to the point of rock failure, suggesting no dilatants.

Haimson (2006) describes the effect of the intermediate principal stress (σ_2) on brittle fracture of rocks, and on their strength criteria. Testing equipment emulating Mogi's but considerably more compact was developed at the University of Wisconsin and used for true triaxial testing of some very strong crystalline rocks. Test results revealed three distinct compressive failure mechanisms, depending on loading mode and rock type: shear faulting resulting from extensile microcrack localization, multiple splitting along the axis, and nondilatant shear failure. The true triaxial

strength criterion for the KTB amphibolite derived from such tests was used in conjunction with logged breakout dimensions to estimate the maximum horizontal in situ stress in the KTB ultra deep scientific hole.

Cai (2008) studied the intermediate principal stress on rock fracturing and strength near excavation boundaries using a FEM/ DEM combined numerical tool. A loading condition of $\sigma_3 = 0$ and $\sigma_1 \neq 0$, and $\sigma_2 \neq 0$ exists at the tunnel boundary, where σ_1 , σ_2 , and σ_3 , are the maximum, intermediate, and minimum principal stress components, respectively. The numerical study is based on sample loading testing that follows this type of boundary stress condition. It is seen from the simulation results that the generation of tunnel surface parallel fractures and microcracks is attributed to material heterogeneity and the existence of relatively high intermediate principal stress (σ_2), as well as zero to low minimum principal stress (σ_3) confinement. A high intermediate principal stress confines the rock in such way that microcracks and fractures can only be developed in the direction parallel to σ_1 and σ_2 . Stress-induced fracturing and microcracking in this fashion can lead to onion-skin fractures, spalling, and slabbing in shallow ground near the opening and surface parallel microcracks further away from the opening, leading to anisotropic behavior of the rock. Consideration of the effect of the intermediate principal stress on rock behavior should focus on the stress-induced anisotropic strength and deformation behavior of the rocks show in Figure 2.3. It is also found that the intermediate principal stress has limited influence on the peak strength of the rock near the excavation boundary.

Walsri et al. (2009) developed polyaxial load frame to determine the compressive and tensile strengths of three types of sandstone under true triaxial stresses. Results from the polyaxial compression tests on rectangular specimens of sandstones suggest

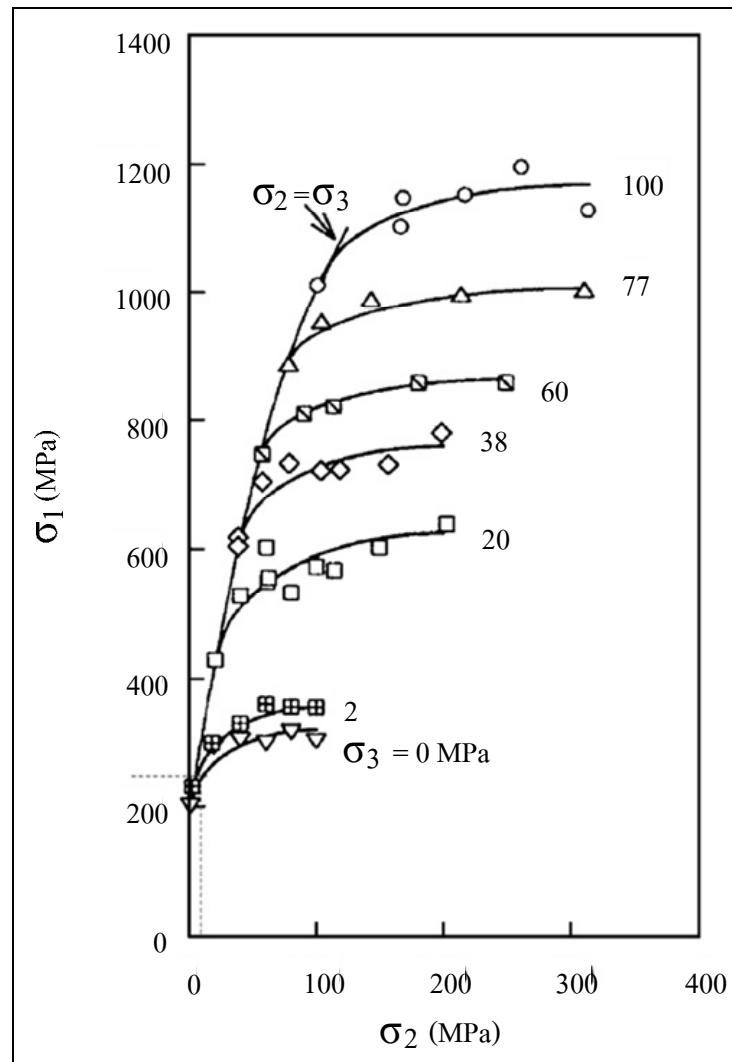


Figure 2.3 Influence of the intermediate principal stress on the strength of Westerly granite. Rapid initial rock strength increases with increasing σ_2 can be seen for low σ_3 (Cai, 2008).

that the rocks are transversely isotropic. The measured elastic modulus in the direction parallel to the bedding planes is slightly greater than that normal to the bed. Poisson's ratio on the plane normal to the bedding planes is lower than those on the parallel ones. Under the same σ_3 , σ_1 at failure increases with σ_2 . Results from the Brazilian tension tests under axial compression reveal the effects of the intermediate principal stress on the rock tensile strength. The Coulomb and modified Wiebols and Cook failure criteria derived from the characterization test results predict the sandstone strengths in term of $J_2^{1/2}$ as a function of J_1 under true triaxial stresses. The modified Wiebols and Cook criterion describes the failure stresses better than does the Coulomb criterion when all principal stresses are in compressions. When the minimum principal stresses are in tension, the Coulomb criterion over-estimate the second order of the stress invariant at failure by about 20% while the modified Wiebols and Cook criterion fails to describe the rock tensile strengths.

2.2 Polyaxial strength criteria

In this research we aim to find which failure criterion, and parameters that best describe the behavior of rock by minimizing the mean standard deviation misfit between the predicted failure stress and the experimental data.

Coulomb criterion indicates that when shear failure takes place across a plane, the normal stress σ_n and the shear stress τ across this plane are related by functional relation characteristics of the material (Jaeger and Cook, 1979):

$$|\tau| = S_0 + \mu_i \sigma_n \quad (2.1)$$

where S_0 is the shear strength or cohesion of the material and μ_i is the coefficient of internal friction of the material. Since the sign of τ only affects the sliding direction, only the magnitude of τ matters. The linearized form of the Mohr failure criterion may also be written as (Jaeger and Cook, 1979):

$$\sigma_1 = \sigma_c + q\sigma_3 \quad (2.2)$$

$$\text{where: } q = \left[(\mu_i^2 + 1)^{1/2} + \mu_i^2 \right]^2 = \tan^2(\pi/4 + \phi/2) \quad (2.3)$$

where σ_1 is the major principal effective stress at failure, σ_3 is the least principal effective stress at failure, σ_c is the uniaxial compressive strength and ϕ is the angle of internal friction equivalent to $\tan^{-1}\mu_i$. This failure criterion assumes that the intermediate principal stress has no influence on failure.

The modified Wiebols and Cook criterion described by Zhou (1994) predicts that a rock fails if:

$$J_2^{1/2} = A + BJ_1 + CJ_1^2 \quad (2.4)$$

$$\text{where: } J_2^{1/2} = \sqrt{(1/6)\{(\sigma_1 - \sigma_2)^2 + (\sigma_1 - \sigma_3)^2 + (\sigma_2 - \sigma_3)^2\}} \quad (2.5)$$

$$J_1 = (\sigma_1 + \sigma_2 + \sigma_3)/3 \quad (2.6)$$

where J_1 is the mean effective confining stress and $J_2^{1/2} = (3/2)^{1/2}\tau_{\text{oct}}$, where τ_{oct} is the octahedral shear stress:

$$\tau_{\text{oct}} = \frac{1}{3} \sqrt{(\sigma_1 - \sigma_2)^2 + (\sigma_1 - \sigma_3)^2 + (\sigma_2 - \sigma_3)^2} \quad (2.7)$$

The constants A, B and C depend on rock materials and the minimum principal stresses (σ_3). They can be determined under the conditions where $\sigma_2 = \sigma_3$, as follows:

$$C = \frac{\sqrt{27}}{2C_1 + (q-1)\sigma_3 - \sigma_c} \times \left(\frac{C_1 + (q-1)\sigma_3 - \sigma_c}{2C_1 + (2q+1)\sigma_3 - \sigma_c} - \frac{q-1}{q+2} \right) \quad (2.8)$$

where: $C_1 = (1 + 0.6\mu_i)\sigma_c$

σ_c = uniaxial compressive strength of the rock

$\mu_i = \tan\phi$

$q = \{(\mu_i^2 + 1)^{1/2} + \mu_i\}^2 = \tan^2(\pi/4 + \phi/2)$

$$B = \frac{\sqrt{3}(q-1)}{q+2} - \frac{C}{3}(2\sigma_c + (q+2)\sigma_3) \quad (2.9)$$

$$A = \frac{\sigma_c}{\sqrt{3}} - \frac{\sigma_c}{3}B - \frac{\sigma_c^2}{9}C \quad (2.10)$$

The rock strength predictions produced using Eq. (2.4) are similar to that of the Wiebols and Cook and thus the model described by Eq. (2.4) represents a modified strain energy criterion, which may be called Modified Wiebols and Cook. For polyaxial states of stress, the predictions made by this criterion are greater than that of the Mohr–Coulomb criterion.

Mogi 1967 empirical criterion indicates the influence of the intermediate stress on failure by performing confined compression tests ($\sigma_1 > \sigma_2 = \sigma_3$), confined extension tests ($\sigma_1 = \sigma_2 > \sigma_3$) and biaxial tests ($\sigma_1 > \sigma_2 > \sigma_3 = 0$) on different rocks. He recognized that the influence of the intermediate principal stress on failure is non-zero, but considerably smaller than the effect of the minimum principal stress. When he plotted the maximum shear stress $(\sigma_1 - \sigma_3)/2$ as a function of $(\sigma_1 + \sigma_3)/2$ for failure of Westerly granite, he observed that the extension curve lied slightly above the compression curve and the opposite happened when he plotted the octahedral shear stress τ_{oct} as a function of the mean normal stress $(\sigma_1 + \sigma_2 + \sigma_3)/3$ for failure of the same rock. Therefore, if $(\sigma_1 + \beta\sigma_2 + \sigma_3)$ is taken as the abscissa (instead of $(\sigma_1 + \sigma_3)$ or $(\sigma_1 + \sigma_2 + \sigma_3)$), the compression and the extension curves become coincidental at a suitable value of β . Mogi argued that this β value is nearly the same for all brittle rocks but we will test this assertion. The empirical criterion has the following formula:

$$(\sigma_1 - \sigma_3)/2 = f_1[(\sigma_1 + \beta\sigma_2 + \sigma_3)/2] \quad (2.11)$$

where β is a constant smaller than 1. The form of the function f_1 in Eq. (2.11) is dependent on rock type and it should be a monotonically increasing function. This criterion postulates that failure takes place when the distortional energy increases to a limiting value, which increases monotonically with the mean normal pressure on the fault plane. The term $\beta\sigma_2$ may correspond to the contribution of σ_2 to the normal stress on the fault plane because the fault surface, being irregular, is not exactly parallel to σ_2 and it would be deviated approximately by $\arcsin(\beta)$.

Mogi 1971 empirical criterion empirical fracture criterion was obtained by generalization of the von Mises's theory. It is formulated by:

$$\tau_{\text{oct}} = f_1(\sigma_1 + \sigma_3) \quad (2.12)$$

where f_1 is a monotonically increasing function. According to Mogi the data points tend to align in a single curve for each rock, although they slightly scatter in some silicate rocks. The octahedral stress is not always constant but increases monotonically with $(\sigma_1 + \sigma_3)$. Failure will occur when the distortional strain energy reaches a critical value that increases monotonically with the effective mean pressure on the slip planes parallel to the σ_2 direction. The effective mean pressure on faulting is $(\sigma_1 + \sigma_3)/2$ or $\sigma_{m,2}$ therefore, τ_{oct} at fracture is plotted against $\sigma_{m,2}$. Mogi applied this failure criterion to different kinds of rocks and it always gave satisfactory results.

Hoek and Brown criterion used to the uniaxial compressive strength of the intact rock material as a scaling parameter, and introduces two dimensionless strength parameters, m' and s . After studying a wide range of experimental data, stated that the relationship between the maximum and minimum stress while these values of m obtained from lab tests on intact rock are intended to represent a good estimate when laboratory tests are not available, they compare them with the values obtained for the five rocks studied. For intact rock materials, $s = 1$ for a completely granulated specimen or a rock aggregate, $s = 0$ (Hoek and Brown, 1980):

$$\sigma_1 = \sigma_3 + \sigma_c \sqrt{m' \frac{\sigma_3}{\sigma_c} + s} \quad (2.13)$$

where m' and s are constants that depend on the properties of the rock and on the extent to which it had been broken before being subjected to the failure stresses σ_1 and σ_3 . The Hoek and Brown failure criterion was originally developed for estimating the strength of rock masses for application to excavation design.

The Lade criterion is a three-dimensional failure criterion for frictional materials with out effective cohesion. It was developed for soils with curved failure envelopes Lade (1977). This criterion is given by

$$((I_1^3/I_3) - 27)(I_1/p_a)^{m'} = \eta \quad (2.14)$$

where: $I_1 = S_1 + S_2 + S_3$

$$I_2 = S_1S_2S_3$$

where p_a is the atmospheric pressure expressed in the same units as the stresses, and m' and η_1 are material constants.

In the modified Lade criterion developed by Ewy (1999), m' was set equal to zero in order to obtain criterion Eq. (2.14), which is able to predict a linear shear strength increase with increasing I_1 . In this way the criterion is similar to that proposed by Lade and Duncan (1975) in which $(I_1)^3/I_3 = k_1$ where k_1 is a constant whose value depends on the density of the soil. For considering materials with cohesion, Ewy (1999) introduced the parameter S and also included the pore pressure as a necessary parameter. Doing all the modifications and defining appropriate stress invariants the following failure criterion was obtained by Ewy (1999):

$$(I_1')^3/I_3' = 27 + \eta \quad (2.15)$$

where: $I_1' = (\sigma_1 + S) + (\sigma_2 + S) + (\sigma_3 + S)$

$$I_3' = (\sigma_1 + S)(\sigma_2 + S)(\sigma_3 + S)$$

where S and η are material constants. The parameter S is related to the cohesion of the rock, while the parameter η represents the internal friction. These parameters can be derived directly from the Mohr–Coulomb cohesion S_0 and internal friction angle ϕ by:

where: $S = S_0/\tan \phi$

$$\eta = 4(\tan\phi)^2(9-7\sin\phi)/(1-\sin\phi)$$

$$S_0 = \sigma_c/(2q^{1/2})$$

The extended von Mises yield criterion or Drucker - Prager criterion was originally developed for soil mechanics. The yield surface of the modified von Mises criterion in principal stress space is a right circular cone equally inclined to the principal-stress axes. The intersection of the π plane with this yield surface is a circle. The yield function used by Drucker and Prager to describe the cone in applying the limit theorems to perfectly plastic soils has the form:

$$J_2^{1/2} = \kappa + \alpha \sigma_m \quad (2.16)$$

where α and k are material constants. The material parameters α and κ can be determined from the slope and the intercept of the failure envelope plotted in the J_1 and $(J_2)^{1/2}$ space. α is related to the internal friction of the material and κ is related to the cohesion of the material, in this way, the Drucker – Prager criterion can be compared to the Mohr –Coulomb criterion. When $\alpha = 0$ it reduces to the Von Mises criterion. The Drucker – Prager criterion can be divided in to an outer bound criterion or Circumscribed Drucker– Prager and an inner bound criterion or Inscribed Drucker

Prager. The set versions of the Drucker – Prager criterion come from comparing the Drucker – Prager criterion with the Mohr–Coulomb criterion. The Inscribed Drucker – Prager criterion is obtained when:

$$\alpha = \frac{3 \sin \phi}{\sqrt{9 + 3 \sin^2 \phi}} \quad (2.17)$$

$$\kappa = \frac{2\sigma_c \cos \phi}{2\sqrt{q}\sqrt{9 + 3 \sin^2 \phi}} \quad (2.18)$$

The Circumscribed Drucker–Prager criterion is obtained when:

$$\alpha = \frac{6 \sin \phi}{\sqrt{3}(3 - \sin \phi)} \quad (2.19)$$

$$\kappa = \frac{\sqrt{3}\sigma_c \cos \phi}{\sqrt{q}(3 - \sin \phi)} \quad (2.20)$$

where ϕ is the angle of internal friction, that is, $\phi = \tan^{-1} \mu_i$.

CHAPTER III

SAMPLE PREPARATION

This chapter describes sample preparation and specifications of the tested rock salt. The method follows as much as practical the standard practices. The salt specimens tested here are obtained from borehole of Pimai salt Co., Ltd., Nakhon Ratchasima province. They are from the Middle members of the Maha Sarakham (MS) formation in the northeastern Thailand. This salt member has long been considered as a host rock for compressed-air energy storage by the Thai Department of Energy. The core specimens are dry cut and ground as shown in Figure 3.1. The core specimens with a nominal diameter of 60 mm tested here were drilled from depths ranging between 170 and 270 m. The salt specimen have a nominal dimension of $5 \times 5 \times 10 \text{ cm}^3$ as shown in Figure 3.2. The rock salt is relatively pure halite with slight amount (less than 1-2%) of anhydrite, clay minerals and ferrous oxide. The average crystal (grain) size is about $5 \times 5 \times 10 \text{ mm}^3$. Warren (1999) gives detailed descriptions of the salt and geology of the basin. Sample preparation is conducted in laboratory facility at the Suranaree University of Technology. A total of 60 specimens are prepared for testing. Table 3.1 summarizes the specimen number, dimensions and density.



Figure 3.1 A salt specimen is dry cut by a cutting machine.

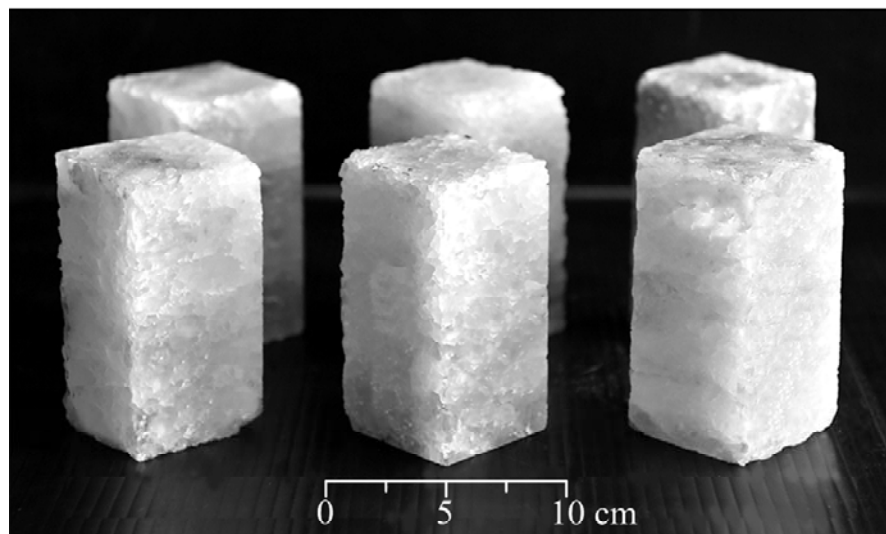


Figure 3.2 Some salt specimens prepared for true triaxial testing.

The nominal dimension is $5 \times 5 \times 10 \text{ cm}^3$.

Table 3.1 Specimen dimensions prepared for polyaxial testing.

Specimen No.	Width (mm.)	Length (mm.)	Height (mm.)	Density (g/cc)
MS-PX-01	52.1	54.3	108.6	2.14
MS-PX-02	56.2	57.4	104.8	2.24
MS-PX-03	53.9	52.7	105.4	2.26
MS-PX-04	55.0	55.3	109.6	2.24
MS-PX-05	54.0	55.1	106.2	2.19
MS-PX-06	57.5	55.1	106.2	2.32
MS-PX-07	53.3	54.5	109.0	2.19
MS-PX-08	54.7	51.2	102.4	2.18
MS-PX-09	56.0	54.9	109.7	2.28
MS-PX-10	55.7	56.1	102.2	2.19
MS-PX-11	55.0	54.5	109.0	2.25
MS-PX-12	53.8	54.5	109.0	2.29
MS-PX-13	54.4	53.5	107.0	2.30
MS-PX-14	53.4	54.3	108.6	2.20
MS-PX-15	51.5	55.0	105.0	2.22
MS-PX-16	54.3	55.6	101.2	2.00
MS-PX-17	54.1	54.3	108.6	2.19
MS-PX-18	55.5	55.3	110.6	2.15
MS-PX-19	55.4	54.4	108.8	2.10
MS-PX-20	54.7	54.7	109.4	2.14
MS-PX-21	54.9	57.5	105.0	2.22
MS-PX-22	54.0	56.6	103.2	2.32
MS-PX-23	56.0	56.1	102.2	2.23
MS-PX-24	57.3	55.4	110.8	2.20
MS-PX-25	56.6	54.8	109.6	2.12
MS-PX-26	54.0	54.7	109.4	2.30
MS-PX-27	57.0	55.7	101.4	2.17
MS-PX-28	56.0	56.2	102.4	2.27
MS-PX-29	54.2	55.6	101.2	2.26
MS-PX-30	55.3	57.1	104.2	2.13
MS-PX-31	54.5	56.4	102.8	2.19
MS-PX-32	56.9	56.1	102.2	2.16
MS-PX-33	57.1	53.5	107.0	2.35
MS-PX-34	54.9	54.5	109.0	2.18
MS-PX-35	56.1	56.7	103.4	2.23
MS-PX-36	55.7	56.2	102.4	2.28
MS-PX-37	54.0	54.3	108.6	2.25

Table 3.1 Specimen dimensions prepared for polyaxial testing (cont.).

Specimen No.	Width (mm.)	Length (mm.)	Height (mm.)	Density (g/cc)
MS-PX-38	55.4	55.1	107.2	2.12
MS-PX-39	56.8	55.9	101.8	2.05
MS-PX-40	55.0	55.3	107.6	2.01
MS-PX-41	53.7	54.2	108.4	2.22
MS-PX-42	54.0	56.5	103.0	2.15
MS-PX-43	54.5	55.2	106.4	2.34
MS-PX-44	54.0	54.6	109.2	2.15
MS-PX-45	55.6	55.6	101.2	2.05
MS-PX-46	53.7	53.9	107.8	2.22
MS-PX-47	53.8	53.1	106.2	2.32
MS-PX-48	56.1	56.5	103.0	2.35
MS-PX-49	55.2	55.5	101.0	2.13
MS-PX-50	53.4	54.6	109.2	2.21
MS-PX-51	54.3	53.8	107.6	2.12
MS-PX-52	54.3	53.4	106.8	2.05
MS-PX-53	54.3	53.4	106.8	2.11
MS-PX-54	53.6	53.0	106.0	2.32
MS-PX-55	57.8	54.0	108.0	2.12
MS-PX-56	54.5	55.0	110.0	2.10
MS-PX-57	54.5	57.0	104.0	2.05
MS-PX-58	54.8	51.2	102.4	2.29
MS-PX-59	54.0	52.0	104.0	2.09
MS-PX-60	54.8	53.0	106.0	2.20
Average				2.20 ± 0.09

CHAPTER IV

POLYAXIAL COMPRESSIVE STRENGTH TESTS

4.1 Introduction

The objective of this chapter is to experimentally determine the compressive strengths of rock salt subjected to anisotropic stress states. This chapter describes the equipment, method, results and analysis of the polyaxial compressive strength tests on the rock. A total of 36 specimens have been tested.

4.2 Test equipment

Figure 4.1 shows the polyaxial load frame (Walsri et al., 2009) used in this test. The polyaxial compression tests are performed to determine the compressive strengths and deformations of the salt specimens under true triaxial stresses. The intermediate (σ_2) and minimum (σ_3) principal stresses are maintained constant while σ_1 maximum stresses is increased until failure is occurred. Here the constant σ_2 is varied from 0 to 80 MPa, and σ_3 from 0 to 28 MPa. Neoprene sheets are used to minimize the friction at all interfaces between the loading platen and the rock surface. Figure 4.2 shows the applied principal stress directions with respect for all specimens. The failure stresses are recorded and mode of failure examined. To meet the load requirement above, two pairs of cantilever beams are used to apply the lateral stresses in mutually perpendicular directions on the specimen. The outer end of each opposite beam is pulled down by dead weight placed in the middle of a steel bar linking the two

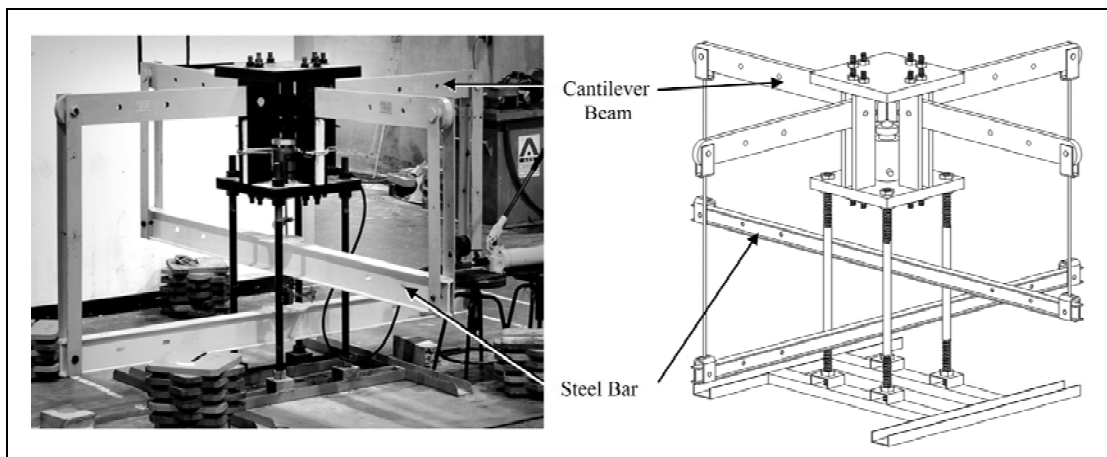


Figure 4.1 Polyaxial load frame developed for compressive strength testing under true triaxial stresses (from Walsri et al., 2009).

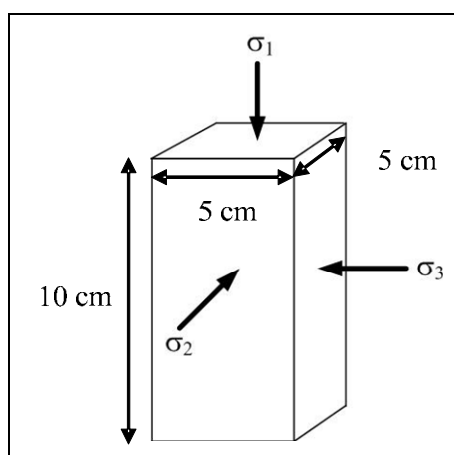


Figure 4.2 Directions of loading with respect to specimen shape.

opposite beams underneath (Figure 4.3). The inner end is hinged by a pin mounted on vertical bars on each side of the frame. During testing all beams are arranged perfectly horizontally, and hence a lateral compressive load results on the specimen placed at the center of the frame. Due to the different distances from the pin to the outer weighting point and from the pin to the inner loading point, a load magnification of 17

to 1 is obtained from load calibration with an electronic load cell. This loading ratio is also used to determine the lateral deformation of the specimen by monitoring the vertical movement of the two steel bars below. The maximum lateral load is designed for 100 kN. The axial load is applied by a 1000-kN hydraulic load cell. The load frame can accommodate specimen sizes from $2.5 \times 2.5 \times 2.5 \text{ cm}^3$ to $10 \times 10 \times 20 \text{ cm}^3$. The different specimen sizes and shapes can be tested by adjusting the distances between the opposite loading platens. Note that virtually all true triaxial and polyaxial cells previously developed elsewhere can test rock samples with the maximum size not larger than $5 \times 5 \times 10 \text{ cm}^3$. σ_1 is obtained from the maximum stresses failure. σ_2 and σ_3 are obtained from calibration by load cell. Figure 4.4 plots the calibrated curves for use in polyaxial compression test. F is load on the rock sample (kN). W is weight on the lower bars (kN).

4.3 Test method

The prepared rock specimen has a nominal dimension of $5 \times 5 \times 10 \text{ cm}^3$. The test produce can be described as follows:

- Use neoprene sheet on six sides of rock specimen.
- Connect hydraulic pump with hydraulic cylinder and check level of oil in the pump.

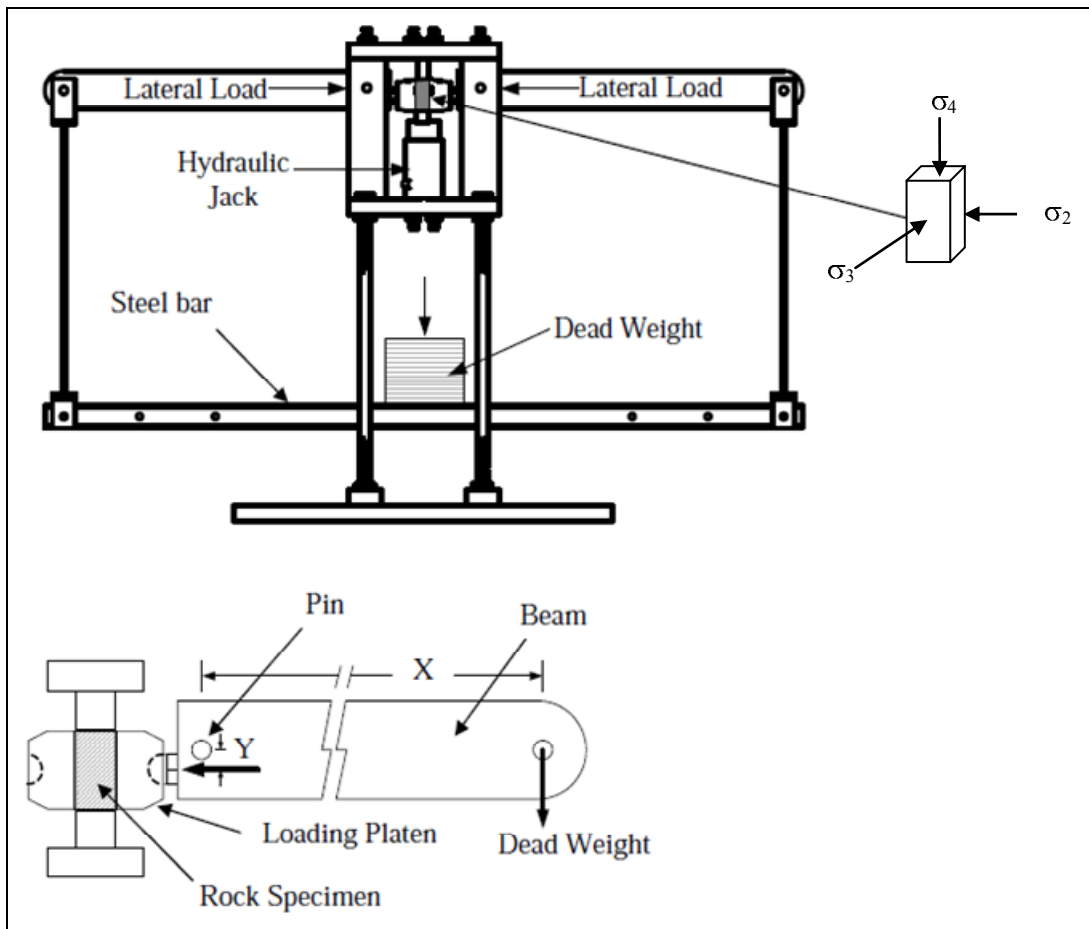


Figure 4.3 Cantilever beam weighed at outer end applies lateral stress to the rock specimen (Walsri et al., 2009).

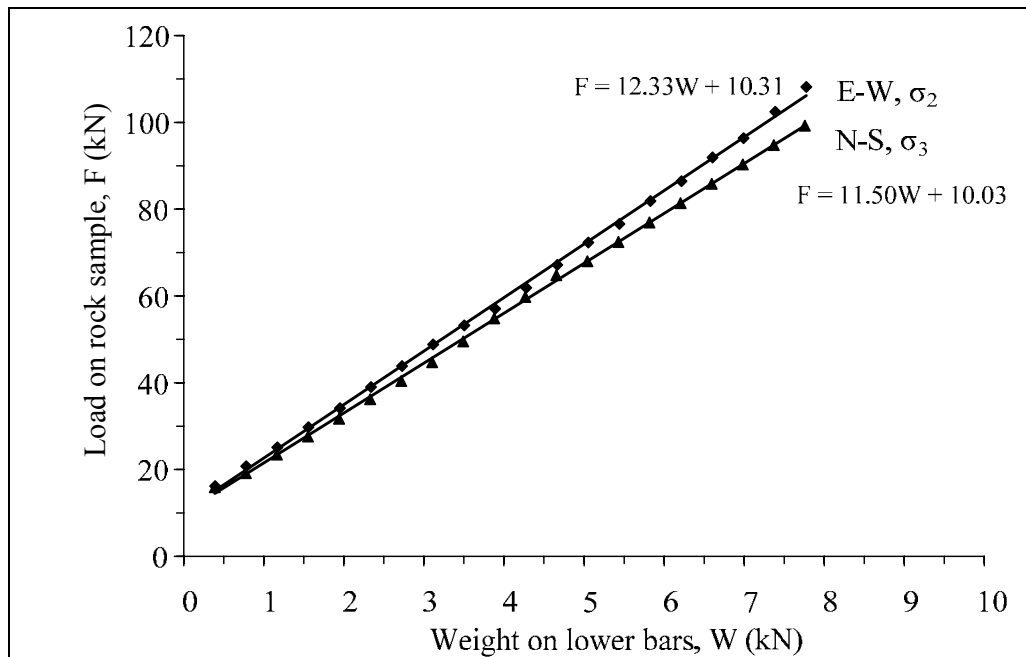


Figure 4.4 Calibrated curves for use in polyaxial compression testing.

- The rock specimen with neoprene is placed on the loading platen.
- The lateral loading platens contact the sides of specimen.
- Raise the cantilever beam in N–S direction.
- Place the rock specimen with neoprene and lateral loading platen into the polyaxial load frame.
- Lateral loading platens must be straight with half spherical bolt.
- Slowly reduce the level of cantilever beam until half spherical bolts and lateral loading platen are in contact.
- Raise the cantilever beam in W–E direction.
- Place the lateral loading platens on the sides of specimen.
- Slowly reduce level of the cantilever beam.
- Place the loading platens on top and bottom of the specimen.

- Increase oil pressure using hydraulic pump until specimen, loading platens and upper steel plates are in contact.
- Put a steel plate (dead weight) on the middle of each beam to increase lateral load.
- Axial load and lateral load must be increased simultaneously up to pre-set pressure so that rock specimen will be in hydrostatic condition.
- Install dial gages in monitoring directions.

4.4 Test results

This section describes test results in terms of strength and elasticity. The measured sample deformations are used to determine the strains along the principal axes during loading. The failure stresses are recorded and mode of failure examined. Appendix A shows the stress-strain curves from the start of loading to failure for the salt specimens in true triaxial stress states.

4.4.1 Strength results

Table 4.1 summarizes the strengths with respect to the orientation of the true triaxial compression stresses. Figure 4.5 plots σ_1 at failure as a function of σ_2 tested under various σ_3 for salt. The results show the effects of the intermediate principal stress, σ_2 , on the maximum stresses at failure by the failure envelopes being offset from the condition where $\sigma_2 = \sigma_3$. For all minimum principal stress levels, σ_1 at failure increases with σ_2 . The effect of σ_2 tends to be more pronounced under a greater σ_3 . These observations agree with those obtained elsewhere (e.g. Haimson and Chang, 2000; Colmenares and Zoback, 2002; Haimson, 2006). The modes of failure were observed from the post-test specimens, and photographs were taken (Figure 4.6).

The observed splitting tensile fractures under relatively high σ_2 suggest that the fracture initiation has no influence from the friction at the loading interface in the σ_2 direction. As a result the increase of σ_1 with σ_2 should not be due to the interface friction.

Figures 4.7 (results of triaxial compressive strength from polyaxial compressive strength tests in terms of Mohr's circles and Coulomb criterion) shows the Mohr circles of the results with shear stress as ordinates and normal stress as abscissas.

Table 4.1 Summary of the strength results on salt specimen of true triaxial compression tests.

Specimen number	Depth (m)	Failure Stresses		
		σ_3 (MPa)	σ_2 (MPa)	σ_1 (MPa)
MS-PX-56	253.75-253.85	0	0	23.0
MS-PX-7	179.66-179.77		10.0	36.2
MS-PX-55	208.40-208.50		25.0	43.1
MS-PX-42	211.60-211.70		35.1	35.1
MS-PX-20	244.47-244.57	1	1.0	26.5
MS-PX-22	246.21-246.31		7.0	43.2
MS-PX-23	245.50-245.60		14.0	56.1
MS-PX-54	208.50-208.60		25.0	60.4
MS-PX-44	210.05-219.15		35.0	62.5
MS-PX-38	211.20-211.30		49.3	49.3
MS-PX-61	178.13-178.23	3	3.0	45.1
MS-PX-53	208.60-208.70		7.0	55.0
MS-PX-52	254.05-254.15		10.0	61.0
MS-PX-5	256.43-256.53		14.0	66.0
MS-PX-57	201.70-201.80		25.0	71.5
MS-PX-35	200.45-200.56		40.0	75.0
MS-PX-43	209.95-210.05		50.0	74.9
MS-PX-40	211.40-211.50		64.9	64.9
MS-PX-27	264.41-264.51	5	5.0	58.6
MS-PX-28	263.31-263.41		14.0	71.2
MS-PX-29	264.67-264.77		21.0	79.2
MS-PX-47	210.35-210.45		30.0	87.4
MS-PX-41	211.50-211.60		40.0	91.6
MS-PX-48	210.45-210.55		50.0	89.3
MS-PX-45	210.15-210.25		65.0	85.0
MS-PX-49	210.55-210.65		79.6	79.6
MS-PX-12	201.23-201.33		7	7.0
MS-PX-13	201.60-201.70	14.0		78.1
MS-PX-19	244.37-244.47	24.0		92.4
MS-PX-25	245.10-245.20	40.0		106.4
MS-PX-50	210.65-210.75	50.0		110.7
MS-PX-46	210.25-210.35	65.0		109.5
MS-PX-10	179.93-180.31	10	10.0	79.6
MS-PX-58	251.79-250.85	12	12.0	81.8
MS-PX-59	212.11-212.21	20	20.0	106.4
MS-PX-60	243.71-243.81	28	28.0	119.7

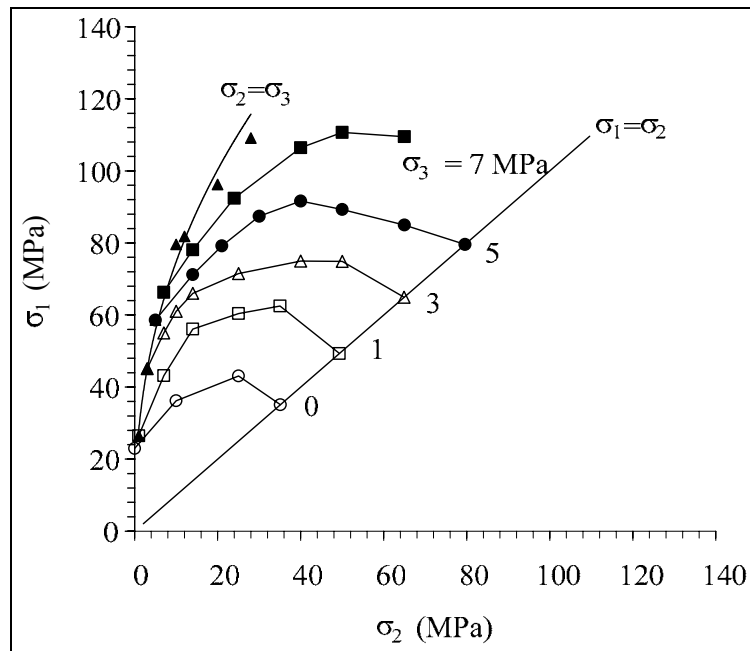


Figure 4.5 Major principal stress (σ_1) at failure as a function of σ_2 for various σ_3 values.

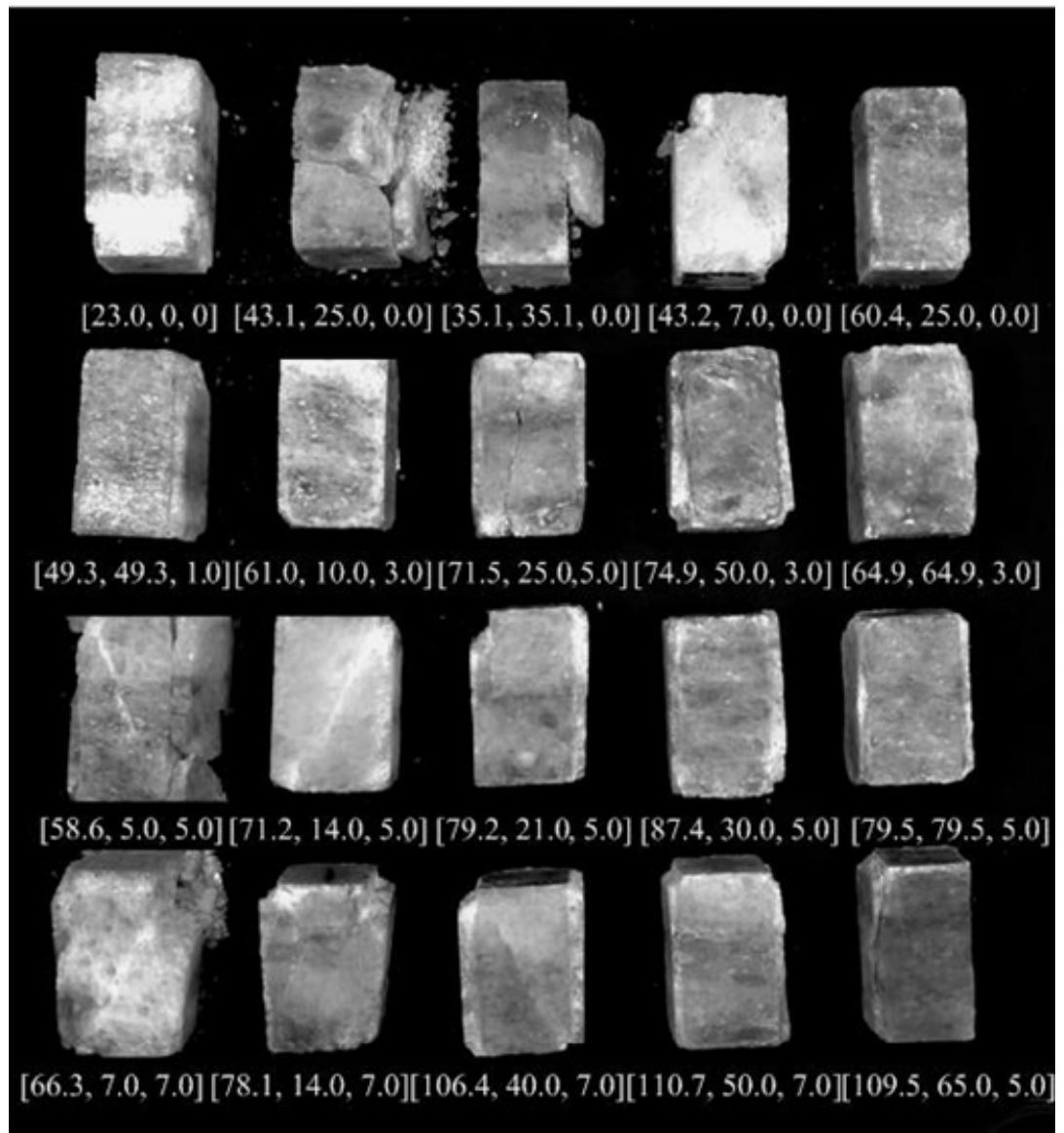


Figure 4.6 Some post-test specimens. Numbers in blankets indicate $[\sigma_1, \sigma_2, \sigma_3]$ at failure.

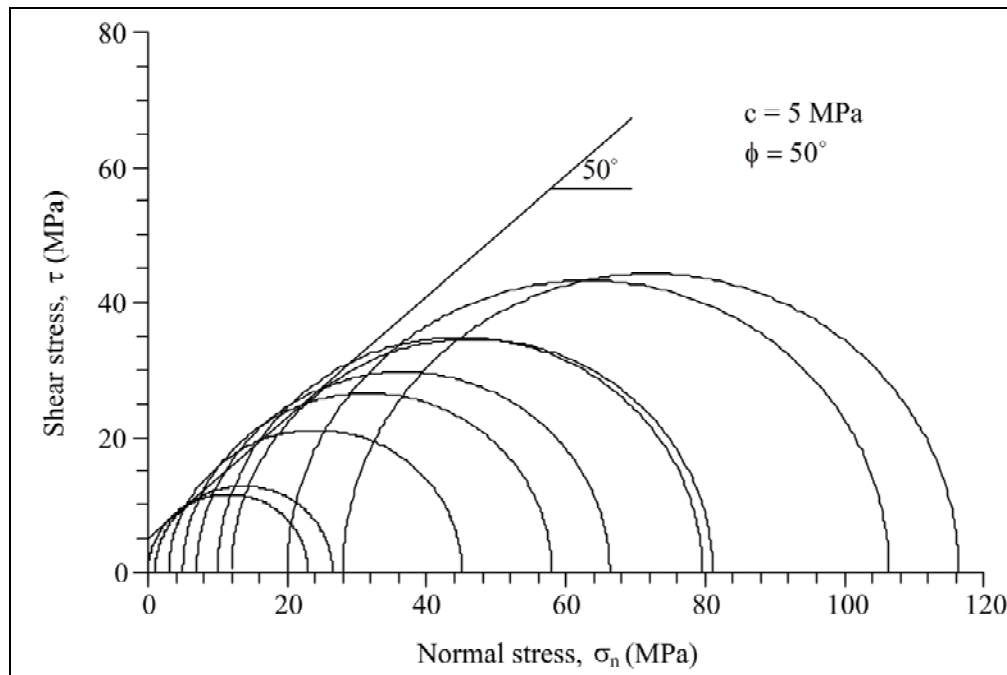


Figure 4.7 Results of triaxial compressive strength from polyaxial compressive strength tests in terms of Mohr's circles and Coulomb criterion.

The relationship can be represented by the Coulomb criterion;

$$\tau = c + \sigma_n \tan \phi \quad (4.1)$$

where τ is the shear stress, c is the cohesion, σ_n is the normal stress and ϕ is the angle of internal friction. The friction angle = 50° and the cohesion = 5 MPa.

4.4.2 Elastic parameter

The elastic parameters are calculated for the three-dimensional principal stress-strain relations, given by Jaeger and Cook (1979). The relation can be simplified to obtain a set of governing equations for an isotropic material as follows:

$$G = (1/2) (\tau_{\text{oct},e} / \gamma_{\text{oct},e}) \quad (4.2)$$

$$3\sigma_{m,e} = (3\lambda + 2G) \Delta \quad (4.3)$$

$$E = 2G (1 + \nu) \quad (4.4)$$

$$\nu = \lambda / 2(\lambda + G) \quad (4.5)$$

where $\tau_{\text{oct},e}$, $\gamma_{\text{oct},e}$, $\sigma_{m,e}$ and Δ are octahedral shear stress and strain, mean stress, and volumetric strain at the point where the elastic parameters are determined.

Table 4.2 summarizes these stress and strain values and their corresponding elastic parameters. The calculations of Elastic parameter are made at 30-40% of the maximum principal stress are shown in Table 4.3.

Table 4.2 Summarizes these stress and strain values and their corresponding elastic parameters.

Specimen number	Failure Stresses			$\sigma_{m,e}$ (MPa)	$\tau_{oct,e}$ (MPa)	$\gamma_{oct,e}$ ($\times 10^{-3}$)	Δ ($\times 10^{-3}$)
	σ_3 (MPa)	σ_2 (MPa)	σ_1 (MPa)				
56	0	0	23	16.3	10.8	0.75	0.72
7		10.0	36.2	25.7	15.3	0.89	0.91
55		25.0	43.1	30.6	17.7	1.08	1.25
42		35.1	35.1	-	-	-	-
20	1	1.0	26.5	18.8	12	0.61	0.62
22		7.0	43.2	30.7	18.9	1.25	1.51
23		14.0	56.1	39.8	23.8	1.42	1.43
54		25.0	60.4	42.9	24.8	1.45	1.64
44		35.0	62.5	-	-	-	-
38		49.3	49.3	-	-	-	-
61	3	3.0	45.1	32.0	19.8	1.32	1.48
53		7.0	55.0	39.1	24.4	1.70	1.74
52		10.0	61.0	43.3	26.7	1.78	1.73
5		14.0	66.0	46.9	28.4	1.96	2.07
57		25.0	71.5	50.8	29.6	1.61	1.71
35		40.0	75.0	53.3	30.6	1.93	2.06
43		50.0	74.9	-	-	-	-
40		64.9	64.9	-	-	-	-
27	5	5.0	58.6	41.6	25.3	1.65	1.90
28		14.0	71.2	50.6	30.8	1.93	1.93
29		21.0	79.2	56.2	33.5	2.10	2.12
47		30.0	87.4	62.1	36.3	2.02	2.08
41		40.0	91.6	-	-	-	-
48		50.0	89.3	63.4	36.5	2.39	2.62
45		65.0	85.0	-	-	-	-
49		79.6	79.6	56.5	37.5	2.79	2.81
12	7	7.0	66.3	47.1	28	2.31	2.49
13		14.0	78.1	55.5	34	1.88	1.83
19		24.0	92.4	65.6	39.1	2.59	2.81
25		40.0	106.4	-	-	-	-
50		50.0	110.7	78.6	45.3	2.71	3.01
46		65.0	109.5	-	-	-	-
10	10	10.0	79.6	56.5	32.8	1.98	2.05
58	12	12.0	81.8	58.1	32.9	1.51	1.64
59	20	20.0	106.4	75.5	40.7	2.65	2.96
60	28	28.0	119.7	85.0	43.2	2.41	2.92

Remark : - is not calculated because $\sigma_1=\sigma_2$, $\sigma_2=\sigma_3$ and not measured.

Table 4.3 Elastic parameters obtained from true triaxial testing.

Specimen number	G (GPa)	λ (GPa)	E (GPa)	ν
MS-PX-56	7.25	2.72	20.3	0.40
MS-PX-7	8.59	3.71	21.8	0.27
MS-PX-55	8.20	2.70	23.3	0.42
MS-PX-20	9.87	3.61	27.7	0.40
MS-PX-22	7.57	1.73	22.0	0.45
MS-PX-23	8.40	3.70	21.6	0.28
MS-PX-54	8.55	3.01	24.1	0.41
MS-PX-61	7.47	2.24	21.4	0.43
MS-PX-53	7.18	2.68	20.1	0.40
MS-PX-52	7.52	3.36	19.9	0.33
MS-PX-5	7.25	2.72	20.3	0.40
MS-PX-57	9.20	3.74	25.4	0.38
MS-PX-35	7.92	3.31	21.7	0.37
MS-PX-27	7.65	2.19	22.0	0.44
MS-PX-28	7.97	3.43	20.2	0.27
MS-PX-29	7.96	3.53	20.6	0.29
MS-PX-47	9.00	3.93	24.3	0.35
MS-PX-48	7.63	2.98	21.2	0.39
MS-PX-49	6.73	2.21	19.1	0.42
MS-PX-12	6.06	2.26	17.0	0.40
MS-PX-13	9.05	4.05	23.7	0.31
MS-PX-19	7.56	2.75	21.2	0.40
MS-PX-50	8.36	3.12	23.4	0.40
MS-PX-10	8.29	3.66	21.4	0.29
MS-PX-58	10.9	4.57	29.9	0.37
MS-PX-59	7.67	3.39	20.5	0.34
MS-PX-60	9.33	3.48	26.1	0.40
Mean \pm Standard Deviation	8.12 \pm 1.01	3.14\pm0.67	22.2 \pm 2.74	0.37 \pm 0.05

CHAPTER V

ASSESSMENT OF THE STRENGTH CRITERIA

5.1 Introduction

This chapter describes the strength analysis and compressive failure criteria under true triaxial compression. The strength criteria used in this study include the Coulomb, Drucker-Prager, modified Lade, modified Weibols and Cook, Hoek and Brown, and the empirical Mogi criteria. The principal stresses at failure can be incorporated to the strength criteria. The mean misfit (\bar{s}) is determined for each criterion.

5.2 Coulomb criterion

The second order stress invariant ($J_2^{1/2}$) and the first order stress invariant or the mean stress (σ_m) is calculated from the test results by the following relations (Jaeger and Cook, 1979):

$$J_2^{1/2} = \sqrt{(1/6)\{(\sigma_1 - \sigma_2)^2 + (\sigma_1 - \sigma_3)^2 + (\sigma_2 - \sigma_3)^2\}} \quad (5.1)$$

$$\sigma_m = (\sigma_1 + \sigma_2 + \sigma_3)/3 \quad (5.2)$$

The Coulomb criterion in from of J_2 and J_1 can be expressed as (Jaeger and Cook, 1979):

$$J_2^{1/2} = \frac{2}{\sqrt{3}} [\sigma_m \sin \phi + c \cdot \cos \phi] \quad (5.3)$$

The Coulomb criterion can also be expressed in terms of the major and minor effective principal stresses, σ_1 and σ_3 written as (Jaeger and Cook, 2007):

$$\sigma_1 = \sigma_c + \tan^2(\pi/4 + \phi/2)\sigma_3 \quad (5.4)$$

where ϕ is friction angle, c is cohesion, σ_m is mean stress and $J_2^{1/2}$ is the second order of stress invariant, σ_1 is the major principal effective stress at failure, σ_3 is the least principal effective stress at failure, σ_c is the uniaxial compressive strength. Based on the Coulomb criterion the internal friction angle from the triaxial loading condition ($\sigma_2 = \sigma_3$) is calculated as 50° , and the cohesion as 5 MPa. Table 5.1 shows the results of the strengths calculation in terms of $J_2^{1/2}$ and σ_m for salt. Figures 5.1 compares the polyaxial test results with those predicted by the Coulomb criterion. The predictions are made for $\sigma_3 = 0, 1, 3, 5$ and 7 MPa. (as used in the tests) and under stress conditions from $\sigma_2 = \sigma_3$ to $\sigma_2 > \sigma_3$. In the $J_2^{1/2} - \sigma_m$ diagram, $J_2^{1/2}$ increases with σ_3 but it is independent of σ_m because the Coulomb criterion ignores σ_2 in the strength calculation. Under low σ_2 and σ_3 the Coulomb prediction tends to agree with the test results obtained from the MS salt. Except for this case, no correlation between the Coulomb predictions and the polyaxial strengths can be found. The inadequacy of the predictability of Coulomb criterion under polyaxial stress states obtained here agrees with a conclusion drawn by Colmenares and Zoback (2002).

5.3 Modified Wiebols and Cook criteria

The modified Wiebols and Cook criterion given by Colmenares and Zoback (2002) defines $J_2^{1/2}$ at failure in terms of J_1 as:

$$J_2^{1/2} = A + BJ_1 + CJ_1^2 \quad (5.5)$$

The modified Wiebols and Cook criterion can also be expressed in terms of the principal stresses as:

$$\sigma_1 = \left[\frac{6(\psi - \chi) - 3(A + B\sigma_m)}{C\sigma_m} \right] - (\sigma_2 + \sigma_3) \quad (5.6)$$

where $\psi = (\sigma_1^2 + \sigma_2^2 + \sigma_3^2)$

$$\chi = (\sigma_1\sigma_2 + \sigma_1\sigma_3 + \sigma_2\sigma_3)$$

$$\sigma_m = (\sigma_1 + \sigma_2 + \sigma_3)/3$$

where σ_1 is maximum principal stress, σ_2 is intermediate principal stress, σ_3 is minimum principal stress. The constants A, B and C depend on rock materials and the minimum principal stresses (σ_3). They can be determined under the conditions where $\sigma_2 = \sigma_3$, as follows (Colmenares and Zoback, 2002):

$$C = \frac{\sqrt{27}}{2C_1 + (q-1)\sigma_3 - \sigma_c} \times \left(\frac{C_1 + (q-1)\sigma_3 - \sigma_c}{2C_1 + (2q+1)\sigma_3 - \sigma_c} - \frac{q-1}{q+2} \right) \quad (5.7)$$

where: $C_1 = (1 + 0.6\mu_i)\sigma_c$

σ_c = uniaxial compressive strength of the rock

$$\mu_i = \tan\phi$$

$$q = \{(\mu_i^2 + 1)^{1/2} + \mu_i\}^2 = \tan^2(\pi/4 + \phi/2)$$

$$B = \frac{\sqrt{3}(q-1)}{q+2} - \frac{C}{3}(2\sigma_c + (q+2)\sigma_3) \quad (5.8)$$

$$A = \frac{\sigma_c}{\sqrt{3}} - \frac{\sigma_c}{3}B - \frac{\sigma_c^2}{9}C \quad (5.9)$$

The numerical values of A, B and C for rock salt are given in Table 5.2 for each σ_3 tested. Substituting these constants into equation (5.4), the upper and lower limits of $J_2^{1/2}$ for each rock type can be defined under conditions where $\sigma_2 = \sigma_3$ and $\sigma_1 = \sigma_2$. The predictions are made for $\sigma_3 = 0, 1, 3, 5$ and 7 . Figure 5.2 compares the test results with those predicted by the modified Wiebols and Cook criterion. The predictions agree well with the test results. This conforms to the results obtained by Colmenares and Zoback (2002). The predictive capability of the modified Wiebols and Cook criterion can be improved as the minimum principal stress increases.

Table 5.1 Strength calculation in terms of $J_2^{1/2}$ and σ_m .

Specimen number	Failure Stresses			σ_m (MPa)	$J_2^{1/2}$ (MPa)
	σ_3 (MPa)	σ_2 (MPa)	σ_1 (MPa)		
MS-PX-56	0	0.0	5.4	7.7	10.8
MS-PX-7		10.0	7.6	15.4	15.3
MS-PX-55		25.0	8.8	22.7	17.7
MS-PX-42		35.1	8.3	23.4	16.5
MS-PX-20	1	1.0	6.0	9.5	12.0
MS-PX-22		7.0	9.5	16.7	18.9
MS-PX-33		14.0	11.9	23.4	23.8
MS-PX-54		25.0	12.4	28.5	24.8
MS-PX-44		35.0	12.8	32.5	25.6
MS-PX-38		49.3	11.6	32.9	23.2
MS-PX-61	3	3.0	9.9	17.0	19.8
MS-PX-53		7.0	12.2	20.7	24.4
MS-PX-52		10.0	13.4	23.7	26.7
MS-PX-5		14.0	14.2	26.7	28.4
MS-PX-57		25.0	14.8	32.2	29.6
MS-PX-35		40.0	15.3	38.3	30.6
MS-PX-43		50.0	15.6	41.6	31.1
MS-PX-40		64.9	15.3	43.3	30.6
MS-PX-27	5	5.0	12.6	22.9	25.3
MS-PX-28		14.0	15.4	28.4	30.8
MS-PX-29		21.0	16.8	33.4	33.5
MS-PX-47		30.0	18.1	39.1	36.3
MS-PX-41		40.0	18.7	43.9	37.5
MS-PX-48		50.0	18.3	46.4	36.5
MS-PX-45		65.0	18.1	50.0	36.3
MS-PX-49		79.6	18.8	53.1	37.5
MS-PX-12	7	7.0	14.0	26.8	28.0
MS-PX-13		14.0	17.0	30.7	34.0
MS-PX-19		24.0	19.6	38.8	39.1
MS-PX-25		40.0	21.9	48.8	43.9
MS-PX-50		50.0	22.6	53.6	45.3
MS-PX-46		65.0	22.5	58.2	45.0
MS-PX-10	10	10.0	16.4	33.2	28.9
MS-PX-58	12	12	16.5	35.3	29.0
MS-PX-59	20	20	20.4	48.8	35.9
MS-PX-60	28	28	21.6	58.6	38.1

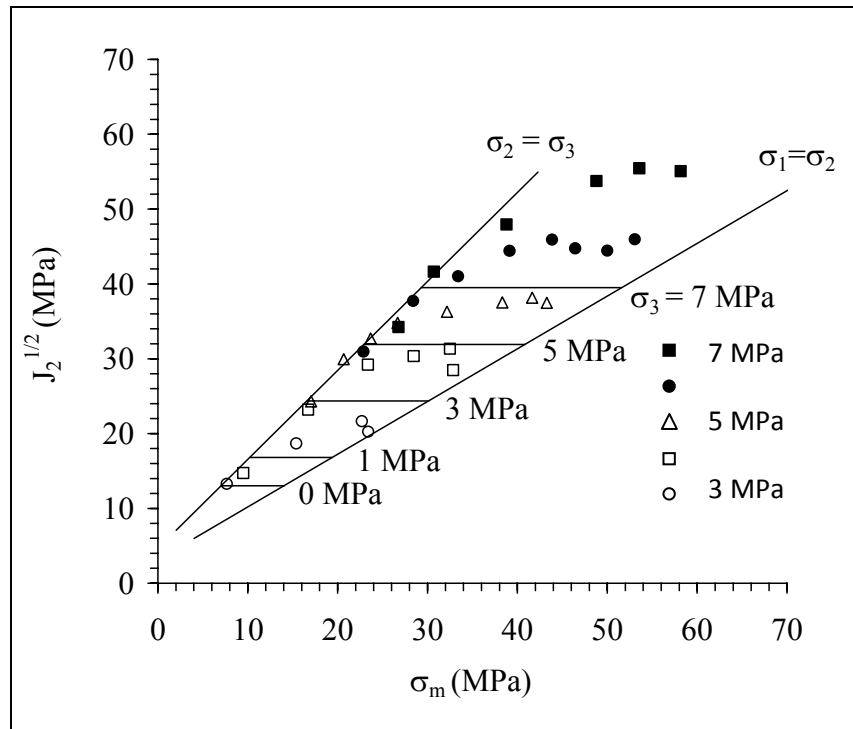


Figure 5.1 $J_2^{1/2}$ as a function of σ_m from testing rock salt compared with the Coulomb criterion predictions (lines).

5.4 Modified Lade criterion

The modified Lade criterion is developed by Ewy (1999) by modifying the criterion of Lade and Duncan (1975). The criterion is written as as:

$$(I_1')^3/I_3' = 27 + \eta \quad (5.10)$$

where: $I_1' = (\sigma_1 + S) + (\sigma_2 + S) + (\sigma_3 + S)$

$$I_3' = (\sigma_1 + S)(\sigma_2 + S)(\sigma_3 + S)$$

where S and η are material constants. The parameter S is related to the cohesion of the rock, while the parameter η represents the internal friction. These parameters can be derived directly from the Mohr–Coulomb cohesion (c) and internal friction angle (ϕ) by:

$$\text{where: } S = S_0 / \tan \phi$$

$$\eta = 4(\tan \phi)^2 (9 - 7 \sin \phi) / (1 - \sin \phi)$$

$$S_0 = \sigma_c / (2q^{1/2})$$

$$q = \{(\mu_i^2 + 1)^{1/2} + \mu_i\}^2 = \tan^2(\pi/4 + \phi/2)$$

Figure 5.3 compares the polyaxial test results with those predicted by the modified Lade criterion. The predictions are made for $\sigma_3 = 0, 1, 3, 5$ and 7 MPa. The predictions can describe the effect of the intermediate principal stress on the test results. The modified Lade criterion overestimates the strengths at all levels of σ_3 .

Table 5.2 Modified Wiebols and Cook parameters for rock salt.

σ_3 (MPa)	Parameters		
	C (MPa ⁻¹)	B	A (MPa)
0	-0.036	1.746	2.031
1	-0.030	1.739	1.698
3	-0.022	1.733	1.281
5	-0.017	1.732	1.027
7	-0.014	1.732	0.853

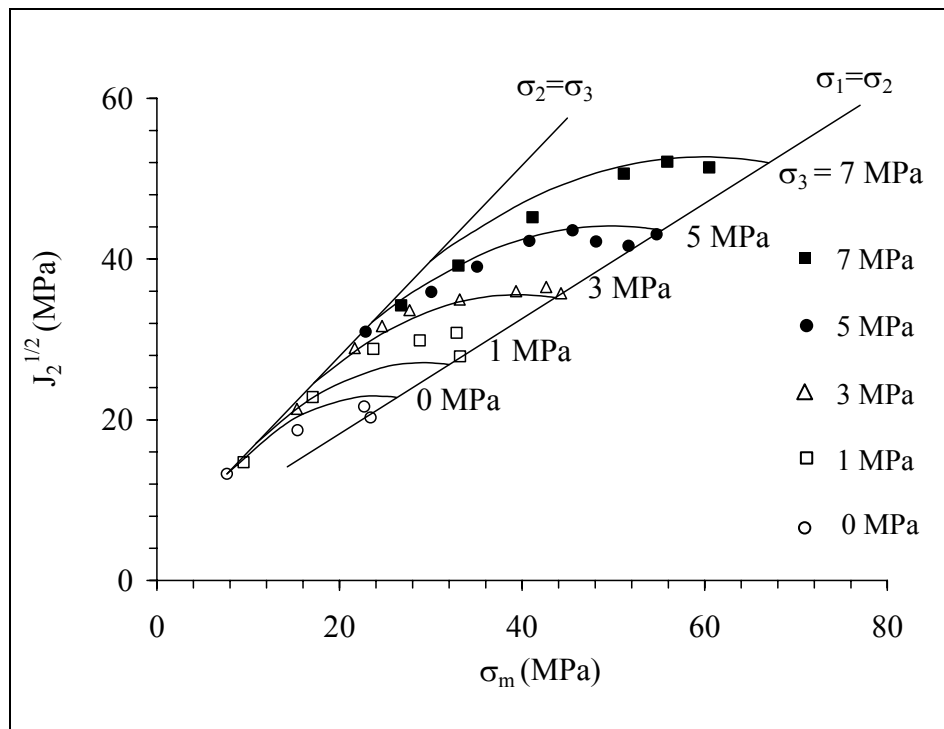


Figure 5.2 $J_2^{1/2}$ as a function of σ_m from testing rock salt compared with the modified Wiebols & Cook criterion predictions (lines).

5.5 Mogi empirical 1971

The mogi 1971 is a generalization from the von Mises's theory. It is formulated by:

$$\tau_{\text{oct}} = f_1(\sigma_{m,2}) \quad (5.11)$$

where f_1 is a monotonically increasing function. τ_{oct} and $\sigma_{m,2}$ are, respectively, The octahedral shear stress and the effective mean stress. The empirical Mogi criterion uses a power law to describe the failure stresses, defines τ_{oct} at failure in terms of $\sigma_{m,2}$ as:

$$\tau_{\text{oct}} = A' \sigma_{m,2}^{B'} \quad (5.12)$$

$$\tau_{\text{oct}} = \sqrt{(1/3)\{(\sigma_1 - \sigma_2)^2 + (\sigma_1 - \sigma_3)^2 + (\sigma_2 - \sigma_3)^2\}} \quad (5.13)$$

$$\sigma_{m,2} = (\sigma_1 + \sigma_3)/2 \quad (5.14)$$

The constants A' and B' depend on rock materials. Figure 5.4 compares the polyaxial test results with those predicted by the empirical Mogi criterion 1971. The predictions are made for $\sigma_3 = 0, 1, 3, 5$ and 7 MPa. The empirical (power law) Mogi criterion tends to underestimate the salt strengths particularly under high σ_3 values.

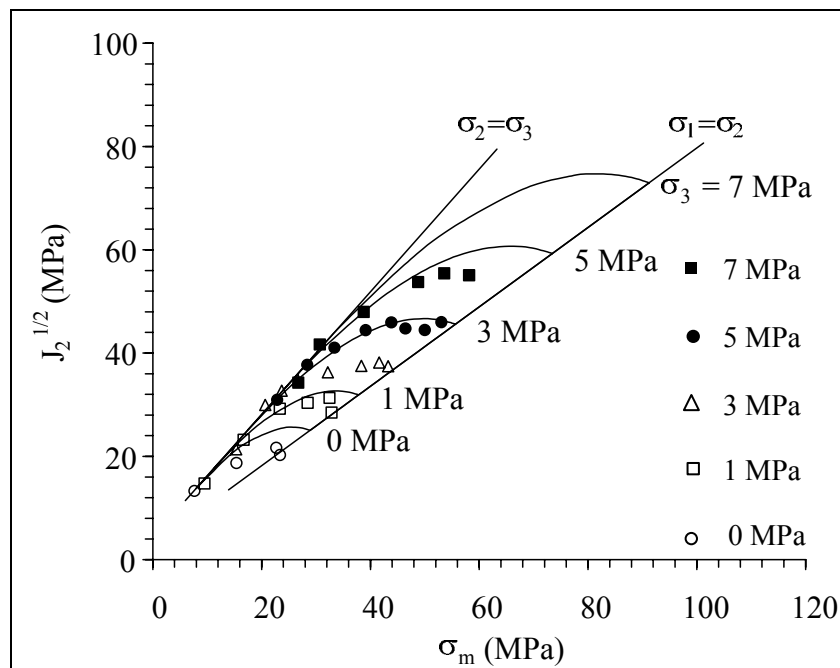


Figure 5.3 $J_2^{1/2}$ as a function of σ_m from testing rock salt compared with the modified Lade criterion predictions (lines).

5.6 Drucker–Prager criterion

The Drucker – Prager criterion given by Drucker – Prager (1952) defines $J_2^{1/2}$ at failure in terms of σ_m as:

$$J_2^{1/2} = \kappa + \alpha \sigma_m \quad (5.15)$$

The Drucker – Prager criterion defines the relationship between the principal stresses:

$$\sigma_1 = \frac{2(\psi - \chi) - \kappa}{\alpha} - (\sigma_2 + \sigma_3) \quad (5.16)$$

where $\psi = (\sigma_1^2 + \sigma_2^2 + \sigma_3^2)$

$$\chi = (\sigma_1\sigma_2 + \sigma_1\sigma_3 + \sigma_2\sigma_3)$$

where σ_1 is maximum principal stress, σ_2 is intermediate principal stress, σ_3 is minimum principal stress, α and κ are material constants. The material parameters α and κ can be determined from the slope and the intercept of the failure envelope plotted in the J_1 and $(J_2)^{1/2}$ space. α is related to the internal friction of the material and κ is related to the cohesion of the material, in this way, the Drucker – Prager criterion can be compared to the Mohr – Coulomb criterion. The Drucker – Prager criterion can be divided in to an outer bound criterion or circumscribed Drucker – Prager and an inner bound criterion or inscribed Drucker – Prager. The set woversions of the Drucker – Prager criterion come from comparing the Drucker – Prager criterion with the Mohr – Coulomb criterion. The inscribed Drucker – Prager criterion is obtained when:

$$\alpha = \frac{3 \sin \phi}{\sqrt{9 + 3 \sin^2 \phi}} \quad (5.17)$$

$$\kappa = \frac{2\sigma_c \cos \phi}{2\sqrt{q}\sqrt{9 + 3 \sin^2 \phi}} \quad (5.18)$$

The Circumscribed Drucker–Prager criterion is obtained when:

$$\alpha = \frac{6 \sin \phi}{\sqrt{3}(3 - \sin \phi)} \quad (5.19)$$

$$\kappa = \frac{\sqrt{3}\sigma_c \cos \phi}{\sqrt{q}(3 - \sin \phi)} \quad (5.20)$$

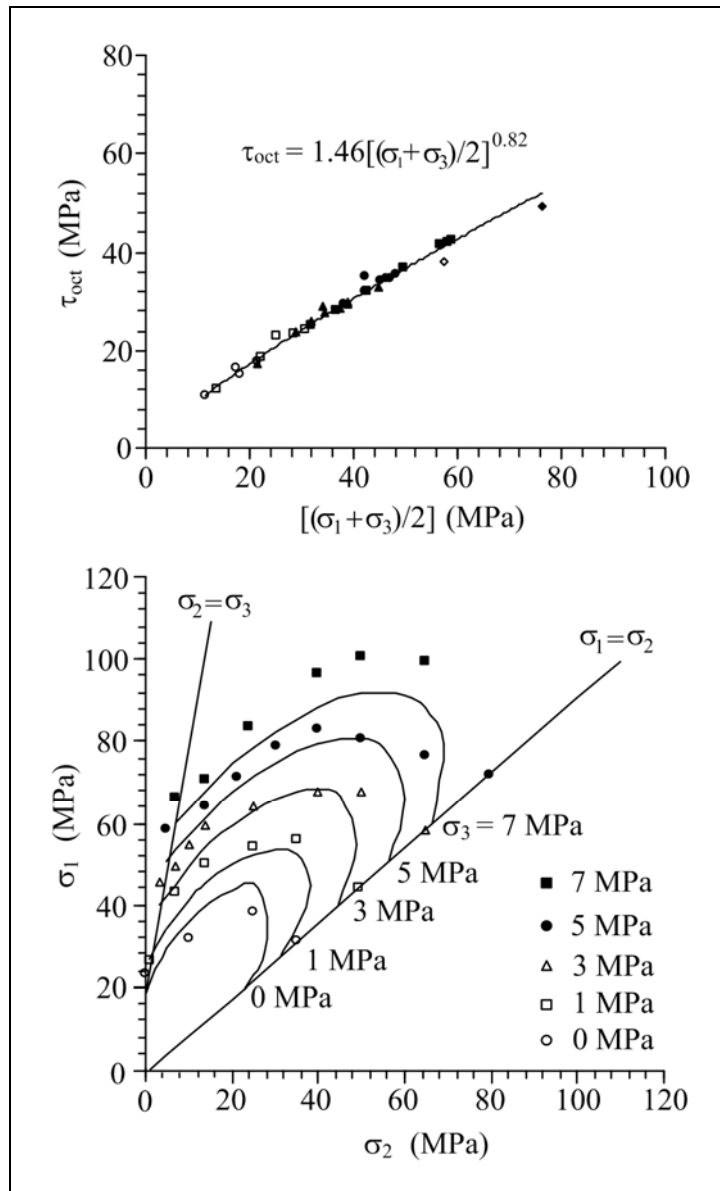


Figure 5.4 Comparisons between the test results with the Mogi empirical 1971.

where ϕ is the angle of internal friction, that is, $\phi = \tan^{-1} \mu_i$. Figure 5.5 compares the polyaxial test results with those predicted by the circumscribed Drucker–Prager criterion. The predictions are made for $\sigma_3 = 0, 1, 3, 5$ and 7 MPa. Both circumscribed and inscribed Drucker–Prager criteria severely underestimate σ_1 at failure for all stress conditions.

5.7 Hoek and Brown criterion

The Hoek and Brown criterion in form of J_2 and $\sigma_{m,2}$ can be expressed as (Hoek and Brown, 1980):

$$J_2^{1/2} = \frac{2}{\sqrt{3}} (\sigma_{m,2}) \quad (5.21)$$

$$\text{where: } \sigma_{m,2} = (\sigma_1 + \sigma_3) / 2 \quad (5.22)$$

The Hoek and Brown criterion defines the relationship between the maximum and minimum stresses (Hoek and Brown, 1980) by:

$$\sigma_1 = \sigma_3 + \sigma_c \sqrt{m' \frac{\sigma_3}{\sigma_c} + s} \quad (5.23)$$

where m and s are constants that depend on the properties of the rock and on the extent to which it had been broken before being subjected to the failure stresses σ_1 and σ_3 . Figure 5.6 compares the polyaxial test results with those predicted by the Hoek and Brown criterion.

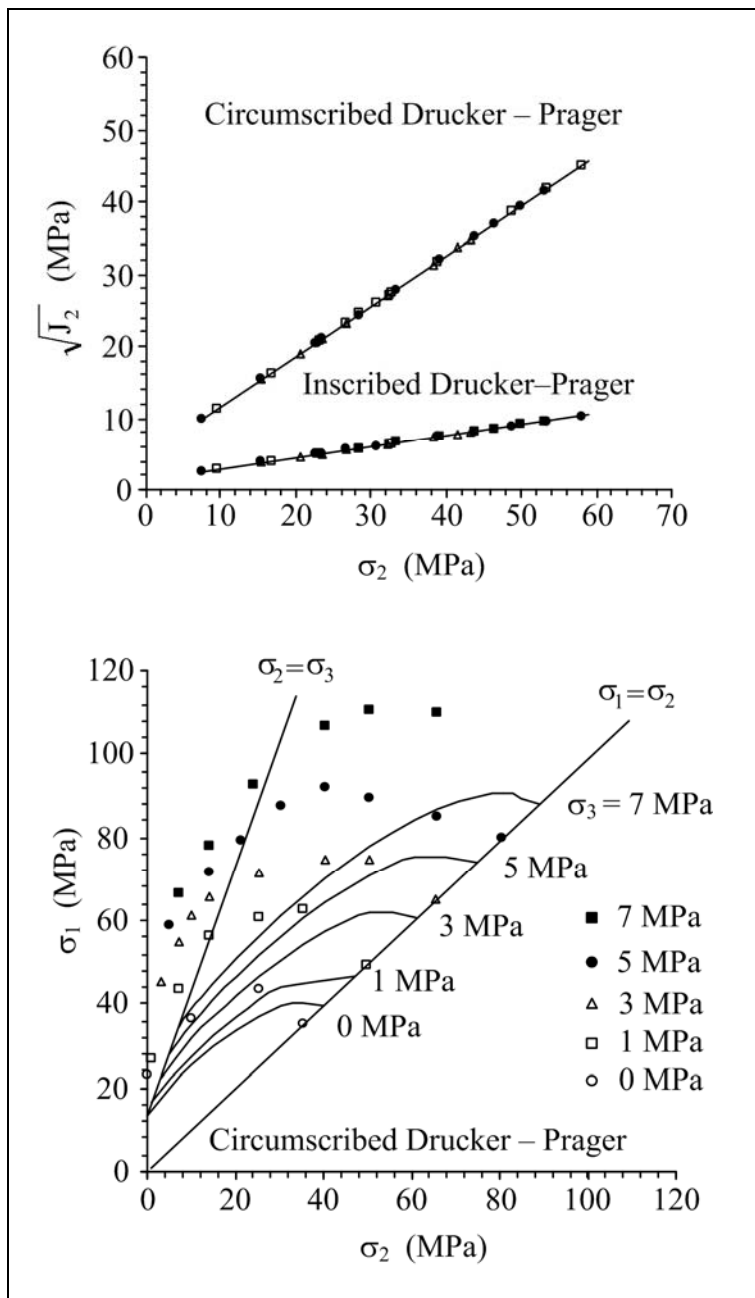


Figure 5.5 Comparisons between the test results with the circumscribed Drucker-Prager criterion.

The predictions are made for $\sigma_3 = 0, 1, 3, 5$ and 7 MPa. and under stress conditions from $\sigma_2 = \sigma_3$ to $\sigma_2 > \sigma_3$. In the $J_2^{1/2} - \sigma_m$ diagram, $J_2^{1/2}$ increases with σ_3 but it is independent of σ_m because the Hoek and Brown criterion ignores σ_2 in the strength calculation. Hoek and Brown criterion can not describe the salt strengths beyond the condition where $\sigma_2 = \sigma_3$, as they can not incorporate the effects of σ_2 . The calculated property parameters of each failure criterion are given in Table 5.3.

Table 5.3 Parameters for each failure criterion.

Criteria	Calibrated parameters
Modified Wiebols and Cook	$\sigma_3 = 0, A = 2.031 \text{ MPa}, B = 1.746,$ $C = -0.036 \text{ MPa}^{-1}$ $\sigma_3 = 1, A = 1.698 \text{ MPa}, B = 1.739,$ $C = -0.030 \text{ MPa}^{-1}$ $\sigma_3 = 3, A = 1.281 \text{ MPa}, B = 1.733,$ $C = -0.022 \text{ MPa}^{-1}$ $\sigma_3 = 5, A = 1.027 \text{ MPa}, B = 1.732,$ $C = -0.017 \text{ MPa}^{-1}$ $\sigma_3 = 7, A = 0.853 \text{ MPa}, B = 1.732,$ $C = -0.014 \text{ MPa}^{-1}$
Mogi 1971	$A' = 1.46$ $B' = 0.82$
Hoek and Brown	$m' = 20.2$ $s = 1$
Modified Lade	$S = 3.66 \text{ MPa}$ $\eta = 88.33$
Coulomb	$\phi = 50$ $c = 5 \text{ MPa}$
Drucker-Prager (Circumscribed)	$\alpha = 0.69$ $\kappa = 4.7 \text{ MPa}$
Drucker-Prager (Inscribed)	$\alpha = 0.15$ $\kappa = 1.38 \text{ MPa}$

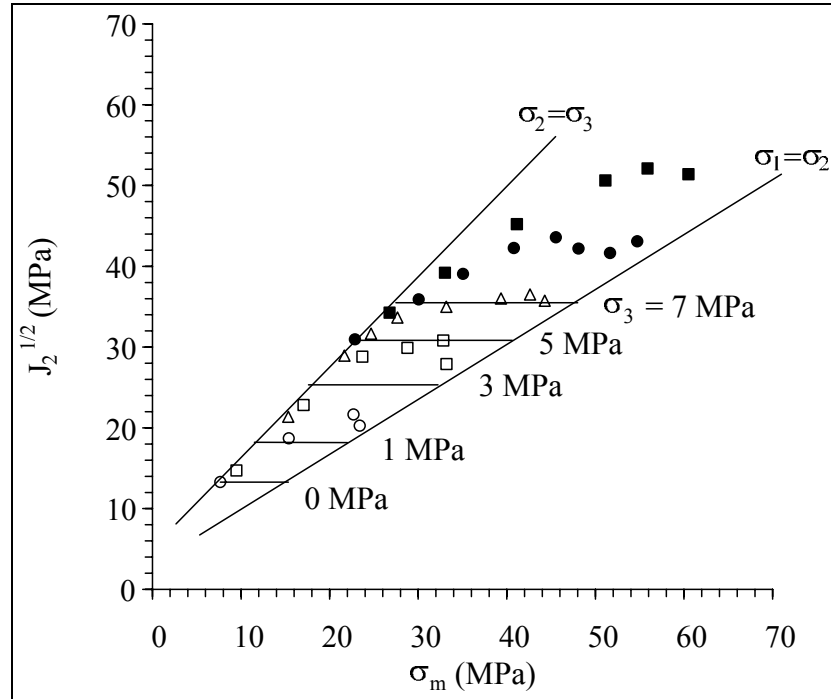


Figure 5.6 $J_2^{1/2}$ as a function of σ_m from testing rock salt compared with the Hoek and Brown criterion predictions (lines).

5.8 Predictability of the strength criteria

The three-dimensional strength criteria are used to compare against the strength data in form of the octahedral shear strength as a function of mean stress, and the major principal stress at failure as a function of the intermediate principal stress. The mean misfit (\bar{s}) is determined for each criterion using an equation (Riley et al., 1998):

$$\bar{s} = \frac{1}{m} \sum_i s_i \quad (5.24)$$

where $s_i = \sqrt{\frac{1}{n} \sum_j (\sigma_{1,j}^{\text{calc}} - \sigma_{1,j}^{\text{test}})^2}$

$\sigma_{1,j}^{\text{calc}}$ = maximum stress predicted from strength criterion

$\sigma_{1,j}^{\text{test}}$ = maximum stress from test data

n = number of data points calculated

m = number of data sets

Table 5.4 describes the calculated mean misfits for each criterion. The effect of σ_2 on the salt strengths can be best described by the modified Wiebols and Cook criterion with the mean misfit = 3.5 MPa. The empirical (power law) Mogi criterion tends to underestimate the salt strengths particularly under high σ_3 values. The modified Lade criterion overestimates the actual strengths at all levels of σ_3 , showing the mean misfit = 15.4 MPa. The Coulomb and Hoek and Brown criteria can not describe the salt strengths beyond the condition where $\sigma_2 = \sigma_3$, as they can not incorporate the effects of σ_2 . Both circumscribed and inscribed Drucker-Prager criteria severely underestimate σ_1 at failure for all stress conditions, showing the largest mean misfit of 19.5 and 34.7 MPa, respectively.

Table 5.4 Mean misfits calculated for each failure criterion.

Strength Criteria	Mean Misfit (MPa)
Modified Wiebols and Cook	3.5
Empirical Mogi	9.6
Hoek and Brown	18.6
Modified Lade	15.4
Coulomb	17.7
Drucker-Prager (Circumscribed)	19.5
Drucker-Prager (Inscribed)	34.7

5.9 Discussions of the test results

The polyaxial loading tests are performed to assess the effect of intermediate principal stress on the MS salt. The results suggest that the intermediate principal stress can affect the maximum stress at failure. Such effect is not linear. The results indicate that the elastic modulus and Poisson's ratio of the MS salt are averaged as 21.5 ± 2.6 GPa and 0.40 ± 0.04 . For the Coulomb criterion, the internal friction angle determined from the triaxial loading condition ($\sigma_2 = \sigma_3$) is 50° , and the cohesion is 5 MPa. The effect of σ_2 on the salt strengths can be best described by the modified Wiebols and Cook criterion. The empirical (power law) Mogi criterion tends to underestimate the salt strengths particularly under high σ_3 values. The modified Lade criterion overestimates at all levels of σ_3 . The Coulomb and Hoek and Brown criteria can not describe the salt strengths beyond the condition where $\sigma_2 = \sigma_3$, as they can not incorporate the effects of σ_2 . Both circumscribed and inscribed Drucker-Prager criteria severely underestimate σ_1 at failure for all stress conditions.

CHAPTER VI

COMPUTER SIMULATIONS

6.1 Introduction

This chapter describes the finite difference analyses using FLAC (Itasca, 1992) to assess the stability of an underground storage cavern in rock salt of the Maha Sarakham. The multi-axial strength criterion, calibrated from the true triaxial strength test results and the conventional approach of using the uniaxial and triaxial strength test data are used to determine the stability conditions of the storage cavern. The computer simulation results are compared against the Coulomb and modified Wiebols and Cook failure criteria. They are selected because the Coulomb criterion has been widely used in actual field applications while the modified Wiebols and Cook criterion has been claimed by many researchers to be one of the best representations of rock strengths under confinements.

6.2 Numerical simulation

A finite element analysis was performed to demonstrate the impact of the intermediated principal stress on the salt behavior around a compressed-air storage cavern subject to the designed minimum storage pressures during retrieval period. Under this condition the minimum cavern pressure (P_{\min}) is reduced to as low as 10% and 20% of the in-situ stress at the casing shoe (above the cavern top), and hence the stress states in the surrounding salt are highly deviatoric. The radial stress is the lowest, representing σ_3 . The axial (vertical) stress is σ_2 , and the tangential stress is the greatest,

representing σ_1 . For this demonstration, the cavern is taken as an upright cylinder with a diameter of 50 m. The top and bottom of the cavern are at 500 m and 700 m depths, shown in Figure 6.1. The cavern configurations and depth represent those designed by the Thai Department of Energy and Suranaree University of Technology for the compressed-air energy storage in the Sakhon Nakhon basin. The project is under site characterization stage. The tentative cavern location is at Maha Sarakham province, northeast of Thailand. The analysis is made in axis symmetry under isothermal condition, and assuming that no nearby underground structure within 1.2 km radius. The elastic modulus and Poisson's ratio for the salt rocks are taken as 21.5 GPa and 0.4, respectively (Sriapai and Fuenkajorn, 2010). Table 6.1 gives summary of the parameters used in numerical simulation.

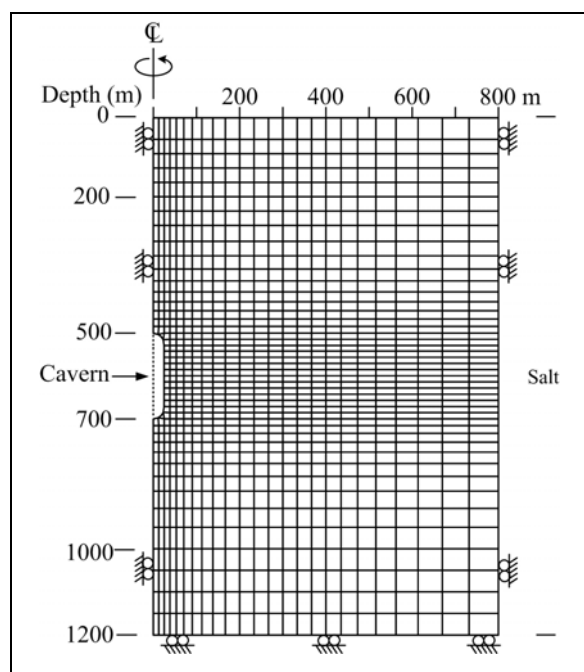


Figure 6.1. Finite difference mesh constructed to simulate a compressed-air storage cavern in the Maha Sarakham salt.

Table 6.1 Material properties and strengths parameter used in FLAC simulations.

Parameters	values
Elastic modulus, E (GPa)	21.5
Possion' ratio, ν	0.4
Friction angle, ϕ (Degree)	50.0
Cohesion, c (MPa)	5.0
Density, ρ (g/cc)	2.2
In-situ stress at casing shoe, σ_{cs} (MPa)	10.8
P_{min} at 20% (MPa)	2.2
P_{min} at 10% (MPa)	1.1

6.3 Results

The FLAC simulations determine the stress distribution assumed the cavern.

The factor of safety (FS) is determined for each criterion by using equations;

6.3.1 Coulomb criterion

The factor of safety is determined by using Coulomb criterion in form of σ_1 which can be expressed as (Jaeger et al, 2007):

$$FS = \sigma_{1,c} / \sigma_{1,f} \quad (6.1)$$

$$\text{where } \sigma_{1,c} = 2S_0 \tan\alpha + \sigma_3 \tan^2\alpha \quad (6.2)$$

$$\alpha = (\pi/4) + (\phi/2)$$

where $\sigma_{1,f}$ is maximum principal stress from FLAC program, σ_3 is minimum principal stress from FLAC program, ϕ is friction angle, S_0 is cohesion.

6.3.2 The modified Wiebols and Cook criterion

The factor of safety (FS) is determined by the modified Wiebols and Cook criterion given by Colmenares and Zoback (2002) defines $J_2^{1/2}$ at failure in terms of J_1 as:

$$FS = J_2^{1/2},c / J_2^{1/2},f \quad (6.3)$$

$$\text{where } J_2^{1/2},c = A + BJ_1 + CJ_1^2 \quad (6.4)$$

$$J_2^{1/2} = \sqrt{(1/6)\{(\sigma_1 - \sigma_2)^2 + (\sigma_1 - \sigma_3)^2 + (\sigma_2 - \sigma_3)^2\}} \quad (6.5)$$

$$J_1 = (\sigma_1 + \sigma_2 + \sigma_3)/3 \quad (6.6)$$

The constants A, B and C depend on rock materials and the minimum principal stresses (σ_3). They can be determined under the conditions where $\sigma_2 = \sigma_3$, as follows (Colmenares and Zoback, 2002):

$$C = \frac{\sqrt{27}}{2C_1 + (q-1)\sigma_3 - C_0} \times \left(\frac{C_1 + (q-1)\sigma_3 - C_0}{2C_1 + (2q+1)\sigma_3 - C_0} - \frac{q-1}{q+2} \right) \quad (6.7)$$

$$\text{where: } C_1 = (1 + 0.6\mu_i)C_0$$

C_0 = uniaxial compressive strength of the rock

$$\mu_i = \tan\phi$$

$$q = \{(\mu_i^2 + 1)^{1/2} + \mu_i\}^2 = \tan^2(\pi/4 + \phi/2)$$

$$B = \frac{\sqrt{3}(q-1)}{q+2} - \frac{C}{3}(2C_0 + (q+2)\sigma_3) \quad (6.8)$$

$$A = \frac{C_0}{\sqrt{3}} - \frac{C_0}{3}B - \frac{C_0^2}{9}C \quad (6.9)$$

For the minimum cavern pressure of 10% σ_{cs} shown in Figure 6.2, the failure at cavern boundary as predicted by modified Wiebols and Cook failure criteria are more appropriated when compared with the Coulomb failure criterion. This is because the modified Wiebols and Cook criteria are developed from true triaxial test results, and hence, they can predict the stability condition more realistic and conservative than the Coulomb criterion. When the cavern pressure is reduced to 20% σ_{cs} no failure occurs around the cavern, as shown in Figure 6.3.

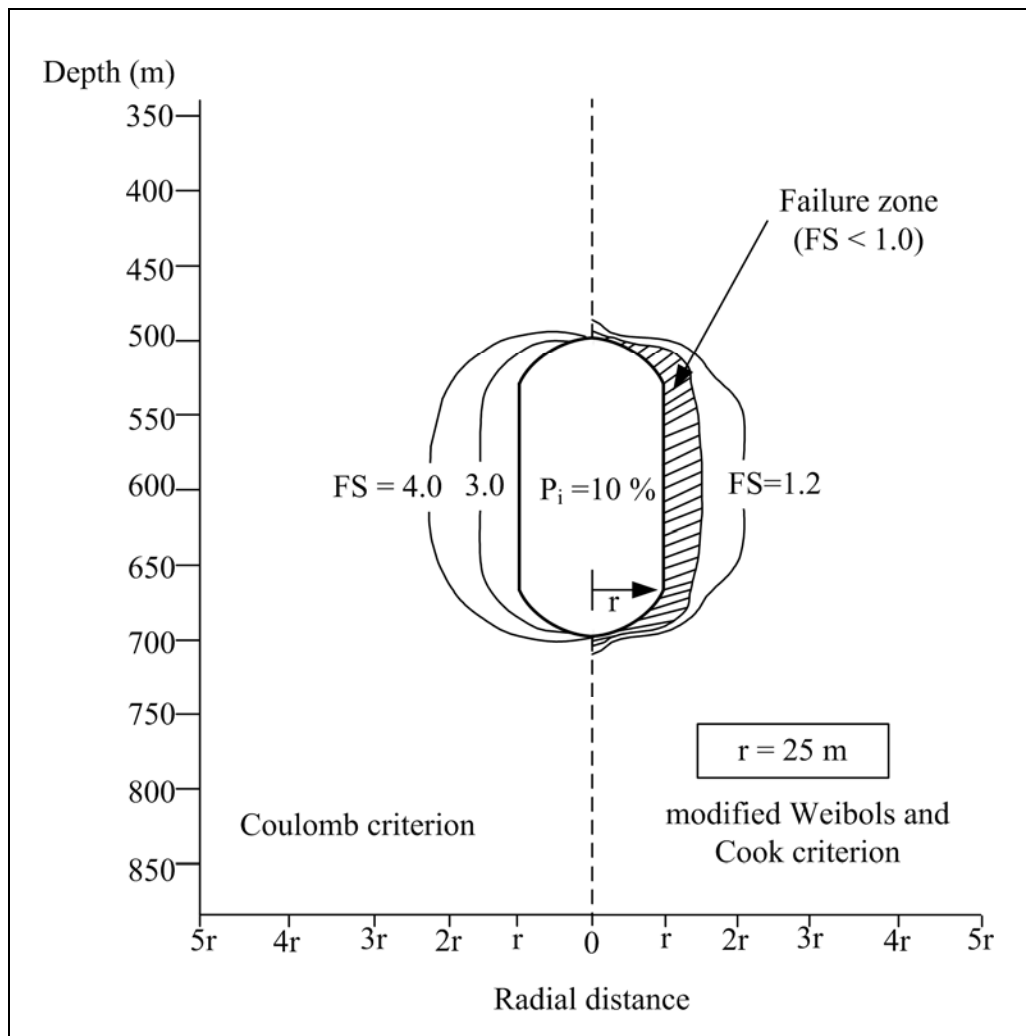


Figure 6.2 Contours of factor of safety calculated from the Coulomb and modified Wiebols and Cook criteria for $P_{\min} = 10\% \sigma_{cs}$, $r = 25$ m.

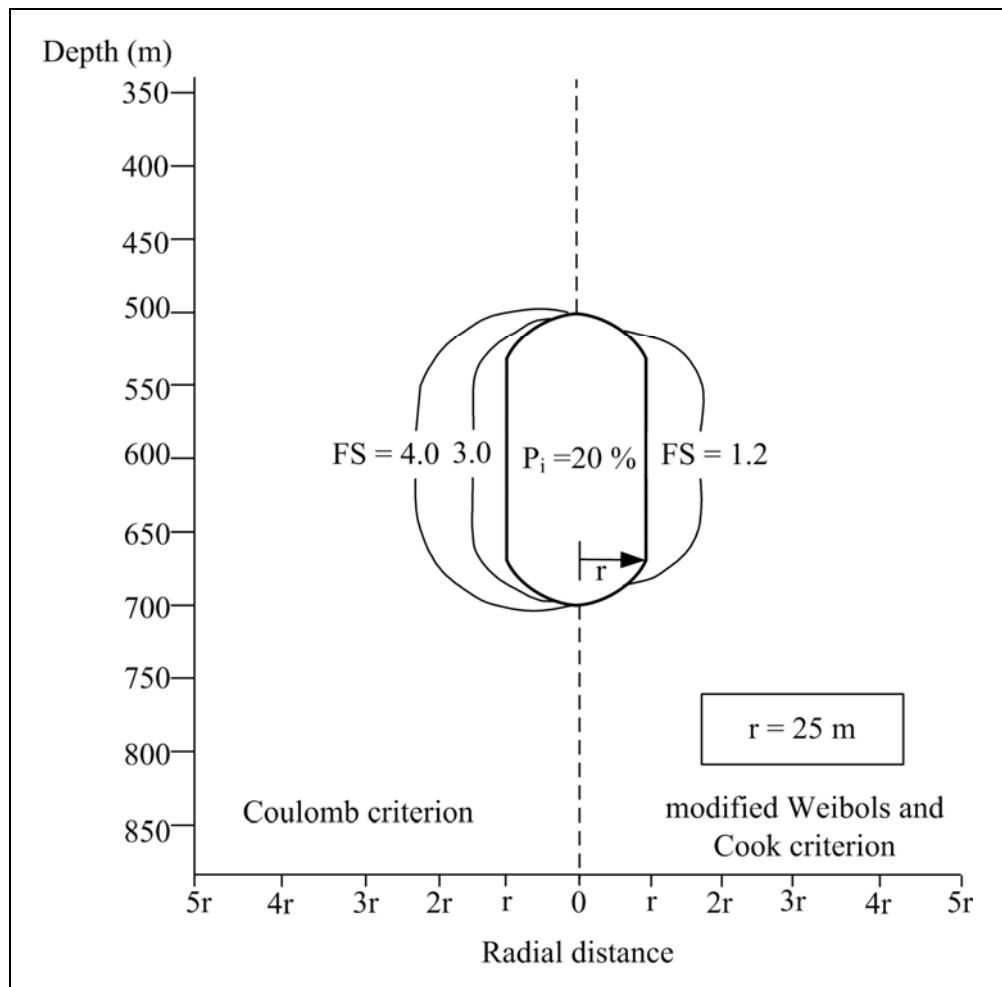


Figure 6.3 Contours of factor of safety calculated from the Coulomb and modified Wiebols and Cook criteria for $P_{\min} = 20\% \sigma_{cs}$, $r = 25$ m.

CHAPTER VII

DISCUSSIONS, CONCLUSIONS, AND RECOMMENDATIONS FOR FUTURE STUDIES

7.1 Discussions and conclusions

True triaxial compressive strengths of Maha Sarakham (MS) salt are determined by using a polyaxial load frame. The salt specimens are cut and ground to obtain rectangular blocks with a nominal dimension of $5 \times 5 \times 10 \text{ cm}^3$. The load frame equipped with two pairs of cantilever beams is used to apply the constant lateral stresses (σ_2 and σ_3) to salt specimen while the axial stress (σ_1) is increased until failure occurs. The deformations induced along the three loading directions are monitored and used to calculate the elastic modulus and Poisson's ratio of the salt. The results indicate that the elastic modulus and Poisson's ratio of the MS salt are averaged as $22.2 \pm 2.7 \text{ GPa}$ and 0.37 ± 0.05 . For the Coulomb criterion the internal friction angle determined from the triaxial loading condition ($\sigma_2 = \sigma_3$) is 50° , and the cohesion is 5 MPa . The effect of σ_2 on the salt strengths can be best described by the modified Wiebols and Cook criterion with the mean misfit = 3.5 MPa . The empirical (power law) Mogi criterion tends to underestimate the salt strengths particularly under high σ_3 values. The modified Lade criterion overestimates the actual strengths at all levels of σ_3 , showing the mean misfit = 15.4 MPa . The Coulomb and Hoek and Brown criteria can not describe the salt strengths beyond the condition where $\sigma_2 = \sigma_3$,

as they can not incorporate the effects of σ_2 . Both circumscribed and inscribed Drucker-Prager criteria severely underestimate σ_1 at failure for all stress conditions, showing the largest mean misfit of 19.5 and 34.7 MPa, respectively.

A finite element analysis was performed to demonstrate the impact of the intermediated principal stress on the salt behavior around a compressed-air storage cavern subject to the designed minimum storage pressures during retrieval period. Under this condition the minimum cavern pressure (P_{\min}) is reduced to as low as 10% and 20% of the in-situ stress at the casing shoe (above the cavern top), and hence the stress states in the surrounding salt are highly deviatoric. The radial stress is the lowest, representing σ_3 . The axial (vertical) stress is σ_2 , and the tangential stress is the greatest, representing σ_1 . The analysis is made in axis symmetry under isothermal condition, and assuming that no nearby underground structure within 1.2 km radius. For the minimum cavern pressure of 10% σ_{cs} failure occurs at cavern boundary as predicted by modified Wiebols and Cook criteria are more appropriated when compared with the Coulomb criterion. This is because the modified Wiebols and Cook criteria are developed from true triaxial test results, and hence, they can predict the stability condition more realistic conservative than the Coulomb criterion. When the cavern pressure is reduced to 20% σ_{cs} no failure occurs around the cavern.

7.2 Recommendations for future studies

The uncertainties and adequacies of the research investigation and results discussed above lead to the recommendations for further studies. The test should be performed on a variety of rock types with different strengths. The effect of friction

at the interface between the loading platen and rock surfaces should be investigated. Size effect on the rock polyaxial strength should also be examined. The effect of temperature should be considered on the true triaxial compressive tested.

REFERENCES

- Alsayed, M.I. (2002). Utilising the hoek triaxial cell for multiaxial testing of hollow rock cylinders. **International Journal of Rock Mechanics & Mining Sciences**. 39: 355-366.
- Cai, M. (2008). Influence of intermediate principal stress on rock fracturing and strength near excavation boundaries—Insight from numerical modeling. **International Journal of Rock Mechanics & Mining Sciences**. 45: 763-772.
- Chang, C., and Haimson, B. (2005). Non-dilatant deformation and failure mechanism in two Long Valley Caldera rocks under true triaxial compression. **International Journal of Rock Mechanics & Mining Sciences**. 42: 402-414.
- Colmenares, L.B., and Zoback, M.D. (2002). A statistical evaluation of intact rock failure criteria constrained by polyaxial test data for five different rocks. **International Journal of Rock Mechanics & Mining Sciences**. 39: 695-729.
- Drucker, D., and Prager., W. (1952). Soil mechanics and plastic analysis or limit design. *Q Appl Math*. 10:157–65.
- Ewy, R. (1999). Wellbore-stability predictions by use of a modified Lade criterion. **SPE Drill Completion**. 14(2): 85–91.
- Hoek, E., and Franklin, J.A, (1970). Developments in triaxial testing equipment. **Rock Mechanics**. 2: 223-228.
- Haimson, B., and Chang, C. (2000). A new true triaxial cell for testing mechanical properties of rock, and its use to determine rock strength and deformability of Westerly granite. **International Journal of Rock Mechanics and Mining Sciences**. 37 (1-2): 285-296.

- Haimson, B. (2006). True triaxial stresses and the brittle fracture of rock. **Pure and Applied Geophysics**. 163 1101-1130.
- Hoek, E., and Brown, E.T. (1980). Underground excavations in rock. **IMM**. London, pp. 133-136.
- Itasca (1992). **User manual for FLAC–fast Lagrangian analysis of continua, version 3.0**. Itasca Consulting Group Inc., Minneapolis, MN.
- Jaeger, J.C., and Cook, N.G.W. (1979). **Fundamentals of Rock Mechanics (3rd. Edn.)**. Chapman & Hall, London, pp. 105-106.
- Jaeger, J.C., Cook, N.G.W., and Zimmerman, R.W. (2007). **Fundamentals of Rock Mechanics (4rd. Edn.)**. Blackwell Publishing, Oxford.
- Kwaśniewski, M., Takahashi, M., and Li, X. (2003). Volume changes in sandstone under true triaxial compression conditions. **ISRM 2003–Technology Roadmap for Rock Mechanics**. South African Institute of Mining and Metallurgy, pp. 683-688.
- Lade, P. (1977). Elasto-plastic stress-strain theory for cohesion less soil with curved yield surfaces. **Int J Solids Struct**. 13: 1019–1035.
- Lade, P., and Duncan, J. (1975). Elasto-plastic stress-strain theory for cohesion less soil. **J Geotech Eng Div ASCE**. 101: 1037–1053.
- Mogi, K. (1967). Effect of the intermediate principal stress on rock failure. **J Geophys. Res.** 72: 5117–5131.
- Mogi, K. (1971). Fracture and flow of rocks under high triaxial compression. **J. Geophys. Res.** 76(5): 1255-1269.

- Rao, K.S., and Tiwari, R.P. (2002). Physical simulation of jointed model materials under biaxial and true triaxial stress states. **Research Report, IIT Delhi, India**, pp. 30.
- Riley, K.F., Hobson, M.P., and Bence, S.J. (1998). **Mathematical Methods for Physics and Engineering**. Cambridge: Cambridge University Press, 1008 pp.
- Sriapai, T., and Fuenkajorn, K. (2010). Polyaxial strengths of Maha Sarakham salt. In **Proceedings of the ISRM International Symposium and the 6th Asian Rock Mechanics Symposium**. Central Board of Irrigation and Power, New Delhi (Published in CD ROM).
- Tiwari, R.P., and Rao, K.S. (2004). Physical modeling of a rock mass under a true triaxial stress state. **International Journal of Rock Mechanics and Mining Sciences**. 41: 1-6.
- Walsri, C., Poonprakon, P., Thosuwat, R., and Fuenkajorn, K. (2009). Compressive and tensile strengths of sandstones under true triaxial stresses. In **Proceeding 2nd Thailand Symposium on Rock Mechanics**. Chonburi, Thailand. 2: 199-218.
- Warren, J. (1999). **Evaporites: Their Evolution and Economics** (pp.235-239). Blackwell Science. Oxford.
- Wiebols, G.A., and Cook, N.G.W. (1968). An energy criterion for the strength of rock in polyaxial compression. **International Journal of Rock Mechanics and Mining Sciences**. 5: 529-549.
- Zhou, S. (1994). A program to model the initial shape and extent of borehole breakout. **Comput Geosci**. 20(7/8):1143–60.

APPENDIX A

LIST OF STRESS-STRAIN CURVES

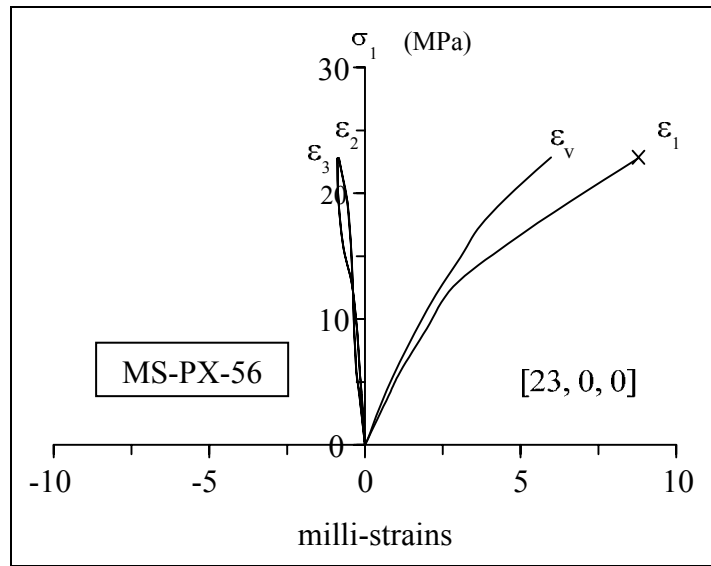


Figure A.1 Stress-strain curves of Maha Sarakham rock salt tested under $\sigma_2 = 0$ MPa and $\sigma_3 = 0$ MPa.

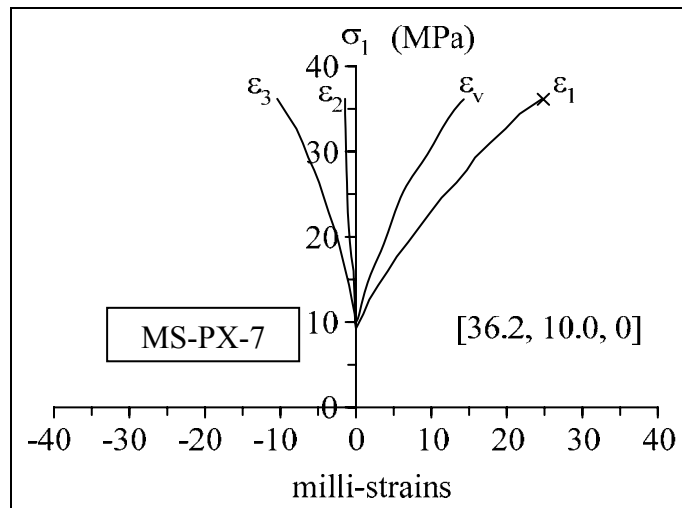


Figure A.2 Stress-strain curves of Maha Sarakham rock salt tested under $\sigma_2 = 10.0$ MPa and $\sigma_3 = 0$ MPa.

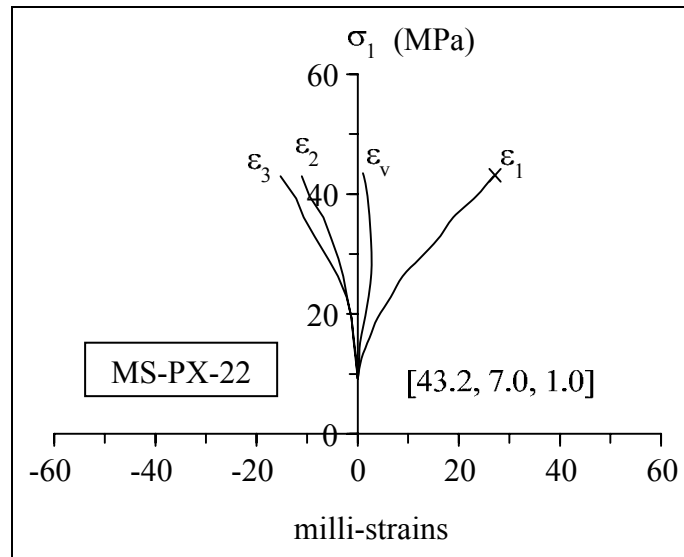


Figure A.3 Stress-strain curves of Maha Sarakham rock salt tested under $\sigma_2 = 7$ MPa and $\sigma_3 = 1.0$ MPa.

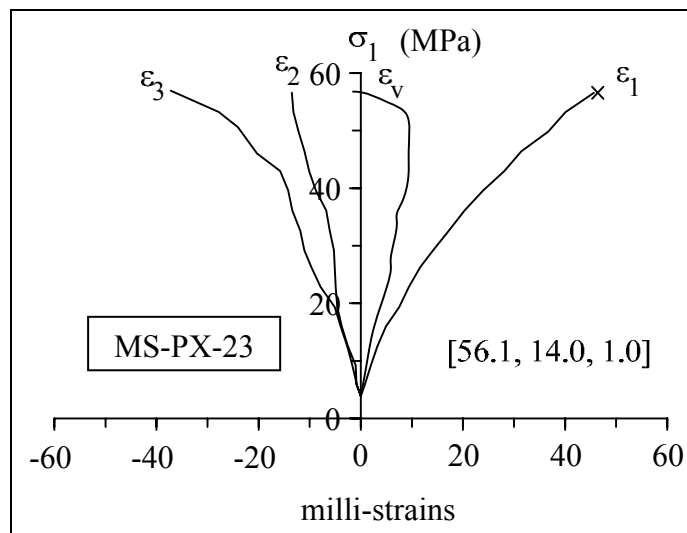


Figure A.4 Stress-strain curves of Maha Sarakham rock salt tested under $\sigma_2 = 14.0$ MPa and $\sigma_3 = 1.0$ MPa.

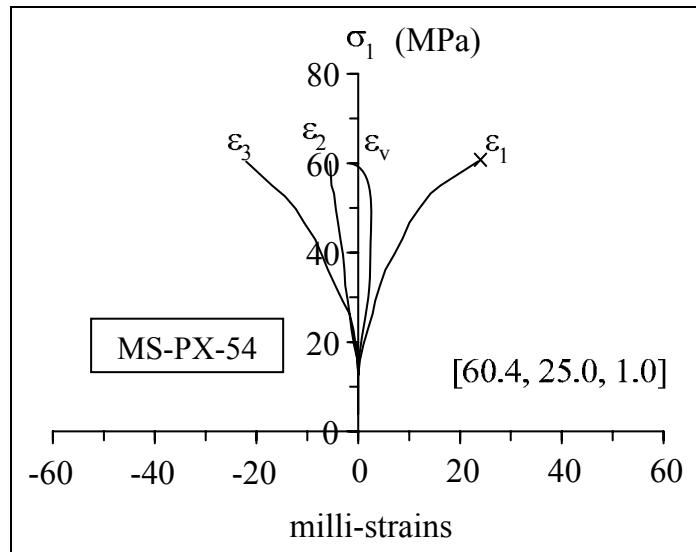


Figure A.5 Stress-strain curves of Maha Sarakham rock salt tested under $\sigma_2 = 25.0$ MPa and $\sigma_3 = 1.0$ MPa.

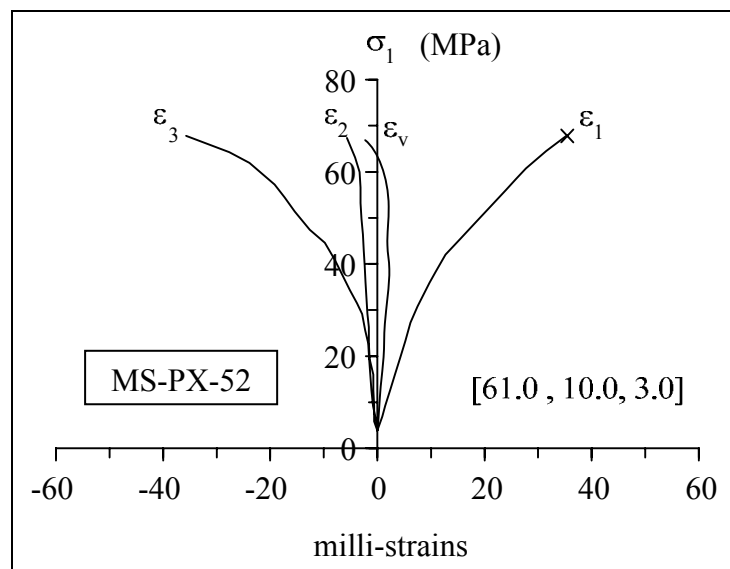


Figure A.6 Stress-strain curves of Maha Sarakham rock salt tested under $\sigma_2 = 10.0$ MPa and $\sigma_3 = 3.0$ MPa.

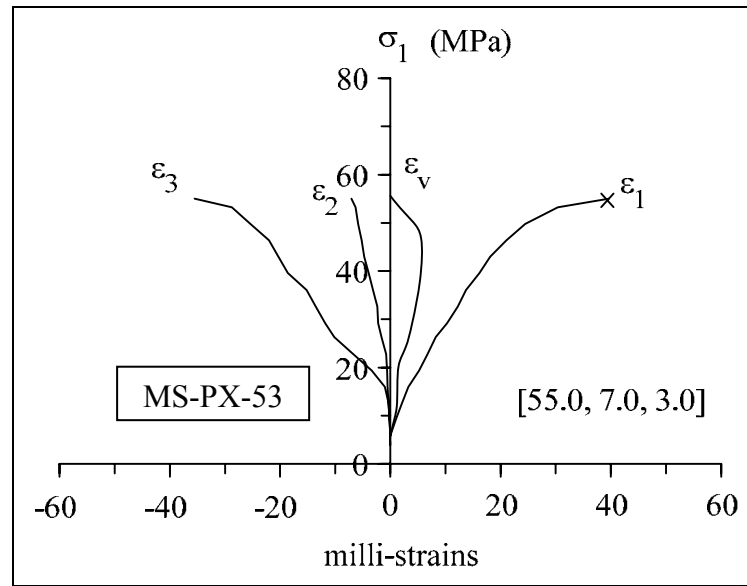


Figure A.7 Stress-strain curves of Maha Sarakham rock salt tested under $\sigma_2 = 7.0$ MPa and $\sigma_3 = 3.0$ MPa.

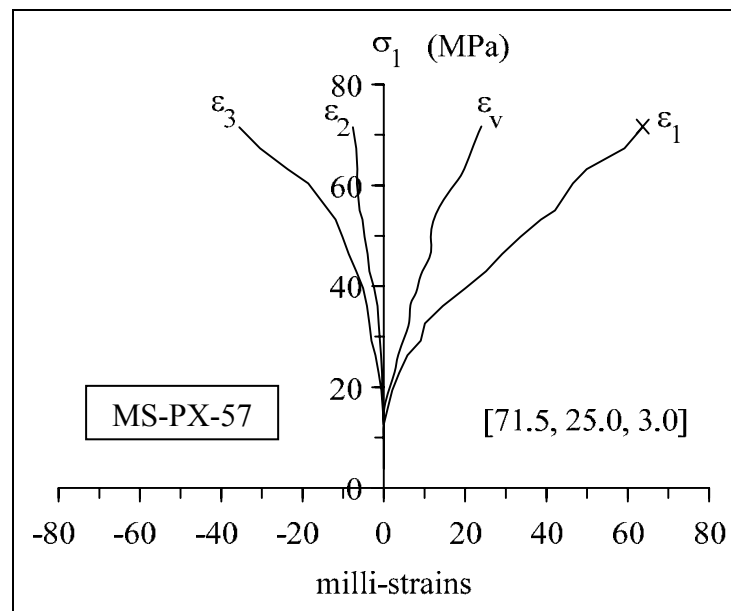


Figure A.8 Stress-strain curves of Maha Sarakham rock salt tested under $\sigma_2 = 25.0$ MPa and $\sigma_3 = 3.0$ MPa.

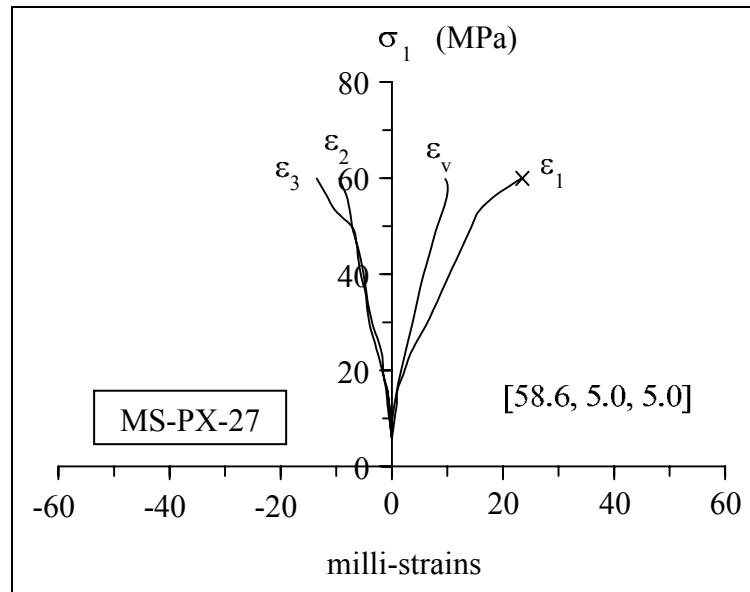


Figure A.9 Stress-strain curves of Maha Sarakham rock salt tested under $\sigma_2 = 5.0$ MPa and $\sigma_3 = 5.0$ MPa.

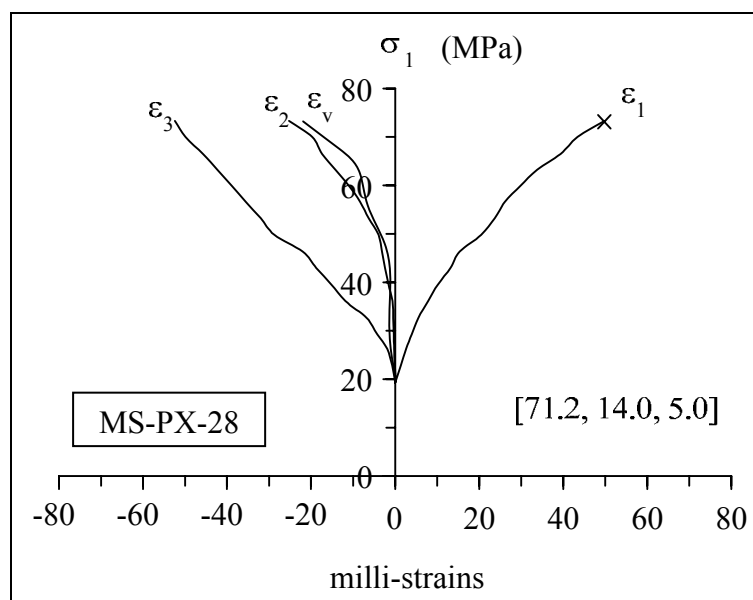


Figure A.10 Stress-strain curves of Maha Sarakham rock salt tested under $\sigma_2 = 14.0$ MPa and $\sigma_3 = 5.0$ MPa.

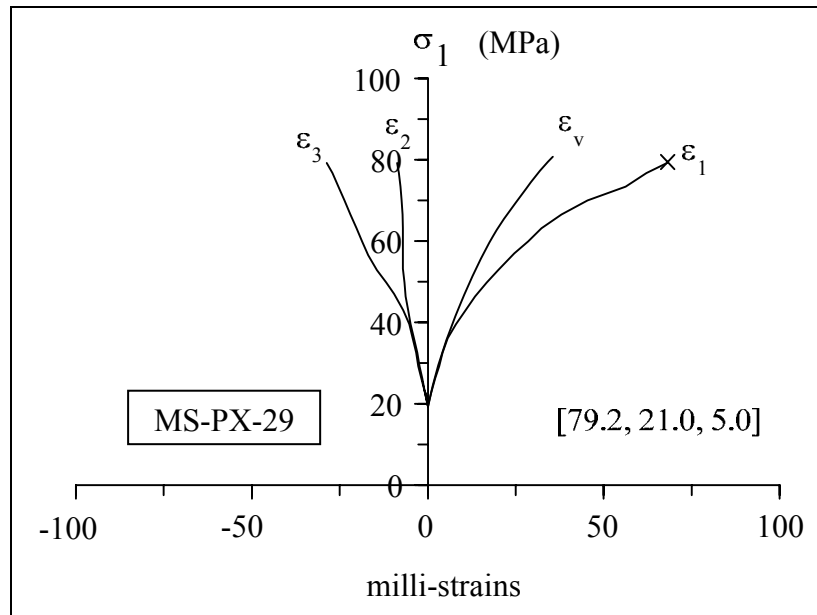


Figure A.11 Stress-strain curves of Maha Sarakham rock salt tested under $\sigma_2 = 21.0$ MPa and $\sigma_3 = 5.0$ MPa.

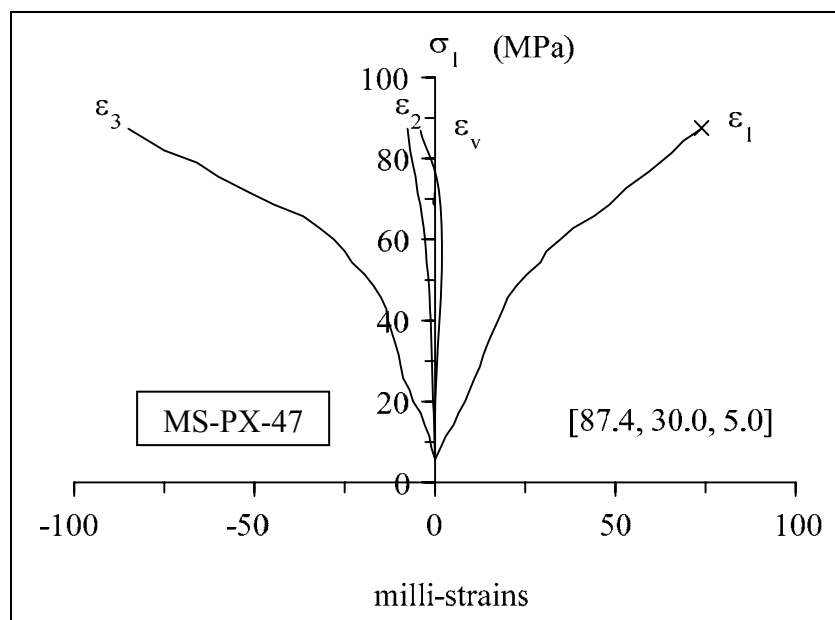


Figure A.12 Stress-strain curves Maha Sarakham rock salt tested under $\sigma_2 = 30.0$ MPa and $\sigma_3 = 5.0$ MPa.

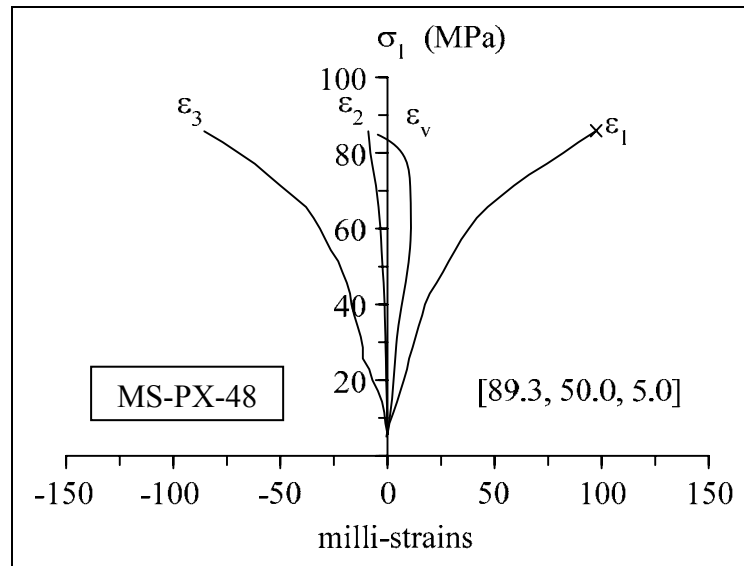


Figure A.13 Stress-strain curves of Maha Sarakham rock salt tested under $\sigma_2 = 50.0$ MPa and $\sigma_3 = 5.0$ MPa.

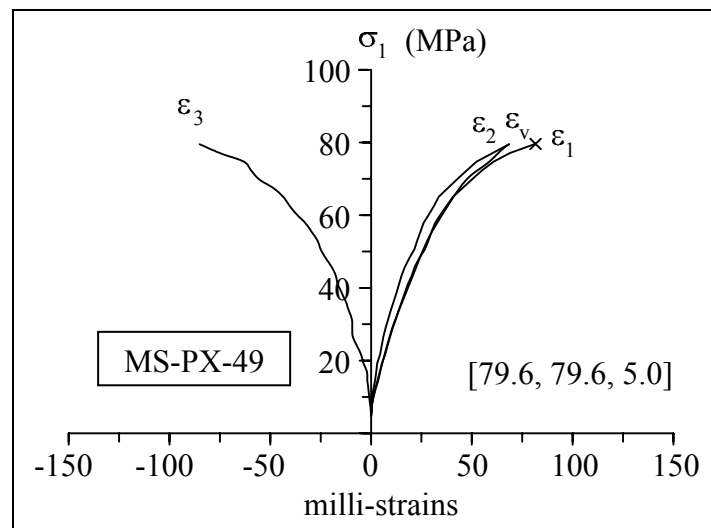


Figure A.14 Stress-strain curves of Maha Sarakham rock salt tested under $\sigma_2 = 79.6$ MPa and $\sigma_3 = 5.0$ MPa.

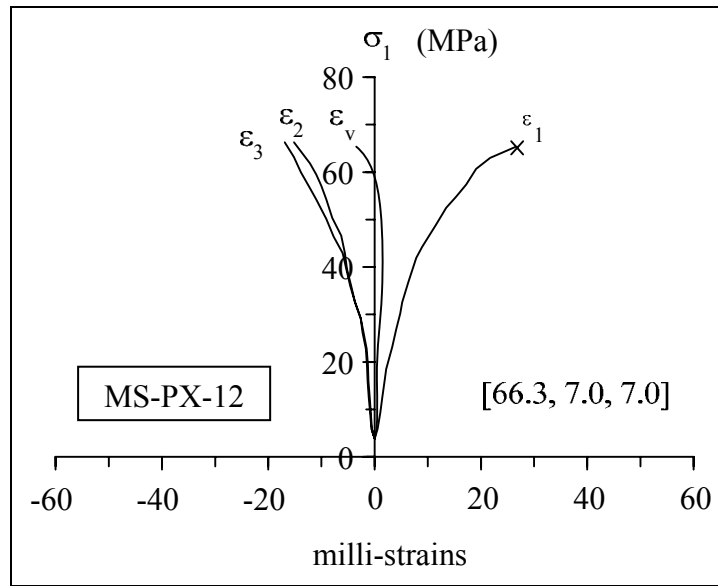


Figure A.15 Stress-strain curves of Maha Sarakham rock salt tested under

$\sigma_2 = 7.0$ MPa and $\sigma_3 = 7.0$ MPa.

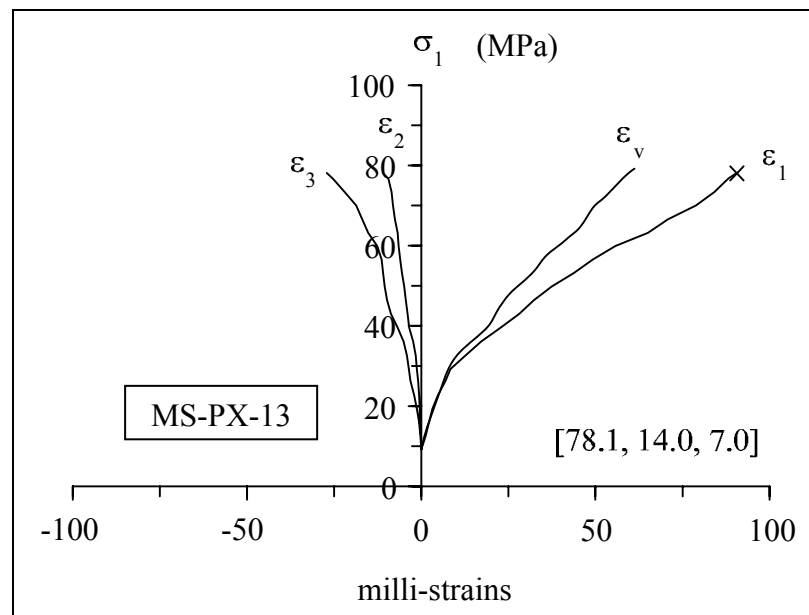


Figure A.16 Stress-strain curves of Maha Sarakham rock salt tested under

$\sigma_2 = 14.0$ MPa and $\sigma_3 = 7.0$ MPa

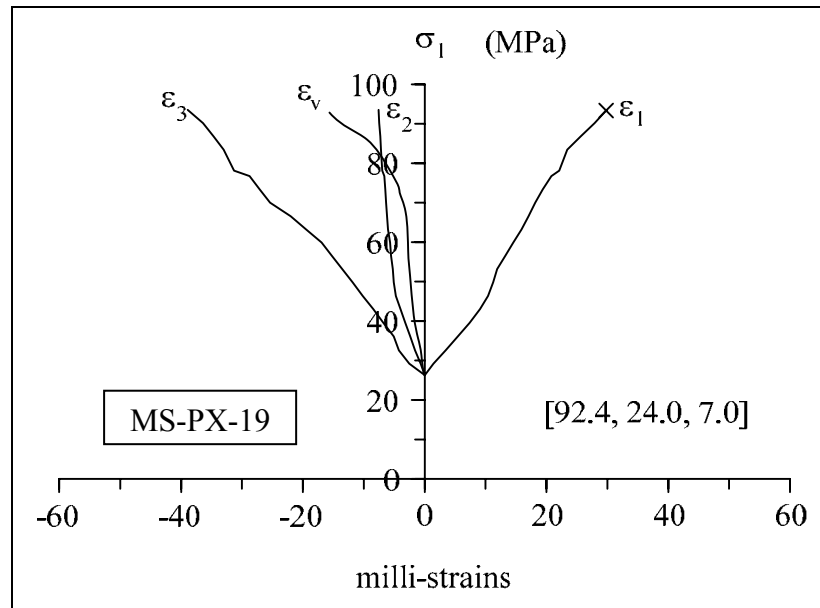


Figure A.17 Stress-strain curves of Maha Sarakham rock salt tested under $\sigma_2 = 24.0$ MPa and $\sigma_3 = 7.0$ MPa.

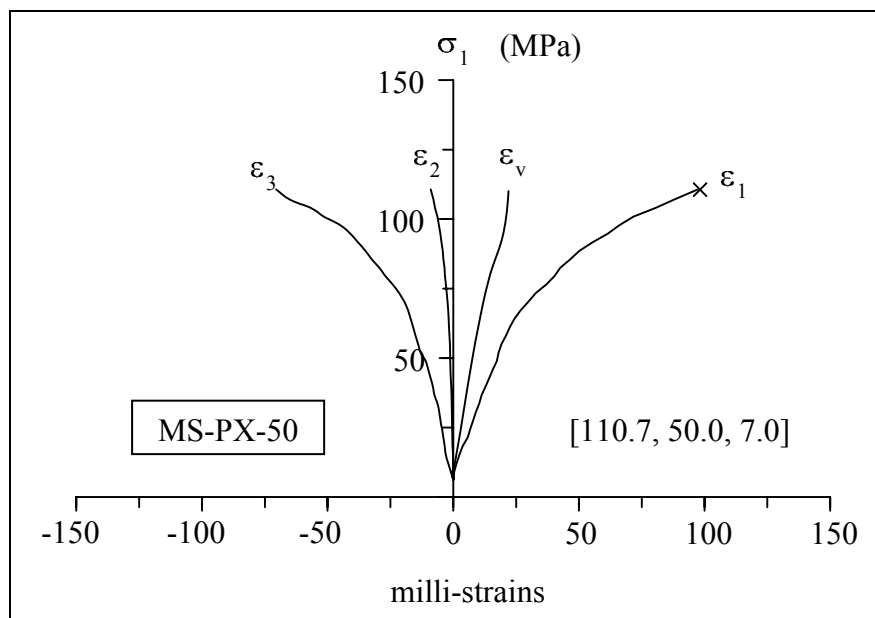


Figure A.18 Stress-strain curves of Maha Sarakham rock salt tested under $\sigma_2 = 50.0$ MPa and $\sigma_3 = 7.0$ MPa.

APPENDIX B

TECHNICAL PUBLICATION

TECHNICAL PUBLICATION

Sriapai, T., and Fuenkajorn, K., (2010). **Polyaxial Strengths of Maha Sarakham Salt**. In Proceeding of 6th Asian Rock Mechanics Symposium – ARMS 2010, New Delhi, India, 23-27 October 2010. (Published in CD ROM).

Sriapai, T. Samsri, P., and Fuenkajorn K., (2011). **Polyaxial strengths of Maha Sarakham salt**, In Proceeding of Third Thai Rock Mechanics Symposium, Petchburi Thailand, 10-11 March 2011.

Tanapol Sriapai, et al

ISRM International Symposium 2010 and 6th Asian Rock Mechanics Symposium - Advances in Rock Engineering
23-27 October, 2010, New Delhi, India

POLYAXIAL STRENGTHS OF MAHA SARAOKHAM SALT

TANAPOL SRIAPAI AND KITTITEP FUENKAJORN

Geomechanics Research Unit, Institute of Engineering, Suranaree University of Technology
111 University Avenue, Nakhon Ratchasima 30000, Thailand

Abstract: True triaxial compressive strengths of Maha Sarakham (MS) salt are determined by using a polyaxial load frame. The salt specimens are cut and ground to obtain rectangular blocks with a nominal dimension of $5.4 \times 5.4 \times 10.8 \text{ cm}^3$. The load frame equipped with two pairs of cantilever beams is used to apply the constant lateral stresses (σ_2 and σ_3) to salt specimen while the axial stress (σ_1) is increased at 0.5-1.0 MPa/s until failure occurs. The deformations induced along the three loading directions are monitored and used to calculate the tangent elastic modulus and Poisson's ratio of the salt. The results indicate that the elastic modulus and Poisson's ratio of the MS salt are averaged as $21.5 \pm 2.6 \text{ GPa}$ and 0.40 ± 0.04 . For the Coulomb criterion the internal friction angle determined from the triaxial loading condition ($\sigma_2 = \sigma_3$) is 50° , and the cohesion is 5 MPa. The effect of σ_2 on the salt strengths can be best described by the modified Wiebols and Cook criterion with the mean misfit = 3.5 MPa. The empirical (power law) Mogi criterion tends to underestimate the salt strengths particularly under high σ_3 values. The modified Lade criterion overestimates the actual strengths at all levels of σ_3 , showing the mean misfit = 15.4 MPa. The Coulomb and Hoek and Brown criteria can not describe the salt strengths beyond the condition where $\sigma_2 = \sigma_3$, as they can not incorporate the effects of σ_2 . Both circumscribed and inscribed Drucker-Prager criteria severely underestimate σ_1 at failure for all stress conditions, showing the largest mean misfit of 19.5 and 34.7 MPa, respectively.

1. INTRODUCTION

The effects of confining pressures at great depths on the mechanical properties of rocks are commonly simulated in a laboratory by performing triaxial compression testing of cylindrical rock core specimens. A significant limitation of these conventional methods is that the intermediate and minimum principal stresses are equal during the test while the actual in-situ rock is normally subjected to an anisotropic stress state where the maximum, intermediate and minimum principal stresses are different ($\sigma_1 \neq \sigma_2 \neq \sigma_3$). It has been commonly found that the compressive strength obtained from conventional triaxial testing can not represent the actual in-situ strength where the rock is subjected to an anisotropic stress state [1-6].

From the experimental results on brittle rocks obtained from Haimson [2], Colmenares & Zoback [7], it can be generally concluded that in a $\sigma_1 - \sigma_2$ diagram, for a given σ_3 , σ_1 at failure initially increases with σ_2 to a certain magnitude, and then it gradually decreases as σ_2 increases. The effect of σ_2 is more pronounced under higher σ_3 . Cai [8] offers an explanation of how the intermediate principal stress affects the rock strength based on the results from numerical simulations on fracture initiation and propagation. This states that the intermediate principal stress confines the rock in such a way that fractures can only be initiated and propagated in the direction parallel to σ_1 and σ_2 . The effect of σ_2 is related to the stress-induced anisotropic properties, and the end effect at the interface between the rock surface and loading platen in the direction of σ_2 application. The effect is smaller in homogeneous and fine-grained rocks than in coarse-grained rocks where pre-existing micro-cracks are not uniformly distributed.

Several failure criteria have been developed to describe the rock strength under true triaxial stress states. Comprehensive reviews of these criteria have recently been given by Haimson [2], Colmenares & Zoback [7], Benz & Schwab [9] and You [10]. Among these several criteria, the Mogi and modified Wiebols and Cook criteria are perhaps the most widely used to describe the rock compressive strengths under true triaxial stresses. Obtaining rock strengths under an anisotropic stress state is not only difficult but also expensive. A special loading device (e.g. polyaxial loading machine or true triaxial load cell) is required. As a result, test data under true triaxial stress conditions have been relatively limited. Most researchers have used the same sets of test data

(some obtained over a decade ago) to compare with their new numerical simulations, or field observations (notably on breakout of deep boreholes) and to verify their new strength criteria and concepts. Due to the cost and equipment availability for obtaining true triaxial strengths, in common engineering practices application of a failure criterion that can incorporate the three-dimensional stresses has been very rare.

The objective of this paper is to determine the effects of the intermediate principal stress on the strength of Maha Sarakham salt. A polyaxial load frame is used to apply constant lateral loads onto the rectangular specimen while the axial load is increased to failure. Assessment of the predictive capability of some commonly used criteria is made.

2. SALT SAMPLES

The salt specimens tested here were collected from the middle members of the Maha Sarakham formation in the Khorat basin, northeastern Thailand. This salt member has long been considered as a host rock for compressed-air energy storage by the Thai Department of Energy. The rectangular block specimens are cut and ground to have a nominal dimension of $5.4 \times 5.4 \times 10.8 \text{ cm}^3$. The rock salt is relatively pure halite with a slight amount (less than 1-2%) of anhydrite, clay minerals and ferrous oxide. The average crystal (grain) size is $5 \times 5 \times 10 \text{ mm}^3$. The core specimens with a nominal diameter of 60 mm tested here were drilled from depths ranging between 170 and 270 m.

3. POLYAXIAL LOAD FRAME

A polyaxial load frame is developed based on three key design requirements: (1) capable of maintaining constant lateral stresses (σ_2 and σ_3) during the test, (2) capable of testing specimen with volume equal to or larger than those used in the conventional triaxial testing, and (3) allowing monitoring of specimen deformation along the principal axes. To meet the load requirement above, two pairs of cantilever beams are used to apply the lateral stresses in mutually perpendicular directions to the rock specimen (Figure 1). The outer end of each opposite beam is pulled down by dead weight placed in the middle of a steel bar linking the two opposite beams underneath. The inner end is hinged by a pin mounted on vertical bars on each side of the frame. During testing all beams are arranged horizontally, and hence a lateral compressive load results on the specimen placed at the center of the frame. Due to the different distances from the pin to the outer weighting point and from the pin to the inner loading point, a load magnification of 12 to 1 is obtained from load calibration with an electronic load cell. This loading ratio is also used to determine the lateral deformation of the specimen by monitoring the vertical movement of the two steel bars below. The maximum lateral load is designed for 100 kN. The axial load is applied by a 1000 kN hydraulic load cell. The load frame can accommodate specimen sizes from $2.5 \times 2.5 \times 2.5 \text{ cm}^3$ to $10 \times 10 \times 20 \text{ cm}^3$. The different specimen sizes and shapes can be tested by adjusting the distances between the opposite loading platens.

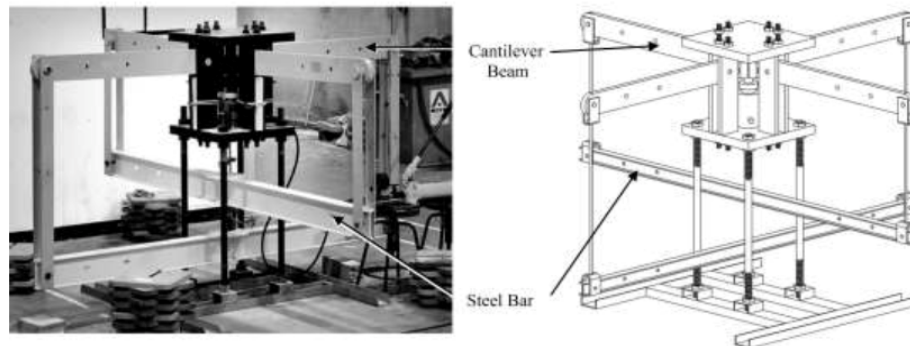


Figure 1. Polyaxial load frame developed for compressive strength testing under true triaxial stress.

4. TRUE TRIAXIAL STRENGTH TESTING

The polyaxial compression tests are performed to determine the compressive strengths and deformations of the salt under true triaxial stresses. The intermediate (σ_2) and minimum (σ_3) principal stresses are maintained constant while σ_1 maximum stresses is increased until failure is occurred. Here the constant σ_2 is varied from 0 to 80 MPa, and σ_3 from 0 to 28 MPa. Neoprene sheets are used to minimize the friction at all interfaces between the loading platen and the rock surface. The measured sample deformations are used to determine the strains along the principal axes during loading. The failure stresses are recorded and mode of failure is examined. Examples of stress-strain curves obtained from polyaxial compressive strength test are shown in Figure 2. The three-dimensional principal stress-strain relations given by Jaeger and Cook [11] can be simplified to obtain a set of governing equations for isotropic material. The calculations of the Poisson's ratios and tangent elastic moduli are made at 50% of the maximum principal stress. The results indicate that the elastic modulus and Poisson's ratio of the MS salt are averaged as 21.5 ± 2.6 GPa and 0.40 ± 0.04 as shown in Table 1. The table also provides the octahedral shear stress (τ_{oct}), mean stress (σ_m), and the second order of the stress deviation ($J_2^{1/2}$) at failure. They can be calculated from the principal stresses at failure ($\sigma_1, \sigma_2, \sigma_3$) [11].

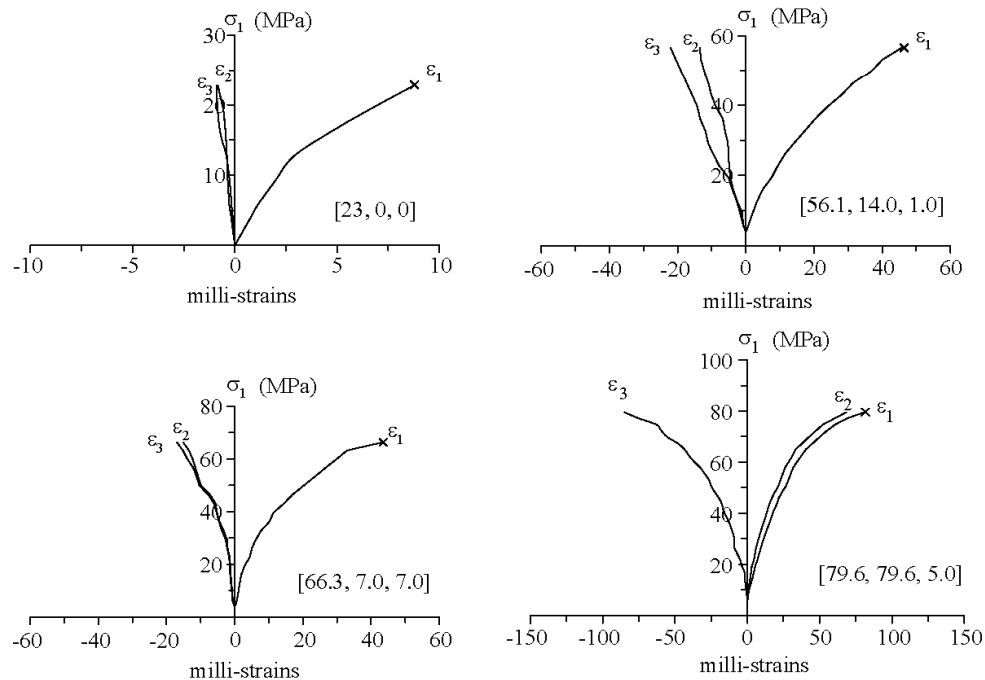


Figure 2. Examples of stress-strain curves obtained from polyaxial compressive strength test, the applied stresses are indicated $[\sigma_1, \sigma_2, \sigma_3]$ in MPa.

5. STRENGTH CRITERIA

The strength criteria used in this study include the Coulomb, Drucker-Prager, modified Lade, modified Weibols and Cook, Hoek and Brown, and the empirical Mogi criteria. Detailed derivations of these criteria are given by Colmenares & Zoback [7], and hence they will not be repeated here. Table 2 summarized the variables and constants used in these criteria. Based on the Coulomb criterion the internal friction angle from the triaxial loading condition ($\sigma_2 = \sigma_3$) is calculated as 50° , and the cohesion as 5 MPa. They are used in the calculation of the constant A, B and C used in the modified Weibols and Cook criteria. The empirical Mogi criterion uses a power law to describe the failure stresses. The parameter α and κ for the Inscribed and Circumscribed Drucker-Prager criteria can be derived from the cohesion and friction angle. The constant "s" in Hoek and Brown criterion is equal to 1 (for intact salt). The constant "m" is determined from the strength data under triaxial condition ($\sigma_2 = \sigma_3$). The modified Lade parameters (η) can also be derived directly from the cohesion and internal friction angle. The calculated property parameters of each failure criterion are given in Table 3.

Tanapol Sriapai

Table 1. Principal stresses at failure and elastic parameters of salt.

Specimen number	Depth (m)	Failure Stresses						Elastic Modulus (GPa)	Poisson's Ratio
		σ_3 (MPa)	σ_2 (MPa)	σ_1 (MPa)	σ_m (MPa)	τ_{oct} (MPa)	$J_2^{1/2}$ (MPa)		
56	253.75-253.85		0.0	23.0	7.7	10.8	5.4	22.4	0.35
7	179.66-179.77	0.0	10.0	36.2	15.4	15.3	7.6	20.7	0.36
55	208.40-208.50		25.0	43.1	22.7	17.7	8.8	23.3	0.42
42	211.60-211.70		35.1	35.1	23.4	16.5	8.3	-	-
20	244.47-244.57		1.0	26.5	9.5	12.0	6.0	25.3	0.46
22	246.21-246.31		7.0	43.2	16.7	18.9	9.5	18.5	0.39
23	245.50-245.60	1.0	14.0	56.1	23.4	23.8	11.9	20.6	0.40
54	208.50-208.60		25.0	60.4	28.5	24.8	12.4	19.3	0.40
44	210.05-219.15		35.0	62.5	32.5	25.6	12.8	-	-
38	211.20-211.30		49.3	49.3	32.9	23.2	11.6	-	-
61	178.13-178.23		3.0	45.1	17.0	19.8	9.9	22.5	0.25
53	208.60-208.70		7.0	55.0	20.7	24.4	12.2	19.8	0.39
52	254.05-254.15		10.0	61.0	23.7	26.7	13.4	23.1	0.40
5	256.43-256.53	3.0	14.0	66.0	26.7	28.4	14.2	15.8	0.38
57	201.70-201.80		25.0	71.5	32.2	29.6	14.8	26.9	0.42
35	200.45-200.56		40.0	75.0	38.3	30.6	15.3	24.3	0.36
43	209.95-210.05		50.0	74.9	41.6	31.1	15.6	-	-
40	211.40-211.50		64.9	64.9	43.3	30.6	15.3	-	-
27	264.41-264.51		5.0	58.6	22.9	25.3	12.6	23.4	0.42
28	263.31-263.41		14.0	71.2	28.4	30.8	15.4	20.8	0.40
29	264.67-264.77		21.0	79.2	33.4	33.5	16.8	18.0	0.35
47	210.35-210.45	5.0	30.0	87.4	39.1	36.3	18.1	21.4	0.39
41	211.50-211.60		40.0	91.6	43.9	37.5	18.7	-	-
48	210.45-210.55		50.0	89.3	46.4	36.5	18.3	23.1	0.39
45	210.15-210.25		65.0	85.0	50.0	36.3	18.1	-	-
49	210.55-210.65		79.6	79.6	53.1	37.5	18.8	24.1	0.42
12	201.23-201.33		7.0	66.3	26.8	28.0	14.0	22.1	0.37
13	201.60-201.70		14.0	78.1	30.7	34.0	17.0	20.0	0.37
19	244.37-244.47	7.0	24.0	92.4	38.8	39.1	19.6	16.0	0.43
25	245.10-245.20		40.0	106.4	48.8	43.9	21.9	-	-
50	210.65-210.75		50.0	110.7	53.6	45.3	22.6	20.2	0.43
46	210.25-210.35		65.0	109.5	58.2	45.0	22.5	-	-
10	179.93-180.31	10.0	10.0	79.6	33.2	32.8	16.4	21.7	0.39
58	251.79-250.85	12.0	12.0	81.8	35.3	32.9	16.5	22.7	0.42
59	212.11-212.21	20.0	20.0	106.4	48.8	40.7	20.4	21.9	0.39
60	243.71-243.82	28.0	28.0	119.7	58.6	43.2	21.6	23.0	0.36
Mean ± Standard Deviation								21.5±2.6	0.4±0.04

6. PREDICTABILITY OF THE STRENGTH CRITERIA

The three-dimensional strength criteria are used to compare against the strength data Figure 3 shows the octahedral shear strength as a function of mean stress, and the major principal stress at failure as a function of the intermediate principal stress. The mean misfit (\bar{s}) is determined for each criterion using equation (1) [13].

Table 2. Summary of the failure criteria.

Criterion	Equation
Modified Wiebols and Cook [7]	$J_2^{1/2} = A + B\sigma_m + C\sigma_m^2$ $A = \frac{C_0}{\sqrt{3}} - \frac{C_0}{3}B - \frac{C_0^2}{9}C$ $B = \frac{\sqrt{3}(q-1)}{q+2} - \frac{C}{3}(2C_0 + (q+2)\sigma_3)$ $C = \frac{\sqrt{27}}{2C_1 + (q-1)\sigma_3 - C_0} \times \left(\frac{C_1 + (q-1)\sigma_3 - C_0}{2C_1 + (2q+1)\sigma_3 - C_0} - \frac{q-1}{q+2} \right)$ $C_1 = (1 + 0.6\mu_i)C_0$ $q = \{(\mu_i^2 + 1)^{1/2} + \mu_i\}^2$ $\mu_i = \tan\phi$
Mogi [2]	$\tau_{oct} = A'[(\sigma_1 + \sigma_3)/2]^{B'}$ <p>A' and B' = Empirical Constant</p>
Hoek & Brown [12]	$\sigma_1 = \sigma_3 + \sigma_c \sqrt{m \frac{\sigma_3}{\sigma_c} + s}$ <p>m and s = Material Constant</p>
Modified Lade [7]	$(I_1')^3/I_3' = 27 + \eta$ $I_1' = (\sigma_1 + S) + (\sigma_2 + S) + (\sigma_3 + S)$ $I_3' = (\sigma_1 + S)(\sigma_2 + S)(\sigma_3 + S)$ $S = S_0/\tan\phi$ $\eta = 4(\tan\phi)^2(9 - 7\sin\phi)/(1 - \sin\phi)$ $S_0 = \sigma_c/(2q^{1/2})$
Coulomb [11]	$J_2^{1/2} = \frac{2}{\sqrt{3}}[\sigma_m \sin\phi + S_0 \cos\phi]$ $\sigma_m = (\sigma_1 + \sigma_2 + \sigma_3)/3$
Drucker-Prager (Circumscribed) [7]	$J_2^{1/2} = \kappa_c + \alpha_c \sigma_m$ $\alpha_c = \frac{6\sin\phi}{\sqrt{3}(3 - \sin\phi)}$ $\kappa_c = \frac{\sqrt{3}C_0 \cos\phi}{\sqrt{q}(3 - \sin\phi)}$
Drucker-Prager (Inscribed) [7]	$J_2^{1/2} = \kappa_i + \alpha_i \sigma_m$ $\alpha_i = \frac{3\sin\phi}{\sqrt{9 + 3\sin^2\phi}}$ $\kappa_i = \frac{2C_0 \cos\phi}{2\sqrt{q}\sqrt{9 + 3\sin^2\phi}}$

Table 3. Parameters for each failure criterion.

Criteria	Calibrated Parameters
Modified Wiebols and Cook	$\sigma_3 = 0$, A = 2.031 MPa, B = 1.746, C = -0.036 MPa ⁻¹
	$\sigma_3 = 1$, A = 1.698 MPa, B = 1.739, C = -0.030 MPa ⁻¹
	$\sigma_3 = 3$, A = 1.281 MPa, B = 1.733, C = -0.022 MPa ⁻¹
	$\sigma_3 = 5$, A = 1.027 MPa, B = 1.732, C = -0.017 MPa ⁻¹
	$\sigma_3 = 7$, A = 0.853 MPa, B = 1.732, C = -0.014 MPa ⁻¹
Mogi 1971	A' = 1.46 B' = 0.82
Hoek & Brown	m = 20.2 s = 1
Modified Lade	S = 3.66 MPa $\eta = 88.33$
Coulomb	$\phi = 50$ c = 5 MPa
Drucker-Prager (Circumscribed)	$\alpha_c = 0.69$ $\kappa_c = 4.7$ MPa
Drucker-Prager (Inscribed)	$\alpha_i = 0.15$ $\kappa_i = 1.38$ MPa

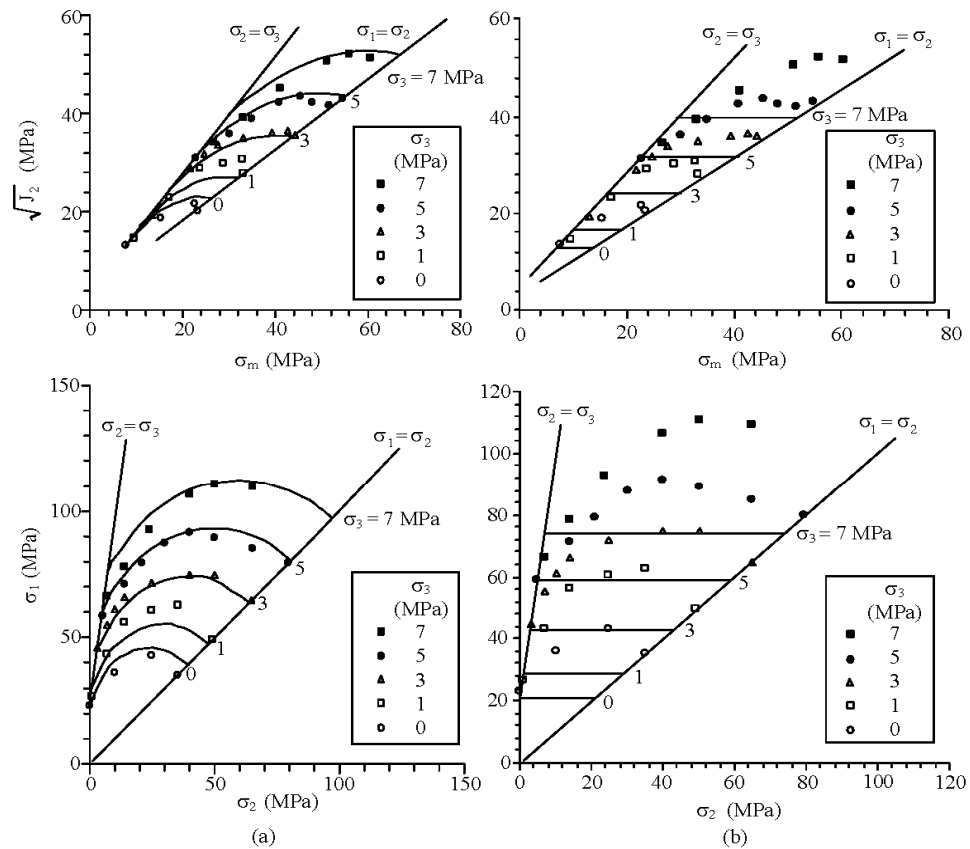


Figure 3. Comparisons between the test results with the modified Wiebols and Cook criterion (a) the Coulomb criterion.

Polyaxial Strengths of Maha Sarakham Salt

$$\bar{s} = \frac{1}{m} \sum_i s_i \quad (1)$$

Where $s_i = \sqrt{\frac{1}{n} \sum_j (\sigma_{1,j}^{\text{calc}} - \sigma_{1,j}^{\text{test}})^2}$

$\sigma_{1,j}^{\text{calc}}$ = maximum stress predicted from strength criterion.

$\sigma_{1,j}^{\text{test}}$ = maximum stress from test data.

n = number of data points calculated.

m = number of data sets.

Table 4 describes the calculated mean misfits for each criterion. The effect of σ_2 on the salt strengths can be best described by the modified Wiebols and Cook criterion with the mean misfit = 3.5 MPa. The empirical (power law) Mogi criterion tends to underestimate the salt strengths particularly under high σ_3 values. The modified Lade criterion is the overestimates the actual strengths at all levels of σ_3 , showing the mean misfit = 15.4 MPa. The Coulomb and Hoek and Brown criteria can not describe the salt strengths beyond the condition where $\sigma_2 = \sigma_3$, as they can not incorporate the effects of σ_2 . Both circumscribed and inscribed Drucker-Prager criteria severely underestimate σ_1 at failure for all stress conditions, showing the largest mean misfit of 19.5 and 34.7 MPa, respectively.

Table 4. Mean misfits calculated for each failure criterion.

Strength Criteria	Mean Misfit (MPa)
Modified Wiebols and Cook	3.5
Empirical Mogi	9.6
Hoek & Brown	18.6
Modified Lade	15.4
Coulomb	17.7
Drucker-Prager (Circumscribed)	19.5
Drucker-Prager (Inscribed)	34.7

7. CONCLUSIONS

The polyaxial loading tests are performed to assess the effect of intermediate principal stress on the MS salt. The results suggest that the intermediate principal stress can affect the maximum stress at failure. Such effect is not linear. The results indicate that the elastic modulus and Poisson's ratio of the MS salt are averaged as 21.5±2.6 GPa and 0.40±0.04. For the Coulomb criterion, the internal friction angle determined from the triaxial loading condition ($\sigma_2 = \sigma_3$) is 50°, and the cohesion is 5 MPa. The effect of σ_2 on the salt strengths can be best described by the modified Wiebols and Cook criterion. The empirical (power law) Mogi criterion tends to underestimate the salt strengths particularly under high σ_3 values. The modified Lade criterion is the overestimates at all levels of σ_3 . The Coulomb and Hoek and Brown criteria can not describe the salt strengths beyond the condition where $\sigma_2 = \sigma_3$, as they can not incorporate the effects of σ_2 . Both circumscribed and inscribed Drucker-Prager criteria severely underestimate σ_1 at failure for all stress conditions.

ACKNOWLEDGEMENT

This research is funded by Suranaree University of Technology. Permission to publish this paper is gratefully acknowledged. We would like to thank Pimai Salt Co. for donating the salt core samples for this research.

Tanapol Sriapai

REFERENCES

- [1] Yang, X. L., Zou, J. F. and Sui, Z. R. (2007). Effect of intermediate principal stress on rock cavity stability. *Journal Central South University Technology*. s1-0165-05
- [2] Haimson, B. (2006). True triaxial stresses and the brittle fracture of rock. *Pure and Applied Geophysics*. 163, 1101-1113.
- [3] Tiwari, R.P. and Rao, K.S. (2006). Post failure behaviour of a rock mass under the influence of triaxial and true triaxial confinement. *Engineering Geology*. 84, 112-129.
- [4] Haimson, B. and Chang, C. (2000). A new true triaxial cell for testing mechanical properties of rock, and its use to determine rock strength and deformability of Westerly granite. *Int. J. Rock Mech. Min. Sci.* 37, 285-296.
- [5] Reddy, K.R., Saxena, S.K. and Budiman, J.S. (1992). Development of a true triaxial testing apparatus. *Geotechnical Testing Journal*. 35 (2), 89-105.
- [6] Smart, B. G. D. (1995). A true triaxial cell for testing cylindrical rock specimens. *International Journal of Rock Mechanics and Mining Sciences*. 32(3): 269-275.
- [7] Colmenares, L.B. and Zoback, M.D. (2002). A statistical evaluation of intact rock failure criteria constrained by polyaxial test data for five different rocks. *Int. J. Rock Mech. Min. Sci.* 39, 695-729.
- [8] Cai, M. (2008). Influence of intermediate principal stress on rock fracturing and strength near excavation boundaries – Insight from numerical modeling. *Int. J. Rock Mech. Min. Sci.* 45, 763-772.
- [9] Benz, T. and Schwab, R. (2008). A quantitative comparison of six rock failure criteria. *International Journal of Rock Mechanics and Mining Sciences*. 45: 1176-1186.
- [10] You, M. (2008). True-triaxial strength criteria for rock. *International Journal of Rock Mechanics and Mining Sciences*. 46, 115-127.
- [11] Jaeger, J.C., and Cook, N.G.W. (1979). *Fundamentals of Rock Mechanics*. London: Chapman and Hall, 593 pp.
- [12] Hoek, E. and Brown, E. T. (1988). The Hoek-Brown Failure Criterion - a 1988 Update. *Proceedings of the 15th Canadian Rock Mechanics Symposium*, University of Toronto. Vol. 1, pp 31-48.
- [13] Riley, K.F., Hobson, M.P., and Bence, S.J. (1998). *Mathematical Methods for Physics and Engineering*. Cambridge: Cambridge University Press, 1008 pp.

BIOGRAPHY

Mr. Tanapol Sriapai graduated in Geotechnology from Suranaree University of Technology, Nakhon Ratchasima, Thailand in 2009. From 2009 to present, he studies Master degree in Geotechnology at Suranaree University of Technology, Nakhon Ratchasima, Thailand. He has worked as a Research Assistant for Geomechanics Research Unit, Institute of Engineering, Suranaree University of Technology.

Dr. Kittitep Fuenkajorn received his M.S. and Ph.D. in Geological Engineering from the University of Arizona. Now he is Associate Professor at the Suranaree University of Technology, Nakhon Ratchasima, Thailand.

Polyaxial strengths of Maha Sarakham salt

T. Sriapai, P. Samsri & K. Fuenkajorn

Geomechanics Research Unit, Suranaree University of Technology, Thailand

Keywords: True triaxial, polyaxial, intermediate principal stress, rock salt, anisotropic

ABSTRACT: True triaxial compressive strengths of Maha Sarakham (MS) salt are determined by using a polyaxial load frame. The salt specimens are cut and ground to obtain rectangular blocks with a nominal dimension of $5.4 \times 5.4 \times 10.8 \text{ cm}^3$. The load frame equipped with two pairs of cantilever beams is used to apply the constant lateral stresses (σ_2 and σ_3) to salt specimen while the axial stress (σ_1) is increased at 0.5-1.0 MPa/s until failure occurs. The deformations induced along the three loading directions are monitored and used to calculate the tangent elastic modulus and Poisson's ratio of the salt. The results indicate that the elastic modulus and Poisson's ratio of the MS salt are averaged as $21.5 \pm 2.6 \text{ GPa}$ and 0.40 ± 0.04 . For the Coulomb criterion the internal friction angle determined from the triaxial loading condition ($\sigma_2 = \sigma_3$) is 50° , and the cohesion is 5 MPa. The effect of σ_2 on the salt strengths can be best described by the modified Wiebols and Cook criterion with the mean misfit=3.5 MPa. The empirical (power law) Mogi criterion tends to underestimate the salt strengths particularly under high σ_3 values. The modified Lade criterion overestimates the actual strengths at all levels of σ_3 , showing the mean misfit=15.4 MPa. The Coulomb and Hoek and Brown criteria can not describe the salt strengths beyond the condition where $\sigma_2 = \sigma_3$, as they can not incorporate the effects of σ_2 . Both circumscribed and inscribed Drucker-Prager criteria severely underestimate σ_1 at failure for all stress conditions, showing the largest mean misfit of 19.5 and 34.7 MPa, respectively.

1 INTRODUCTION

The effects of confining pressures at great depths on the mechanical properties of rocks are commonly simulated in a laboratory by performing triaxial compression testing of cylindrical rock core specimens. A significant limitation of these conventional methods is that the intermediate and minimum principal stresses are equal during the test while the actual in-situ rock is normally subjected to an anisotropic stress state where the maximum, intermediate and minimum principal stresses are different ($\sigma_1 \neq \sigma_2 \neq \sigma_3$). It has been commonly found that the compressive strength obtained from conventional triaxial testing can not represent the actual in-situ strength where the rock is subjected to an anisotropic stress state (Yang et al., 2007; Haimson, 2006; Tiwari & Rao, 2004, 2006; Haimson & Chang, 1999).

Polyaxial strengths of Maha Sarakham salt

From the experimental results on brittle rocks obtained from Colmenares & Zoback, (2002), Haimson, (2006), it can be generally concluded that in a $\sigma_1 - \sigma_2$ diagram, for a given σ_3 , σ_1 at failure initially increases with σ_2 to a certain magnitude, and then it gradually decreases as σ_2 increases. The effect of σ_2 is more pronounced under higher σ_3 . Cai (2008) offers an explanation of how the intermediate principal stress affects the rock strength based on the results from numerical simulations on fracture initiation and propagation. This states that the intermediate principal stress confines the rock in such a way that fractures can only be initiated and propagated in the direction parallel to σ_1 and σ_2 . The effect of σ_2 is related to the stress-induced anisotropic properties, and the end effect at the interface between the rock surface and loading platen in the direction of σ_2 application. The effect is smaller in homogeneous and fine-grained rocks than in coarse-grained rocks where pre-existing micro-cracks are not uniformly distributed.

Several failure criteria have been developed to describe the rock strength under true triaxial stress states. Comprehensive reviews of these criteria have recently been given by Haimson (2006), Colmenares & Zoback (2002), Benz & Schwab (2008), and You (2008). Among these several criteria, the Mogi and modified Wiebols and Cook criteria are perhaps the most widely used to describe the rock compressive strengths under true triaxial stresses. Obtaining rock strengths under an anisotropic stress state is not only difficult but also expensive. A special loading device (e.g. polyaxial loading machine or true triaxial load cell) is required. As a result, test data under true triaxial stress conditions have been relatively limited. Most researchers have used the same sets of test data (some obtained over a decade ago) to compare with their new numerical simulations, or field observations (notably on breakout of deep boreholes) and to verify their new strength criteria and concepts. Due to the cost and equipment availability for obtaining true triaxial strengths, in common engineering practices application of a failure criterion that can incorporate the three-dimensional stresses has been very rare.

The objective of this paper is to determine the effects of the intermediate principal stress on the strength of Maha Sarakham salt. A polyaxial load frame is used to apply constant lateral loads onto the rectangular specimens while the axial load is increased to failure. Assessment of the predictive capability of some commonly used criteria is made.

2 SALT SAMPLES

The salt specimens tested here were collected from the middle members of the Maha Sarakham formation in the Khorat basin, northeastern Thailand. This salt member has long been considered as a host rock for compressed-air energy storage by the Thai Department of Energy. The rectangular block specimens are cut and ground to have a nominal dimension of $5.4 \times 5.4 \times 10.8 \text{ cm}^3$. The rock salt is relatively pure halite with a slight amount (less than 1-2%) of anhydrite, clay minerals and ferrous oxide. The average crystal (grain) size is $5 \times 5 \times 10 \text{ mm}^3$. The core specimens with a nominal diameter of 60 mm tested here were drilled from depths ranging between 170 and 270 m.

3 POLYAXIAL LOAD FRAME

A polyaxial load frame is developed based on three key design requirements: (1) capable of maintaining constant lateral stresses (σ_2 and σ_3) during the test, (2) capable of testing specimen with volume equal to or larger than those used in the conventional triaxial testing, and (3) allowing monitoring of specimen deformation along the principal axes. To meet the

load requirement above, two pairs of cantilever beams are used to apply the lateral stresses in mutually perpendicular directions to the rock specimen (Figure 1). The outer end of each opposite beam is pulled down by dead weight placed in the middle of a steel bar linking the two opposite beams underneath. The inner end is hinged by a pin mounted on vertical bars on each side of the frame. During testing all beams are arranged horizontally, and hence a lateral compressive load results on the specimen placed at the center of the frame. Due to the different distances from the pin to the outer weighting point and from the pin to the inner loading point, a load magnification of 12 to 1 is obtained from load calibration with an electronic load cell. This loading ratio is also used to determine the lateral deformation of the specimen by monitoring the vertical movement of the two steel bars below. The maximum lateral load is designed for 100 kN. The axial load is applied by a 1000 kN hydraulic load cell. The load frame can accommodate specimen sizes from $2.5 \times 2.5 \times 2.5 \text{ cm}^3$ to $10 \times 10 \times 20 \text{ cm}^3$. The different specimen sizes and shapes can be tested by adjusting the distances between the opposite loading platens.

4 TRUE TRIAXIAL STRENGTH TESTING

The polyaxial compression tests are performed to determine the compressive strengths and deformations of the salt under true triaxial stresses. The intermediate (σ_2) and minimum (σ_3) principal stresses are maintained constant while σ_1 maximum stresses is increased until failure is occurred. Here the constant σ_2 is varied from 0 to 80 MPa, and σ_3 from 0 to 28 MPa. Neoprene sheets are used to minimize the friction at all interfaces between the loading platen and the rock surface. The measured sample deformations are used to determine the strains along the principal axes during loading. The failure stresses are recorded and mode of failure is examined. Examples of stress-strain curves obtained from polyaxial compressive strength test are shown in Figure 2. The three-dimensional principal stress-strain relations given by Jaeger & Cook (1979) can be simplified to obtain a set of governing equations for isotropic material. The calculations of the Poisson's ratios and tangent elastic moduli are made at 50% of the maximum principal stress. The results indicate that the elastic modulus and Poisson's ratio of the MS salt are averaged as $21.5 \pm 2.6 \text{ GPa}$ and 0.40 ± 0.04 as shown in Table 1. The table also provides the octahedral shear stress (τ_{oct}), mean stress (σ_m), and the second order of the stress deviation ($J_2^{1/2}$) at failure. They can be calculated from the principal stresses at failure ($\sigma_1, \sigma_2, \sigma_3$).

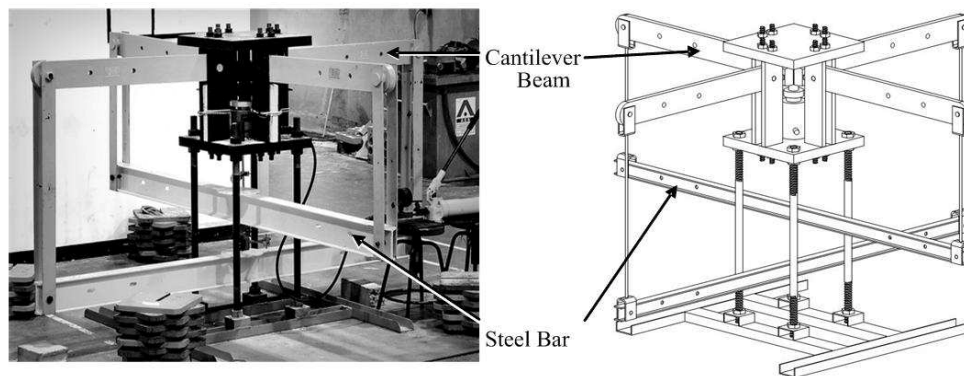


Figure 1. Polyaxial load frame developed for compressive strength testing under true triaxial stress.

Polyaxial strengths of Maha Sarakham salt

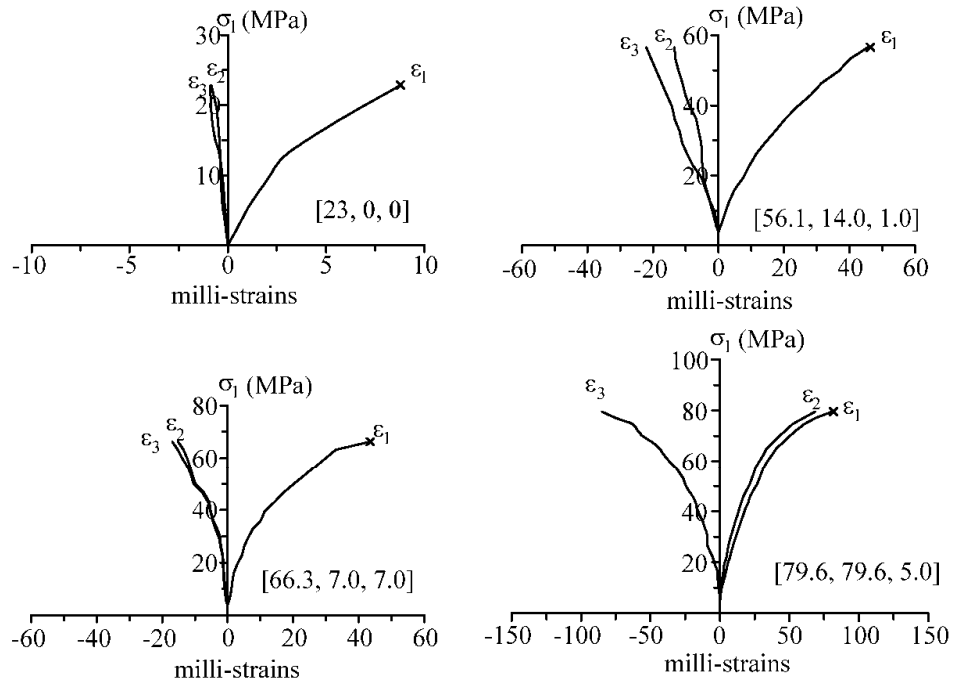
Figure 2. Examples of stress-strain curves obtained from polyaxial compressive strength test, the applied stresses are indicated $[\sigma_1, \sigma_2, \sigma_3]$ in MPa.

Table 1. Principal stresses at failure and elastic parameters of salt.

Specimen number	Depth (m)	Failure Stresses			σ_m (MPa)	τ_{oct} (MPa)	$J_2^{1/2}$ (MPa)	Elastic Modulus (GPa)	Poisson's Ratio
		σ_3 (MPa)	σ_2 (MPa)	σ_1 (MPa)					
56	253.75-253.85	0.0	0.0	23.0	7.7	10.8	5.4	22.4	0.35
7	179.66-179.77		10.0	36.2	15.4	15.3	7.6	20.7	0.36
55	208.40-208.50		25.0	43.1	22.7	17.7	8.8	23.3	0.42
42	211.60-211.70		35.1	35.1	23.4	16.5	8.3	-	-
20	244.47-244.57	1.0	1.0	26.5	9.5	12.0	6.0	25.3	0.46
22	246.21-246.31		7.0	43.2	16.7	18.9	9.5	18.5	0.39
23	245.50-245.60		14.0	56.1	23.4	23.8	11.9	20.6	0.40
54	208.50-208.60		25.0	60.4	28.5	24.8	12.4	19.3	0.40
44	210.05-219.15		35.0	62.5	32.5	25.6	12.8	-	-
38	211.20-211.30		49.3	49.3	32.9	23.2	11.6	-	-
61	178.13-178.23	3.0	3.0	45.1	17.0	19.8	9.9	22.5	0.25
53	208.60-208.70		7.0	55.0	20.7	24.4	12.2	19.8	0.39
52	254.05-254.15		10.0	61.0	23.7	26.7	13.4	23.1	0.40
5	256.43-256.53		14.0	66.0	26.7	28.4	14.2	15.8	0.38
57	201.70-201.80		25.0	71.5	32.2	29.6	14.8	26.9	0.42
35	200.45-200.56		40.0	75.0	38.3	30.6	15.3	24.3	0.36
43	209.95-210.05		50.0	74.9	41.6	31.1	15.6	-	-

Table 1. Principal stresses at failure and elastic parameters of salt (cont).

Specimen number	Depth (m)	Failure Stresses			σ_m (MPa)	τ_{oct} (MPa)	$J_2^{1/2}$ (MPa)	Elastic Modulus (GPa)	Poisson's Ratio
		σ_3 (MPa)	σ_2 (MPa)	σ_1 (MPa)					
40	211.40-211.50		64.9	64.9	43.3	30.6	15.3	-	-
27	264.41-264.51	5.0	5.0	58.6	22.9	25.3	12.6	23.4	0.42
28	263.31-263.41		14.0	71.2	28.4	30.8	15.4	20.8	0.40
29	264.67-264.77		21.0	79.2	33.4	33.5	16.8	18.0	0.35
47	210.35-210.45		30.0	87.4	39.1	36.3	18.1	21.4	0.39
41	211.50-211.60		40.0	91.6	43.9	37.5	18.7	-	-
48	210.45-210.55		50.0	89.3	46.4	36.5	18.3	23.1	0.39
45	210.15-210.25		65.0	85.0	50.0	36.3	18.1	-	-
49	210.55-210.65		79.6	79.6	53.1	37.5	18.8	24.1	0.42
12	201.23-201.33		7.0	7.0	66.3	26.8	28.0	14.0	22.1
13	201.60-201.70	14.0		78.1	30.7	34.0	17.0	20.0	0.37
19	244.37-244.47	24.0		92.4	38.8	39.1	19.6	16.0	0.43
25	245.10-245.20	40.0		106.4	48.8	43.9	21.9	-	-
50	210.65-210.75	50.0		110.7	53.6	45.3	22.6	20.2	0.43
46	210.25-210.35	65.0		109.5	58.2	45.0	22.5	-	-
10	179.93-180.31	10.0	10.0	79.6	33.2	32.8	16.4	21.7	0.39
58	251.79-250.85	12.0	12.0	81.8	35.3	32.9	16.5	22.7	0.42
59	212.11-212.21	20.0	20.0	106.4	48.8	40.7	20.4	21.9	0.39
60	243.71-243.82	28.0	28.0	119.7	58.6	43.2	21.6	23.0	0.36
		Mean \pm Standard Deviation						21.5 \pm 2.6	0.4 \pm 0.04

5 STRENGTH CRITERIA

The strength criteria used in this study include the Coulomb, Drucker-Prager, modified Lade, modified Weibols and Cook, Hoek and Brown, and the empirical Mogi criteria. Detailed derivations of these criteria are given by Colmenares & Zoback (2006), and hence they will not be repeated here. Table 2 summarized the variables and constants used in these criteria. Based on the Coulomb criterion the internal friction angle from the triaxial loading condition ($\sigma_2=\sigma_3$) is calculated as 50° , and the cohesion as 5 MPa. They are used in the calculation of the constant A, B and C used in the modified Weibols and Cook criteria. The empirical Mogi criterion uses a power law to describe the failure stresses. The parameter α and κ for the Inscribed and Circumscribed Drucker-Prager criteria can be derived from the cohesion and friction angle. The constant "s" in Hoek and Brown criterion is equal to 1 (for intact salt). The constant "m" is determined from the strength data under triaxial condition ($\sigma_2=\sigma_3$). The modified Lade parameters (η) can also be derived directly from the cohesion and internal friction angle. The calculated property parameters of each failure criterion are given in Table 3.

BIOGRAPHY

Mr. Tanapol Sriapai was born on June 8, 1987 in Nakhon Ratchasima province, Thailand. He received his Bachelor's Degree in Engineering (Geotechnology) from Suranaree University of Technology in 2009. For his post-graduate, he continued to study with a Master's degree in the Geological Engineering Program, Institute of Engineering, Suranaree university of Technology. During graduation, 2009-2011, he was a part time worker in position of research assistant at the Geomechanics Research Unit, Institute of Engineering, Suranaree University of Technology. He has published two technical papers related to rock mechanics as; In 2010, **“Polyaxial strength of Maha Sarakham rock salt”** published in the Proceedings of the ISRM International Symposium and the 6th Asian Rock Mechanics Symposium. Central Board of Irrigation and Power, New Delhi, India, In 2011 **“Polyaxial strengths of Maha Sarakham salt”** published in the Proceeding of Third Thai Rock Mechanics Symposium, Petchburi, Thailand.

Polyaxial strengths of Maha Sarakham salt

Table 2. Summary of the failure criteria.

Criterion	Equations
Modified Wiebols and Cook	$J_2^{1/2} = A + B\sigma_m + C\sigma_m^2$ $A = \frac{C_0}{\sqrt{3}} - \frac{C_0}{3}B - \frac{C_0^2}{9}C$ $B = \frac{\sqrt{3}(q-1)}{q+2} - \frac{C}{3}(2C_0 + (q+2)\sigma_3)$ $C = \frac{\sqrt{27}}{2C_1 + (q-1)\sigma_3 - C_0} \times \left(\frac{C_1 + (q-1)\sigma_3 - C_0}{2C_1 + (2q+1)\sigma_3 - C_0} - \frac{q-1}{q+2} \right)$ $C_1 = (1 + 0.6\mu_i)C_0$ $q = \{(\mu_i^2 + 1)^{1/2} + \mu_i\}^2$ $\mu_i = \tan \phi$
Mogi	$\tau_{oct} = A'[(\sigma_1 + \sigma_3)/2]^{B'}$ <p>A' and B' = Empirical Constant</p>
Hoek & Brown	$\sigma_1 = \sigma_3 + \sigma_c \sqrt{m \frac{\sigma_3}{\sigma_c} + s}$ <p>m and s = Material Constant</p>
Modified Lade	$(I_1')^3/I_3' = 27 + \eta$ $I_1' = (\sigma_1 + S) + (\sigma_2 + S) + (\sigma_3 + S)$ $I_3' = (\sigma_1 + S)(\sigma_2 + S)(\sigma_3 + S)$ $S = S_0/\tan \phi$ $\eta = 4(\tan \phi)^2(9 - 7\sin \phi)/(1 - \sin \phi)$ $S_0 = \sigma_c/(2q^{1/2})$
Coulomb	$J_2^{1/2} = \frac{2}{\sqrt{3}}[\sigma_m \sin \phi + S_0 \cos \phi]$ $\sigma_m = (\sigma_1 + \sigma_2 + \sigma_3)/3$
Drucker-Prager (Circumscribed)	$J_2^{1/2} = \kappa_c + \alpha_c \sigma_m$ $\alpha_c = \frac{6 \sin \phi}{\sqrt{3}(3 - \sin \phi)}$ $\kappa_c = \frac{\sqrt{3}C_0 \cos \phi}{\sqrt{q}(3 - \sin \phi)}$
Drucker-Prager (Inscribed)	$J_2^{1/2} = \kappa_i + \alpha_i \sigma_m$ $\alpha_i = \frac{3 \sin \phi}{\sqrt{9 + 3 \sin^2 \phi}}$ $\kappa_i = \frac{2C_0 \cos \phi}{2\sqrt{q}\sqrt{9 + 3 \sin^2 \phi}}$

Table 3. Parameters for each failure criterion.

Criteria	Calibrated Parameters
Modified Wiebols and Cook	$\sigma_3 = 0$, A = 2.031 MPa, B = 1.746, C = -0.036 MPa ⁻¹ $\sigma_3 = 1$, A = 1.698 MPa, B = 1.739, C = -0.030 MPa ⁻¹ $\sigma_3 = 3$, A = 1.281 MPa, B = 1.733, C = -0.022 MPa ⁻¹ $\sigma_3 = 5$, A = 1.027 MPa, B = 1.732, C = -0.017 MPa ⁻¹ $\sigma_3 = 7$, A = 0.853 MPa, B = 1.732, C = -0.014 MPa ⁻¹
Mogi 1971	A' = 1.46 B' = 0.82
Hoek & Brown	m = 20.2 s = 1
Modified Lade	S = 3.66 MPa $\eta = 88.33$
Coulomb	$\phi = 50$ c = 5 MPa
Drucker-Prager (Circumscribed)	$\alpha_c = 0.69$ $\kappa_c = 4.7$ MPa
Drucker-Prager (Inscribed)	$\alpha_i = 0.15$ $\kappa_i = 1.38$ MPa

6 PREDICTABILITY OF THE STRENGTH CRITERIA

The three-dimensional strength criteria are used to compare against the strength data. Figure 3 shows the octahedral shear strength as a function of mean stress, and the major principal stress at failure as a function of the intermediate principal stress. The mean misfit (\bar{s}) is determined for each criterion using equation (1) (Riley et al., 1988). Table 4 describes the calculated mean misfits for each criterion. The effect of σ_2 on the salt strengths can be best described by the modified Wiebols and Cook criterion with the mean misfit=3.5 MPa. The empirical (power law) Mogi criterion tends to underestimate the salt strengths particularly under high σ_3 values. The modified Lade criterion is the overestimates the actual strengths at all levels of σ_3 , showing the mean misfit=15.4 MPa. The Coulomb and Hoek and Brown criteria can not describe the salt strengths beyond the condition where $\sigma_2=\sigma_3$, as they can not incorporate the effects of σ_2 . Both circumscribed and inscribed Drucker-Prager criteria severely underestimate σ_1 at failure for all stress conditions, showing the largest mean misfit of 19.5 and 34.7 MPa, respectively.

$$\bar{s} = \frac{1}{m} \sum_i s_i \quad (1)$$

$$\text{Where } s_i = \sqrt{\frac{1}{n} \sum_j (\sigma_{1,j}^{\text{calc}} - \sigma_{1,j}^{\text{test}})^2}$$

$\sigma_{1,j}^{\text{calc}}$ = maximum stress predicted from strength criterion.

$\sigma_{1,j}^{\text{test}}$ = maximum stress from test data.

N = number of data points calculated.

M = number of data sets.

Polyaxial strengths of Maha Sarakham salt

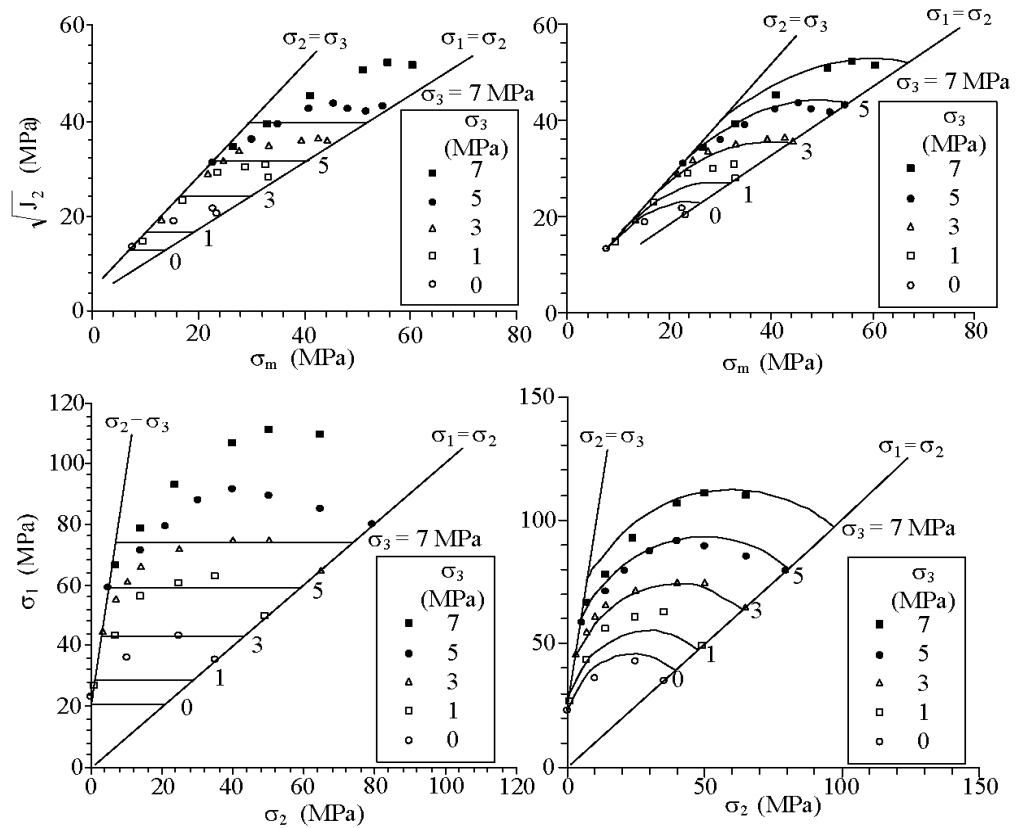


Figure 3. Comparisons between the test results with the modified Wiebols and Cook criterion (right) the Coulomb criterion (left).

Table 4. Mean misfits calculated for each failure criterion.

Strength Criteria	Mean Misfit (MPa)
Modified Wiebols and Cook	3.5
Empirical Mogi	9.6
Hoek & Brown	18.6
Modified Lade	15.4
Coulomb	17.7
Drucker-Prager (Circumscribed)	19.5
Drucker-Prager (Inscribed)	34.7

7 CONCLUSIONS

The polyaxial loading tests are performed to assess the effect of intermediate principal stress on the MS salt. The results suggest that the intermediate principal stress can affect the maximum stress at failure. Such effect is not linear. The results indicate that the elastic modulus and Poisson's ratio of the MS salt are averaged as 21.5 ± 2.6 GPa and 0.40 ± 0.04 . For

the Coulomb criterion, the internal friction angle determined from the triaxial loading condition ($\sigma_2=\sigma_3$) is 50° , and the cohesion is 5 MPa. The effect of σ_2 on the salt strengths can be best described by the modified Wiebols and Cook criterion. The empirical (power law) Mogi criterion tends to underestimate the salt strengths particularly under high σ_3 values. The modified Lade criterion is the overestimates at all levels of σ_3 . The Coulomb and Hoek and Brown criteria can not describe the salt strengths beyond the condition where $\sigma_2=\sigma_3$, as they can not incorporate the effects of σ_2 . Both circumscribed and inscribed Drucker-Prager criteria severely underestimate σ_1 at failure for all stress conditions.

ACKNOWLEDGEMENT

This research is funded by Suranaree University of Technology. Permission to publish this paper is gratefully acknowledged. We would like to thank Pimai Salt Co. for donating the salt core samples for this research.

REFERENCES

- Benz, T. & Schwab, R., 2008. A quantitative comparison of six rock failure criteria. *International Journal of Rock Mechanics and Mining Sciences*. 45: 1176-1186.
- Cai, M., 2008. Influence of intermediate principal stress on rock fracturing and strength near excavation boundaries—Insight from numerical modeling, *International Journal of Rock Mechanics & Mining Sciences*. 45: 763-772.
- Colmenares, L.B. & Zoback, M.D., 2002. A statistical evaluation of intact rock failure criteria constrained by polyaxial test data for five different rocks. *International Journal of Rock Mechanics & Mining Sciences*. 39: 695-729.
- Haimson, B. & Chang, C., 2000. A new true triaxial cell for testing mechanical properties of rock, and its use to determine rock strength and deformability of Westerly granite. *International Journal of Rock Mechanics and Mining Sciences*. 37: 285-296.
- Haimson, B., 2006. True triaxial stresses and the brittle fracture of rock. *Pure and Applied Geophysics*. 163: 1101-1113.
- Hoek, E. & Brown, E. T. 1988. The Hoek-Brown Failure Criterion - a 1988 Update. *Proceedings of the 15th Canadian Rock Mechanics Symposium*, Vol. 1, pp 31-48. University of Toronto.
- Jaeger, J.C., & Cook, N.G.W. 1979. *Fundamentals of Rock Mechanics*. London: Chapman and Hall, 593 pp.
- Reddy, K.R., Saxena, S.K. & Budiman, J.S., 1992. Development of a True Triaxial Testing Apparatus. *Geotechnical Testing Journal*. 15(2): 89-105.
- Riley, K.F., Hobson, M.P., & Bence, S.J. 1998. *Mathematical Methods for Physics and Engineering*. Cambridge: Cambridge University Press, 1008 pp.
- Smart, B. G. D., 1995. A true triaxial cell for testing cylindrical rock specimens. *International Journal of Rock Mechanics and Mining Sciences*. 32(3): 269-275.
- Tiwari, R.P. & Rao, K.S., 2006. Post failure behaviour of a rock mass under the influence of triaxial and true triaxial confinement. *Engineering Geology*. 84: 112-129.
- Yang, X. L., Zou, J. F. & SUI, Z. R., 2007. Effect of intermediate principal stress on rock cavity stability. *Journal Central South University Technology*. s1-0165-05
- You, M., 2008. True-triaxial strength criteria for rock. *International Journal of Rock Mechanics and Mining Sciences*. 46: 115-127.

BIOGRAPHY

Mr. Tanapol Sriapai was born on June 8, 1987 in Nakhon Ratchasima province, Thailand. He received his Bachelor's Degree in Engineering (Geotechnology) from Suranaree University of Technology in 2009. For his post-graduate, he continued to study with a Master's degree in the Geological Engineering Program, Institute of Engineering, Suranaree university of Technology. During graduation, 2009-2011, he was a part time worker in position of research assistant at the Geomechanics Research Unit, Institute of Engineering, Suranaree University of Technology. He has published two technical papers related to rock mechanics as; In 2010, **“Polyaxial strength of Maha Sarakham rock salt”** published in the Proceedings of the ISRM International Symposium and the 6th Asian Rock Mechanics Symposium. Central Board of Irrigation and Power, New Delhi, India, In 2011 **“Polyaxial strengths of Maha Sarakham salt”** published in the Proceeding of Third Thai Rock Mechanics Symposium, Petchburi, Thailand.